Charles University in Prague

Faculty of Science

Department of Genetics and Microbiology

PhD Study Program: Molecular and Cellular Biology, Genetics and Virology

Formation of splicing machinery in the context of the cell nucleus

PhD Thesis

Eva Stejskalová

2014

Supervisor: doc. Mgr. David Staněk, PhD

Department of RNA Biology, Institute of Molecular Genetics AS CR, v. v. i.

DISCLAIMER:

I hereby declare that this thesis is my own original work and has not been submitted before to obtain another academic degree. I have acknowledged all sources used and have cited these in the reference section.

Prague, 3rd November 2014

Signature:

Eva Stejskalová

ACKNOWLEDGEMENT

I would like to express my thanks to my supervisor, David Staněk, for his ideas, advice and support during my graduate studies. I would like to thank all my colleagues from Laboratory of RNA Biology, IMG ASCR, for creating a great working atmosphere and especially for all the ice-creams in the sun.

Thanks to my family for their generous support and encouragement. Special thanks go to Fanda for keeping me sane and for simply everything, as always.

ABSTRACT

Most of the protein coding genes of higher eukaryotes contain introns which have to be removed from primary transcripts to make mRNA which can be used as a template for protein synthesis. This crucial step in the pre-mRNA processing is carried out by the spliceosome, a complex ribonucleoprotein machine formed from small ribonucleoprotein particles (snRNPs). snRNPs biogenesis is a complex process composed of several steps which take place in both the cytoplasm and the nucleus. Spliceosome assembly is highly dynamic and tightly regulated and pre-mRNA splicing depends not only on the sequence of the pre-mRNA itself but also on the nuclear context, such as the chromatin modifications.

How do cells regulate where and when the spliceosome would be assembled? What determines which introns will be spliced? These are fundamental, yet unanswered, biological questions. In this work we analyzed the formation of splicing machinery in the context of the cell nucleus from several different points of view.

First, we investigated the unexpected connection between splicing factor U1-70K and the survival of motor neurons (SMN) complex which is a major player in the snRNP biogenesis pathway. We revealed that U1-70K interacts with the SMN complex and that this interaction is crucial for the stability of nuclear gems, small non-membrane organelles associated with neurodegenerative diseases.

Secondly, we explored the role of an SR-like protein RNA binding motif 39 (RBM39) in the regulation of alternative splicing of the vascular endothelial growth factor (VEGF) gene. We showed that RBM39 is a part of the early spliceosomal complex where it interacts with proteins U1-70K and U2AF35.

Finally, we characterized the interactions of the histone acetylation reader protein Brd2 with acetylated chromatin *in vivo*.

ABSTRAKT ČESKY

Většina genů kódujících proteiny vyšších eukaryot obsahuje introny, které musí být odstraněny z primárních transkriptů. Vznikající mRNA může být poté použita jako templát pro syntézu proteinů. Sestřih intronů probíhá za pomoci složitého sestřihového komplexu, který se skládá z malých jaderných ribonukleoproteinových částic. Tyto částice vznikají během několika postupných kroků, které se odehrávají jak v jádře, tak v cytoplazmě. Sestřihový komplex se poté postupně skládá na molekule pre-mRNA. Jedná se o velmi dynamický a přesně regulovaný proces, který závisí nejen na sekvenci samotné pre-mRNA, ale záleží i na stavu celého jádra, např. na modifikacích chromatinu.

Mezi základní nezodpovězené biologické otázky patří například: Jak buňky řídí, kdy a kde se sestřihový komplex poskládá? Co předurčuje, které introny budou vystřiženy? V této práci zkoumáme sestřihový komplex a jeho skládání v kontextu buněčného jádra z několika různých úhlů pohledu.

Za prvé se věnujeme neočekávané souvislosti mezi sestřihovým faktorem U1-70K a komplexem SMN (z angl. *survival of motor neurons*), který je hlavním účastníkem biosyntetické dráhy malých jaderných ribonukleoproteinových částic. Podařilo se nám odhalit, že protein U1-70K interaguje s komplexem SMN a že tato interakce je klíčová pro stabilitu gems, malých nemembránových jaderných organel, jejichž absence souvisí se vznikem neurodegenerativních onemocnění.

Za druhé jsme zkoumali úlohu proteinu RBM39 (z angl. *RNA binding motif 39*) v regulaci alternativního sestřihu genu pro vaskulární endotheliální růstový faktor. Ukázali jsme, že RBM39 je součástí časného sestřihového komplexu, kde interaguje s proteiny U1-70K a U2AF35.

Nakonec jsme popsali interakce a dynamiku proteinu Brd2, který váže acetylované histony, s acetylovaným chromatinem *in vivo*.

TABLE OF CONTENTS

ABBREVIATIONS

3'ss	3' splice site
5'ss	5' splice site
aa	aminoacid
ACF	autocorrelation function
ATP	adenosine triphosphate
BD	bromodomain
BET	bromodomain extra-terminal protein family
CB	Cajal body
CBC	cap binding complex
cDNA	complementary DNA
CRM1	**c**hromosome region maintenance 1
CTD	C-terminal domain of RNA polymerase II
DABCO	1,4-diazabicyclo[2.2.2]octane
DAPI	4',6-diamidino-2-phenylindole
DMEM	Dulbecco's modified Eagle medium
DSE	distal sequence element
(E)CFP	(enhanced) cyan fluorescent protein
(E)GFP	(enhanced) green fluorescent protein
ESE/ISE	exonic/intronic splicing enhancer
ESS/ISS	exonic/intronic splicing silencer
EST	expressed sequence tag

ET	extra-terminal domain
(E)YFP	(enhanced) yellow fluorescent protein
FISH	fluorescence *in situ* hybridization
FL	full-length
FRAP	fluorescence recovery after photobleaching
FRET	Förster resonance energy transfer
FUS	fused in sarcoma
gem	Gemini of Cajal bodies
GTFs	general transcription factors
H	histone
H3K9	Lysine 9 of histone 3
HDAC	histone deacetylase
hnRNPs	heterogeneous nuclear ribonucleoproteins
IF	indirect immunofluorescence
impβ	importin beta
IP	immunoprecipitation
LEC	little elongation complex
m^7G-cap	7-methylguanosine cap
mRNA	messenger RNA
mut	mutant
NaBu	sodium butyrate
nt	nucleotide
PAGE	polyacrylamide gel electrophoresis

PBS	phosphate buffer saline
PCR	polymerase chain reaction
PHAX	phosphorylated adapter RNA export protein
pICln	chloride ion current inducer protein
Pol II	RNA polymerase II
Pol III	RNA polymerase III
PRMT5	protein arginine methylase 5
Prp5	pre-mRNA processing protein 5
PSE	proximal sequence element
RBM39	RNA-binding motif protein 39 (aka HCC1, RNPC2, CAPER alpha)
RICS	raster image correlation spectroscopy
RNA	ribonucleic acid
RRM	RNA recognition motif
Rsd1	RNA-binding protein rsd1
RT-PCR	reverse transcription followed by polymerase chain reaction
scaRNA	small Cajal body RNA
SDS	sodium dodecylsulphate
SF	splicing factor
SIM	structural illumination microscopy
siRNA	silencer RNA
SMN	survival of motor neurons
SNAPc	snRNA activating protein complex
snRNA	small nuclear RNA

snRNP	small nuclear ribonucleoprotein particle
Spn1	snurportin 1
SR proteins	proteins from serine/arginine rich protein family
SRSF1	serine/arginine-rich splicing factor 1
TGS1	trimethylguanosine synthase 1
TMG	trimethylguanosine cap
TRIS	2-amino-2-hydroxymethylpropan-1,3-diol
TSS	transcription start site
U1-70K	U1 small nuclear ribonucleoprotein 70 kDa
U1A	U1 small nuclear ribonucleoprotein A
U1C	U1 small nuclear ribonucleoprotein C
U2AF	U2 auxiliary factor
UHM	U2AF homology motif
VEGF	vascular endothelial growth factor
WB	western blotting
WD45	WD repeat-containing protein 45
wt	wild-type
Y/R	pyrimidine/purine

SUMMARY

Pre mRNA splicing is complex and tightly regulated process carried out by the spliceosome, a megadalton molecular machine composed of multiple proteins and molecules of RNA. In this work I focused on interactions during early phase of spliceosome assembly. I aimed to characterize an interaction between the U1 snRNP and SMN, which was recently detected in early spliceosome complexes (Makarov et al., 2012), and the role of RNA binding motif protein 39 (RBM39) in U1-U2 snRNPs communication during intron definition. To study early splicing events, I established several microscopy techniques (e. g. Förster resonance energy transfer (FRET), fluorescence recovery after photobleaching (FRAP) or super-resolution microscopy) and I applied these advanced microscopy techniques to measure interactions and dynamics of Brd2, a protein that binds acetylated histones and modulates alternative splicing. For this thesis, I divided my experimental results into three closely connected projects.

In the first project we characterized a novel interaction between U1 snRNP core protein U1-70K and the SMN complex and the unexpected importance of U1-70K protein for the integrity of nuclear gems. In this project we used molecular cloning and biochemical methods, such as co-immunoprecipitation (co-IP) and western blotting, together with advanced fluorescent microscopy approaches, such as FRET, high-content microscopy with automated image analysis and super-resolution structured illumination. To assay for physiological function of U1-70K

protein in the process of gem formation we used siRNA mediated RNA interference.

In the second project we analyzed interaction partners of RBM39 and its role in regulation of alternative splicing. We used molecular cloning, co-IP and western blotting to dissect the role of distinct domains of RBM39. We monitored the interactions of RBM39 *in situ* in fixed cells by FRET microscopy. To analyze RBM39 role in the alternative splicing regulation we utilized the siRNA mediated RNA interference followed by RNA isolation and reverse transcription combined with polymerase chain reaction (RT-PCR).

In the third project we characterized interactions of the histone acetylation reader protein Brd2 with chromatin. For this we took advantage of the advanced fluorescent microscopy techniques, such as raster image correlation microscopy (RICS) and FRAP followed by mathematical modelling. To decipher the contribution of particular domains of the Brd2 protein to the overall interactions with chromatin we used molecular cloning.

AIMS

In this work we focus on the formation of spliceosomal machinery. We study interactions of spliceosomal components and processes involved in splicing regulation. We use various biochemical and microscopic approaches to answer these main questions:

- to address U1 snRNP interactions with the survival of motor neurons complex
- to analyze interactions of the SR-like protein RBM39 with splicing machinery and assess RBM39 role in spliceosome assembly and alternative splicing regulation
- to characterize the interaction of a bromodomain-extraterminal family protein Brd2 with acetylated chromatin in live cells

INTRODUCTION

Genes of higher eukaryotes consist of the protein-coding sequences (exons) interrupted by the intervening sequences (introns). Introns have to be removed from the nascent transcripts (pre-mRNA) and the exons joined together to form mature mRNA. This crucial step in gene expression, pre-mRNA splicing, is carried out by the spliceosome, a macromolecular complex consisting of five snRNPs.

1 Biogenesis of spliceosomal snRNPs

Each snRNP consists of a uridine-rich snRNA molecule (U1, U2, U5 and U4/U6) and a set of specific proteins (Will and Luhrmann, 2011). However, they share a common feature – a ring of seven small Sm proteins (LSm in the case of the U6 snRNA) bound to a conserved uridine-rich sequence motif (Branlant et al., 1982; Urlaub et al., 2001). This common Sm core RNP structure serves various purposes in the complex biogenesis pathway which takes place in both the nucleus and the cytoplasm (Fig. 1).

1.1 snRNA synthesis and export

All snRNAs except U6 are transcribed by RNA polymerase II (Pol II). U6 is synthesized by RNA polymerase III (Pol III) (Reddy et al., 1987). All snRNA genes contain similar regulatory sequences, termed proximal and distal sequence element (PSE and DSE), within the promoter region (Fig. 2, (Hernandez, 2001;

Egloff et al., 2008)). These sequences serve as binding sites for snRNA-specific transcription factors Oct-1 (Murphy et al., 1992; Murphy, 1997) and snRNA activating protein complex SNAPc (Sadowski et al., 1993; Wong et al., 1998). In addition to these factors, the TATA-box binding protein and several general transcription factors are required for the initiation of transcription (Bernues et al., 1993; Kuhlman et al., 1999).

After the transcription is initiated, Pol II transcripts are co-transcriptionally capped (Salditt-Georgieff et al., 1980) with the 7-methylguanosine cap (m^7G-cap) and the snRNA coding region is transcribed. U6 snRNA can be capped post-transcriptionally (Gupta et al., 1990).

Pol II-transcribed snRNA genes terminate transcription at the so-called 3'-box, a sequence located approx. 200 nts downstream of the 3'-end of the mature snRNA

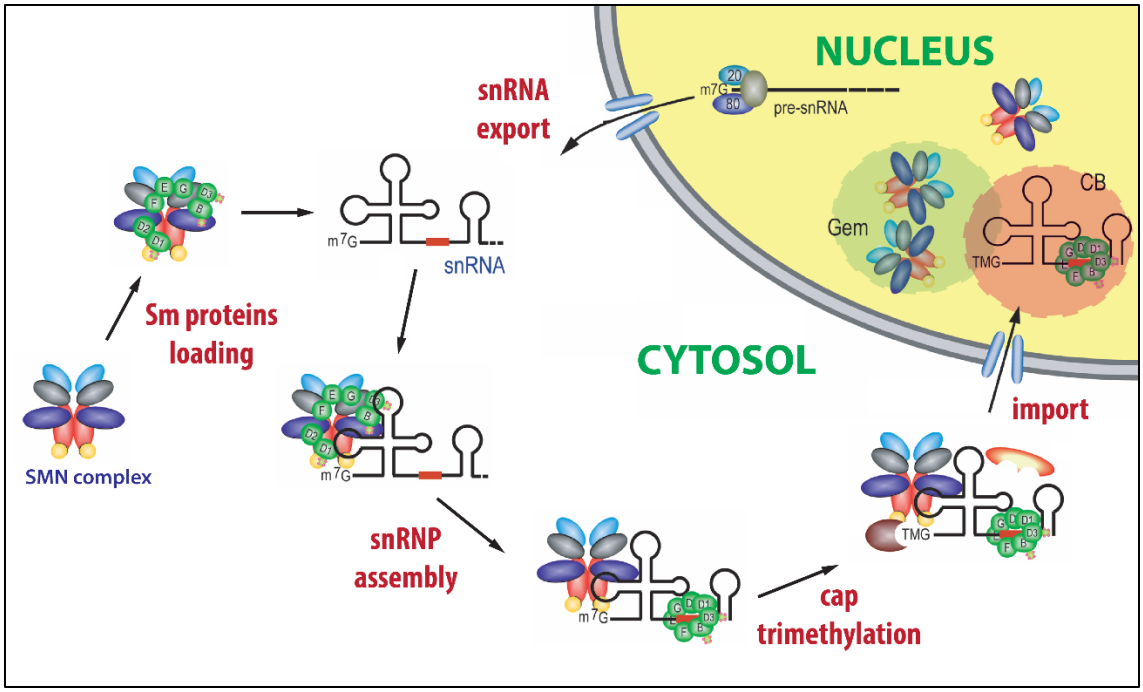

Fig. 1: snRNP biogenesis pathway. snRNA is transcribed in the nucleus and exported to the cytoplasm, where it interacts with the SMN complex. SMN complex loads the Sm ring onto the snRNA which is then further modified and imported back into the nucleus where it first emerges in the Cajal bodies. Adapted from (Battle et al., 2006b).

(Huang et al., 1997; Mougin et al., 2002). Co-transcriptional endonucleolytic cleavage of the snRNA is mediated by the Integrator, a large multiprotein complex which binds specifically phosphorylated C-terminal domain (CTD) of Pol II (Baillat et al., 2005; Egloff et al., 2007). U6 snRNA transcription terminates at a series of uridine residues at the 3'-end (Hamada et al., 2000; Huang and Maraia, 2001).

Pol II transcribed snRNAs are then exported to the cytoplasm via active receptor-mediated transport through nuclear pores (Fig. 3, (Cullen, 2003)). The m^7G-cap, which serves as an export signal, is bound by the cap binding complex (CBC, (Izaurralde et al., 1992)). CBC recruits the PHAX protein (Ohno et al., 2000) which has a nuclear export signal recognized by the export receptor CRM1 (Fornerod et al., 1997; Stade et al., 1997) associated with Ran-GTP (Drivas et al., 1990; Moore, 1998). The formation of the export complex is thought to be facilitated by Cajal bodies (CBs, (Suzuki et al., 2010); CBs are storage, assembly and remodeling sites of spliceosomal snRNPs (Machyna et al., 2013)). After the formation of the export complex, the snRNA is translocated through the nuclear pore to the cytoplasm, GTP bound to Ran is hydrolyzed to GDP and PHAX is

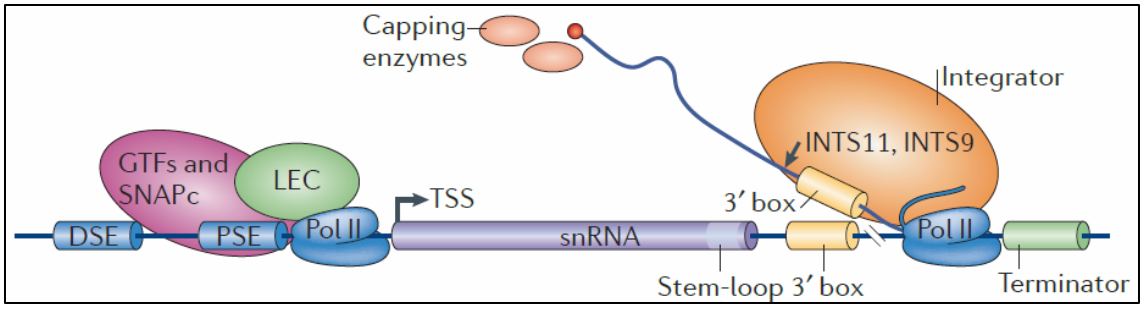

Fig. 2: Simplified scheme of transcription and processing of Pol II class snRNAs. Promoters recruit general transcription factors (GTFs), snRNA-activating protein complex (SNAPc) and the little elongation complex (LEC). The multisubunit Integrator complex recognizes the downstream processing signals, such as the 3'-box. 5'-end capping and 3'-end cleavage probably occur co-transcriptionally. TSS, transcription start site. Adapted from (Matera and Wang, 2014).

dephosphorylated, trigerring the dissociation of the export complex and release of the transported snRNA to the cytoplasm (Ohno et al., 2000; Kitao et al., 2008).

1.2 Assembly of nascent snRNPs in the cytoplasm

Newly exported snRNAs are recruited by the survival of motor neurons (SMN) complex, consisting of SMN protein (Lefebvre et al., 1995; Otter et al., 2007), gemins 2-8 (Fischer et al., 1997; Charroux et al., 1999; Charroux et al., 2000; Baccon et al., 2002; Gubitz et al., 2002; Pellizzoni et al., 2002b; Carissimi et al., 2006) and unrip (Carissimi et al., 2005). SMN complex loads a ring of seven Sm proteins onto the specific sequence in the snRNA called the Sm site (Fig. 4, (Mattaj and De Robertis, 1985)).

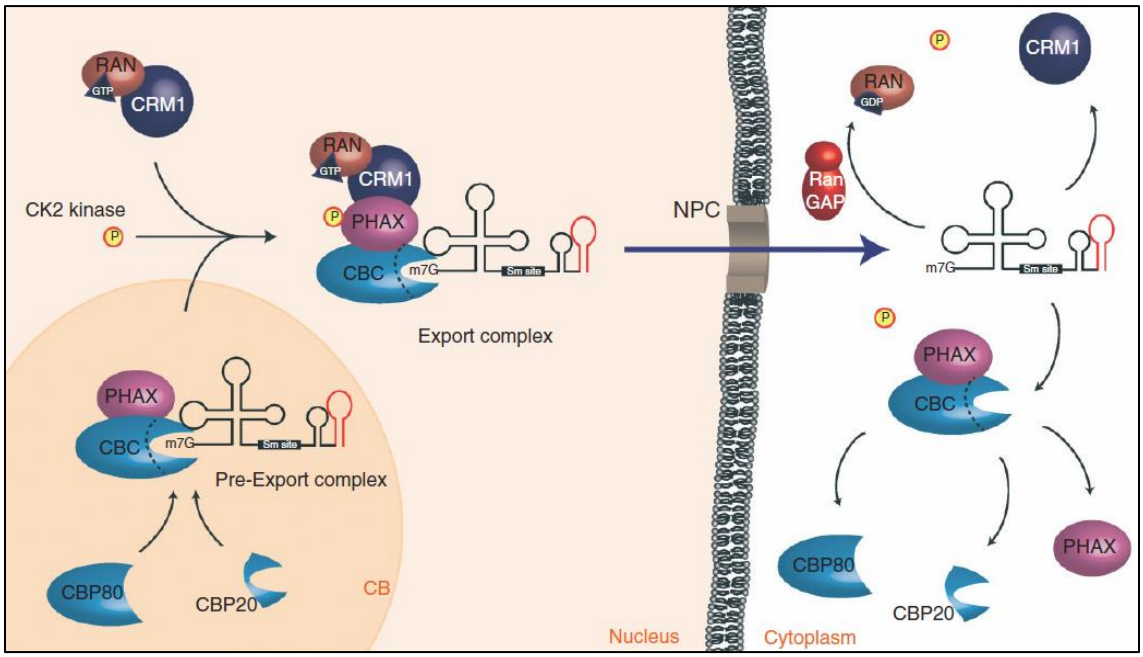

Fig. 3: Export of snRNAs. The export complex consisting of the CBC heterodimer, phosphorylated PHAX and CRM1 with Ran-GTP assembles on the m^7G-cap of the snRNA in the nucleus. The export complex is then transported through the nuclear pore to the cytoplasm, where it dissociates from the snRNA. Adapted from (Fischer et al., 2011).

Sm proteins are able to spontaneously form a ring in the presence of the appropriate RNA *in vitro* (Raker et al., 1996; Kambach et al., 1999; Leung et al., 2011). However, the Sm ring assembly *in vivo* is a tightly regulated process which requires whole SMN complex and ATP (Meister et al., 2001a). SMN complex binds both snRNA and Sm proteins (Friesen and Dreyfuss, 2000; Yong et al., 2002) bringing them together and preventing unspecific Sm ring formation on improper RNAs (Pellizzoni et al., 2002a).

Sm proteins are organized into three heterooligomers SmB-SmD3, SmD1-SmD2 and SmE-SmF-SmG (Raker et al., 1996). Sm proteins are sequestered by the protein arginine methylase 5 (PRMT5) complex consisting of WD45, pICln and PRMT5 methylase, which symmetrically methylates designated C-terminal

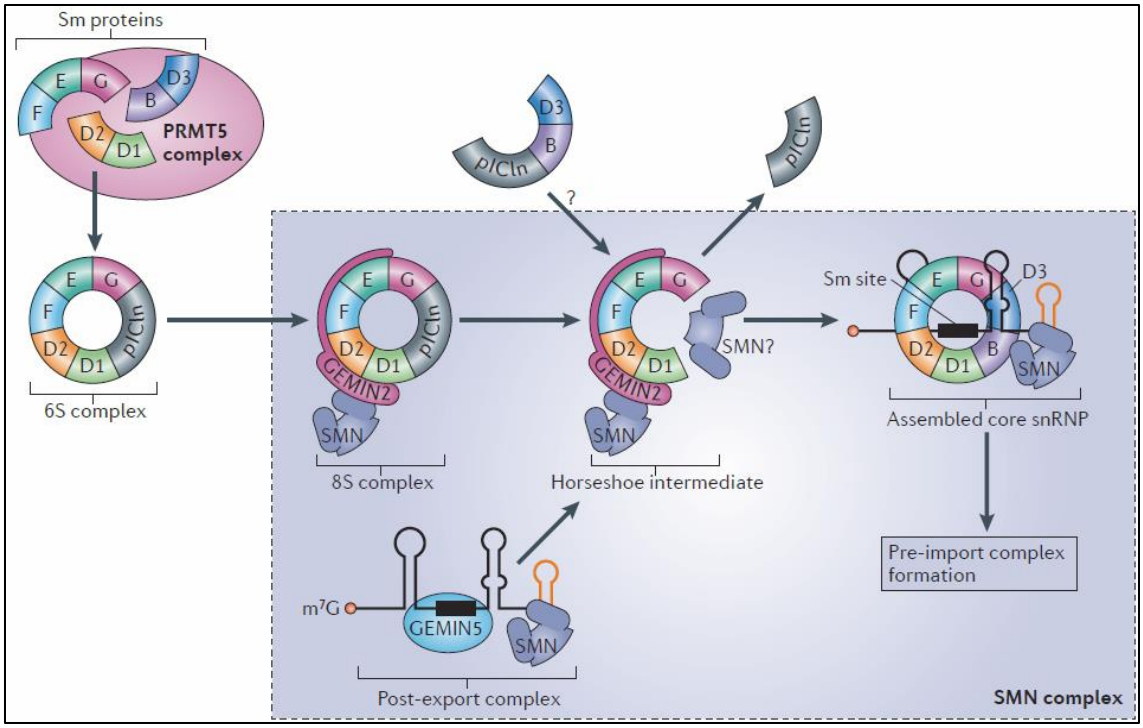

Fig. 4: Sm ring assembly. Sm proteins are symmetrically dimethylated by PRMT5 complex and the Sm pentamer 6S complex is delivered to the SMN complex. SMN complex brings together the Sm proteins bound by gemin2 and the nascent snRNA bound by gemin5. Then a series of not completely understood rearrangements occur resulting in a core snRNP assembly. Adapted from (Matera and Wang, 2014).

arginines in SmB, SmD1 and SmD3 (Friesen et al., 2001; Meister et al., 2001b). pICln then chaperones the delivery of the Sm subcomplexes to the SMN complex (Meister and Fischer, 2002; Chari et al., 2008; Grimm et al., 2013) where they are bound by gemin 2 and form a so-called horseshoe intermediate (Fig. 4, (Zhang et al., 2011)).

In parallel, gemin 5 recognizes the Sm site with adjacent specific stem-loop in the snRNA, thus ensuring the specificity of snRNA binding to the SMN complex (Battle et al., 2006a; Yong et al., 2010). The precise mechanism of the structural rearrangements enabling the final assembly of Sm ring onto the snRNA is still poorly understood.

Sm ring protects the snRNA from degradation by nucleases and initiates further processing steps. Sm core domain provides a binding platform for the trimethylguanosine synthase 1 (TGS1) which hypermethylates the m^7G-cap to the 2,2,7-trimethyl-guanosine cap (TMG, (Mattaj, 1986; Mouaikel et al., 2003)). At the same time, nucleotide extensions at 3'-end of the snRNA are cleaved by an exonuclease and thus trimmed to their mature length (Dahlberg et al., 1990). TMG cap together with the assembled Sm core serve as a nuclear-localization signal (Fig. 5 (Fischer and Luhrmann, 1990; Fischer et al., 1993; Narayanan et al., 2004)).

1.3 Nuclear import of nascent snRNPs

After the m^7G-cap is trimethylated, TGS1 dissociates from nascent snRNP and TMG cap is bound by snurportin 1 (Spn1, (Huber et al., 1998; Strasser et al., 2005)). Spn1 is a snRNP specific import adaptor which binds to the import receptor

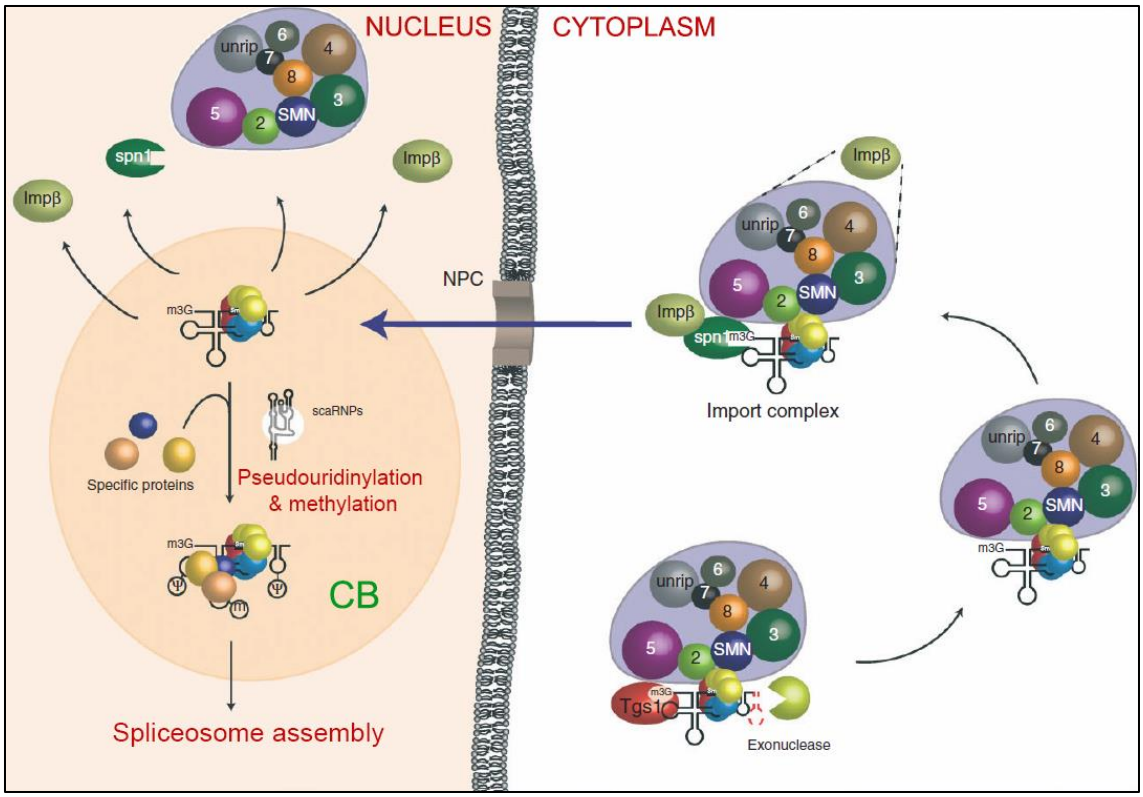

Fig. 5: Nuclear import and final remodeling of snRNPs. After hypermethylation of the 5'-cap, trimethylguanosine synthase 1 (Tgs1) is replaced by snurportin 1 (spn1) associated with importin β (impβ) that mediate its transport through the nuclear pore. The nascent snRNP then emerges in a CB where the snRNA is methylated and pseudouridinylated by scaRNPs and snRNP-specific proteins associate resulting in a mature splicing-competent snRNP. Adapted from (Fischer et al., 2011).

importin β (impβ, (Palacios et al., 1997; Huber et al., 2002; Wohlwend et al., 2007)). SMN complex probably also interacts with impβ and is co-imported to the nucleus while binding the Sm core domain (Narayanan et al., 2002; Narayanan et al., 2004).

After the assembly of the import complex, nascent snRNPs are transported back into the nucleus via Ran-independent transport mechanism (Huber et al., 2002; Wohlwend et al., 2007). SMN complex is thought to dissociate from snRNPs soon after the import. Newly imported snRNPs localize in CBs, where they are further modified (Sleeman and Lamond, 1999; Jady et al., 2003). Fully mature

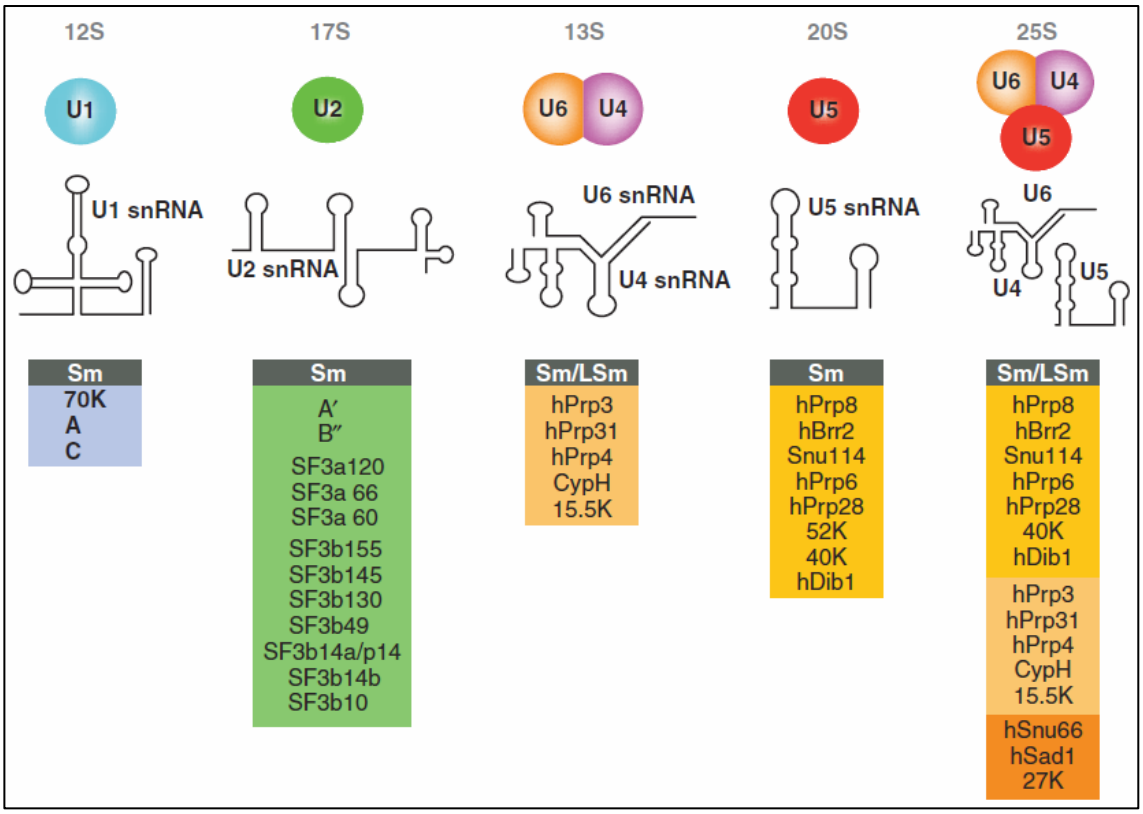

Fig. 6: Human spliceosome protein composition and schematics of snRNA secondary structures. Complete set of Sm or LSm proteins is indicated at the top of the boxes. Adapted from (Will and Luhrmann, 2011).

snRNPs (Fig. 6) are then prepared to participate in the process of pre-mRNA splicing.

1.4 Nuclear compartments and their role in snRNP biogenesis

There are several nuclear subdomains highly enriched in splicing factors, snRNP components and parts of snRNP biogenesis machinery. Among them are nuclear speckles, or interchromatin granule clusters, which are believed to be the storage sites of splicing factors (Lamond and Spector, 2003). Speckles form a variably sized and irregularly shaped localization pattern in the nucleoplasm (Fig. 7). Most of the splicing activity probably takes place on the border between

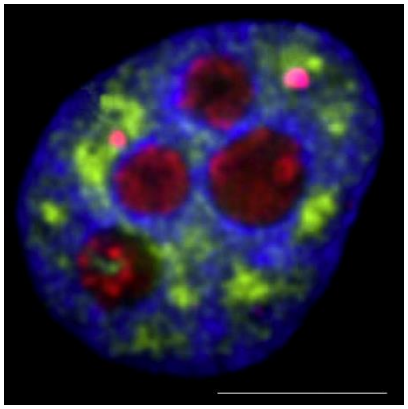

Fig. 7: Nuclear organelles. Chromatin is stained with DAPI (blue) in a HeLa cell expressing the SmB protein tagged with YFP (green) localizing in the nuclear speckles. The dense fibrillar components of nucleoli are stained with antibodies to fibrillarin (red) while anti-fibrillarin and anti-coilin both stain Cajal bodies (pink). Scale bar 10 μm. Adapted from (Sleeman and Trinkle-Mulcahy, 2014).

speckles and chromatin domains (Hall et al., 2006). It was shown recently that spliceosomes involved in post-transcriptional splicing accumulate in nuclear speckles (Girard et al., 2012).

Another non-membrane nuclear organelle important for snRNP biogenesis are CBs (Stanek and Neugebauer, 2006). Coilin, the marker protein of CBs, was shown to be essential for their function in zebrafish (Strzelecka et al., 2010). In addition to coilin and snRNP components, CBs contain CB-specific RNAs (scaRNAs) which guide covalent modifications (pseudouridinylation and 2'-O-ribose methylation) of the snRNAs (Yu et al., 1998; Jady and Kiss, 2001; Jady et al., 2003). CBs were also shown to be the site of several snRNP specific proteins association with the nascent snRNPs (Nesic et al., 2004; Schaffert et al., 2004). Moreover, CBs play role in the *de novo* assembly as well as post-splicing recycling of the U4/U6 di-snRNP and U4/U6·U5 tri-snRNP (Stanek et al., 2003; Staněk and Neugebauer, 2004; Klingauf et al., 2006; Stanek et al., 2008; Novotný et al., 2011).

Another important non-membrane bodies which often localize adjacent to CBs are called Gemini of Cajal bodies or simply gems (Liu and Dreyfuss, 1996; Malatesta et al., 2004). Nuclear population of SMN complexes accumulates in these

bodies which are also enriched in proteins involved in transcription and RNA processing. Physiological function of gems is currently unclear, however, their loss from the nucleus correlates with severity of neurodegenerative diseases such as spinal muscular atrophy and amyotrophic lateral sclerosis (Shan et al., 2010; Kariya et al., 2012; Yamazaki et al., 2012).

2 Spliceosome assembly

The spliceosomal complex forms from the snRNPs step-by-step directly on a pre-mRNA molecule (see below). The splicing of an intron then entails two trans-esterification reactions catalyzed by snRNAs assisted by spliceosomal proteins (Madhani and Guthrie, 1992; Valadkhan, 2010).

2.1 Spliceosome assembly overview

Spliceosome assembly starts with U1 snRNPs interaction with the 5'-splice site (5'ss, Fig. 8) resulting in the formation of the early complex (E-complex, Fig. 9, (Hartmuth et al., 2002)). 5'ss is recognized via base-pairing of U1 snRNA with the consensus sequence and by U1-snRNP specific U1C protein (Du and Rosbash,

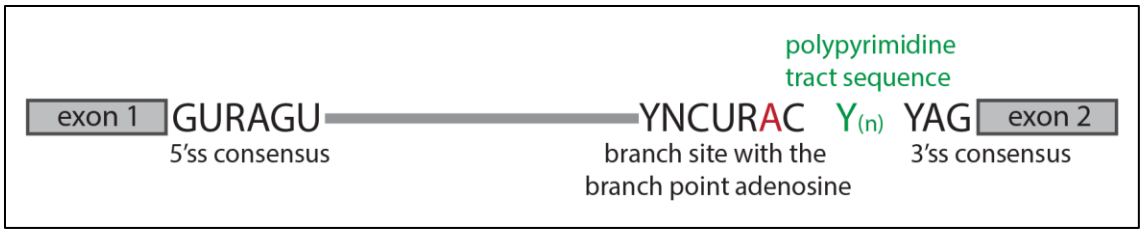

Fig. 8: Conserved sequences defining the introns in metazoan pre-mRNA. Y stands for pyrimidine, R for purine. Adapted from (Will and Luhrmann, 2011).

2002). The binding of U1 snRNP to the pre-mRNA within the E-complex is ATP-independent and stabilized by interactions with SR proteins (Staknis and Reed, 1994; Cho et al., 2011). The 3'ss is recognized by U2 auxiliary factor heterodimer (U2AF) and splicing factor 1 (SF1, (Valcarcel et al., 1996; Berglund et al., 1998)). U2 snRNP is then recruited to the 3'ss of the E-complex in an ATP-dependent process catalyzed by the DExD/H helicases and the pre-spliceosomal A-complex is established (Gozani et al., 1996; Behzadnia et al., 2007).

Pre-assembled U4/U6·U5 tri-snRNP then joins the spliceosome to form the B-complex (Bindereif and Green, 1987; Deckert et al., 2006). After several

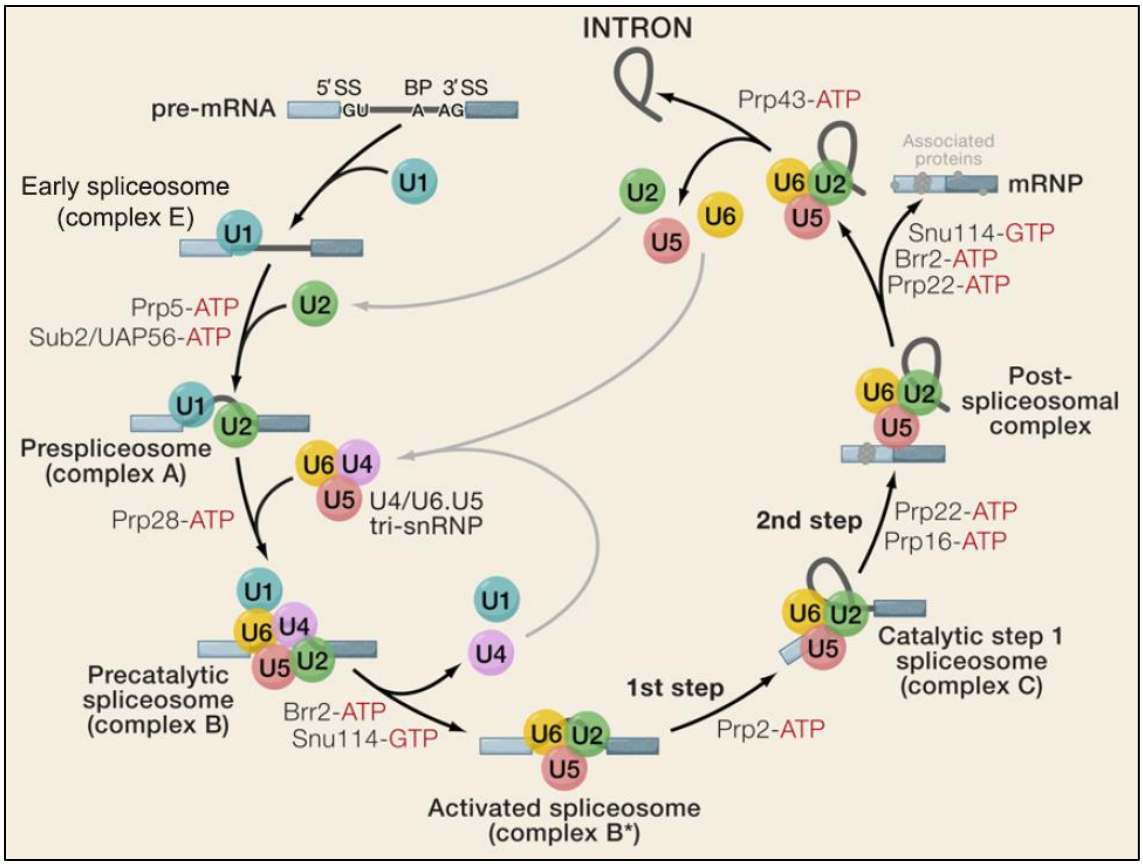

Fig. 9: Stepwise spliceosomal assembly. Simplified scheme of spliceosome assembly in budding yeast. Key steps are conserved in humans. Adapted from (Wahl et al., 2009).

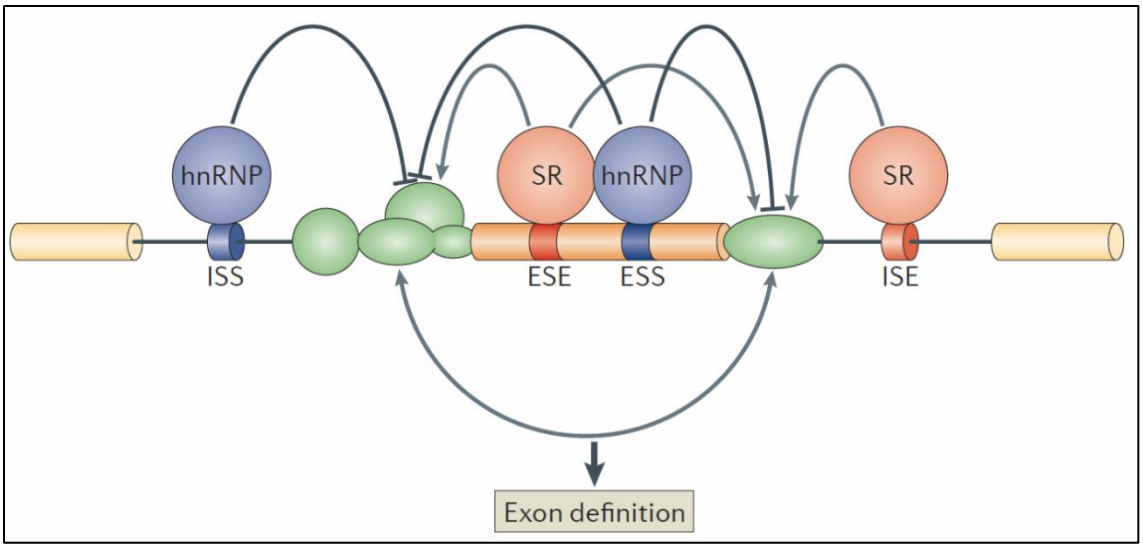

Fig. 10: Splicing regulatory sequences and factors. Splicing is governed by *cis*-regulatory sequences in the pre-mRNA (exonic/intronic splicing enhancers and silencers (ESEs/ISEs and ESSs/ISSs) which are recognized by two main families of splicing regulatory proteins, SR and hnRNPs proteins. These regulatory proteins target components of the spliceosome (green) either by blocking or promoting their interaction with the 5' and the 3'ss. Adapted from (Kornblihtt et al., 2013).

compositional and conformational rearrangements catalyzed by multiple helicases U1 and U4 snRNPs are released from the spliceosome (Raghunathan and Guthrie, 1998; Makarova et al., 2004) and a catalytically active B*-complex emerges (Jurica et al., 2002; Makarov et al., 2002). B*-complex subsequently catalyzes the first trans-esterification reaction resulting in formation of the C-complex (Konarska et al., 2006; Bessonov et al., 2008) which executes the second step of splicing catalysis during which the exons are ligated and the intron is excised in the form of a lariat (Brody and Abelson, 1985). Mature mRNA is then released from the spliceosome and U2, U5 and U6 snRNPs dissociate from the intron lariat to be used for the next round of splicing (Schwer and Gross, 1998; Fourmann et al., 2013; Ilagan et al., 2013).

2.2 Intron definition

Intron recognition is not based solely on consensus sequences at its 5' and 3' ends (Fig. 8). There are additional *cis*-acting elements within pre-mRNA which modulate splicing. These RNA elements (exonic/intronic splicing enhancers or silencers) are bound by regulatory proteins that consequently recruit other parts of splicing machinery (Fig. 10, (Matlin et al., 2005)). Enhancer sequences are typically bound by proteins from Ser/Arg-rich (SR) protein family whereas silencer sequences recruit heterogeneous nuclear ribonucleoproteins (hnRNP, (Busch and Hertel, 2012)). SR proteins and hnRNP proteins often antagonistically regulate splice site usage (Caceres et al., 1994; Zhu et al., 2001).

In case of short introns (approx. up to 250 nts) the E-complex assembles across an intron (Fox-Walsh et al., 2005). However, most pre-mRNAs of higher eukaryotes contain multiple introns with size reaching up to several thousand

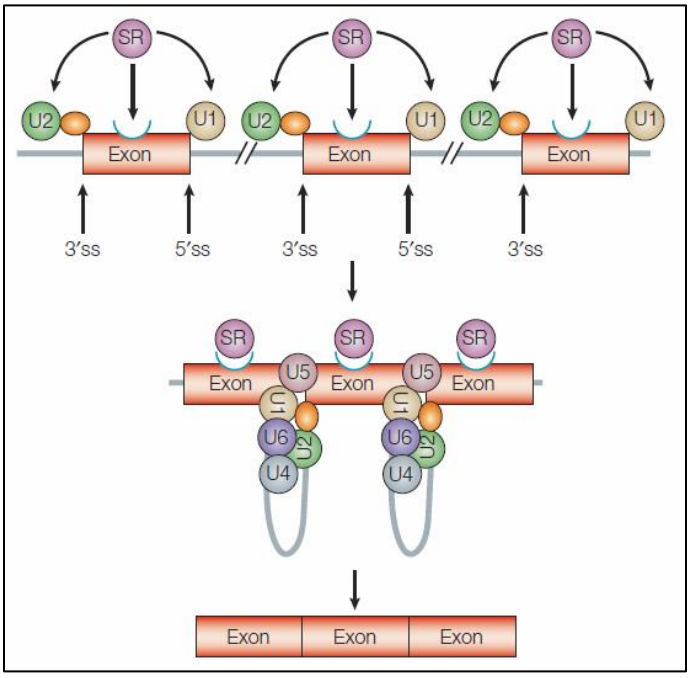

Fig. 11: Exon definition. SR proteins bind to ESEs, recruiting U1 snRNP to the downstream 5′ss and U2AF (represented by orange circle) to the upstream polypyrimidine tract and the 3′ss. U2AF then recruits U2 snRNP to the branch site. Adapted from (Ast, 2004).

nucleotides (Deutsch and Long, 1999) whereas the length of exons is rather fixed (around 120 nts on average (Ast, 2004)). When the intron length exceeds approx. 250 nts, the spliceosome is first assembled across the exon (Berget, 1995). This process called the exon definition (Fig. 11) is mediated by a network of protein-protein interactions between SR proteins which stabilize the exon-defined complex (Hoffman and Grabowski, 1992; Reed, 2000). The exon-defined spliceosomal complex is then converted into the cross-intron spliceosome in a poorly understood switch (House and Lynch, 2006; Bonnal et al., 2008; Sharma et al., 2008; Schneider et al., 2010).

A protein-protein interaction network determining intron recognition in *S. pombe* was recently described (Shao et al., 2012). Using copurification assays, Rsd1 protein was identified as a bridging factor between U1 and U2 snRNPs. Rsd1 interacts with U1 snRNP core protein U1A and at the same time with Prp5 ATPase which binds to U2 snRNP core protein SF3b, thus mediating communication between splice sites during intron recognition (Fig. 12). Rsd1 has a human homolog, RNA-binding motif protein 39 (RBM39, also known as HCC1, RNPC2 or CAPER alpha).

Possible role of RBM39 protein in the human E-complex assembly

Human RBM39 was first identified as a nuclear autoantigen isolated from the sera of a patient with hepatocellular carcinoma. Based on its localization mainly in nuclear speckles, it was proposed that RBM39 may be associated with splicing activities (Imai et al., 1993). This hypothesis was later confirmed by mass

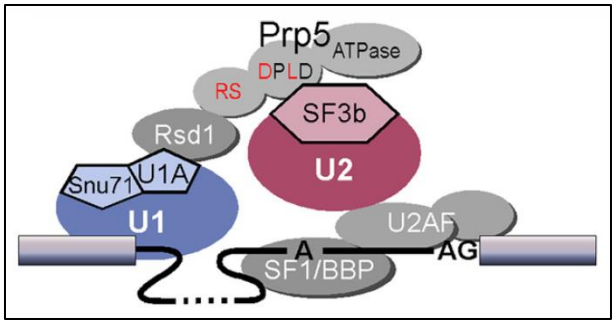

Fig. 12: Protein interaction network for U1-U2 snRNP communication during E-complex assembly in *S. pombe*. U1A binds to an SR-like protein Rsd1 which interacts with SpPrp5 via its RS-domain. SpPrp5 interacts via its conserved DPLD motif with SF3b protein of the U2 snRNP. Adapted from (Shao et al., 2012).

spectrometry studies of purified human spliceosomal complexes (Rappsilber et al., 2002) which showed RBM39 copurified mainly with prespliceosomal E-complex (Hartmuth et al., 2002).

RBM39 is an SR-like protein highly homologous to U2AF65 (Imai et al., 1993; Jung et al., 2002). In addition to the RS domain, RBM39 has two canonical RRMs and one UHM domain (U2AF homology motif, a structural motif which forms a hydrophobic pocket able to bind tryptophan residues of a ligand protein, thus promoting protein-protein interactions (Kielkopf et al., 2004)).

RBM39 functions as a hormone-dependent splicing cofactor. It was shown that it regulates alternative splicing of vascular endothelial growth factor (VEGF) gene (Dowhan et al., 2005; Huang et al., 2012). However, a molecular mechanism of this regulation is not known. It was shown that UHM domain of another SR-like splicing factor SPF45 is required for regulation of FAS alternative splicing in HeLa cells (Corsini et al., 2007). Thus it is tempting to speculate that RBM39 regulates the alternative splicing of the VEGF via its UHM domain.

3 Splicing regulation & alternative splicing

The consensus sequences of 5' and 3'ss are rather short and abundant (Fig. 8). Despite this fact the sequences which are not *bona fide* splice sites are very rarely spliced even if they have a similar level of consensus as the authentic splice sites (Sun and Chasin, 2000). Moreover, most genes in higher eukaryotes (nearly 95% in case of mammalian genes (Pan et al., 2008)) undergo alternative splicing which produces distinct mRNA isoforms leading to proteins with different functions (Fig. 13, (Kornblihtt et al., 2013)). Regulation of spliceosome assembly is the key control point for the fidelity of pre-mRNA splicing and it is achieved via synergy of multiple factors which will be discussed below.

3.1 Spliceosome assembly regulation

Depending on the level of consensus and thus their affinity for cognate splicing factors, splice sites can be considered either as strong (constitutively used) or

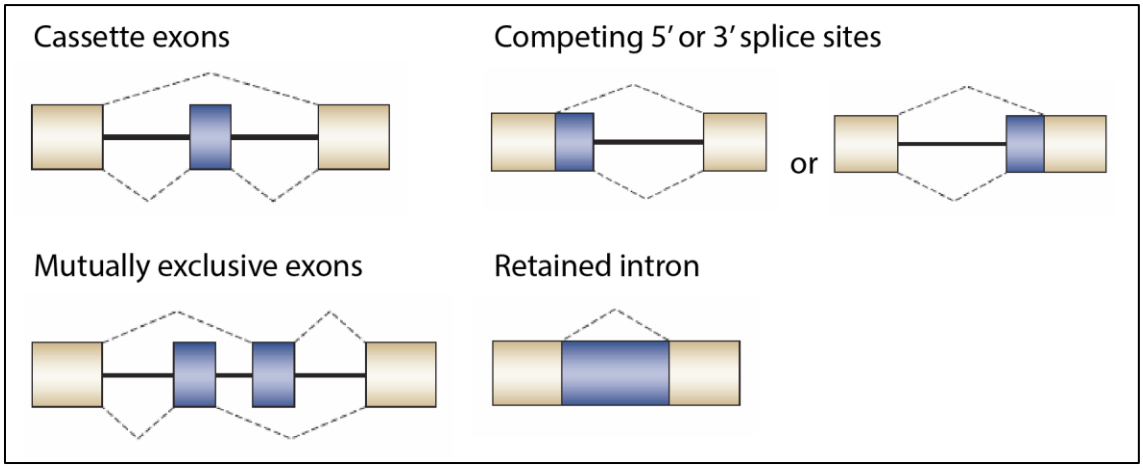

Fig. 13: Graphical representation of the elementary alternative splicing events. Different modes of alternative splicing comprise alternative exon inclusion or modification (alternative usage of different 5' or 3'ss) or intron retention. Adapted from (Kielkopf et al., 2004; Matlin et al., 2005).

weak (the usage varies depending on the cellular context). The usage of the weak splice sites is regulated by *cis*-acting regulatory sequences (splicing enhancers and silencers) and *trans*-acting splicing factors binding to them. In most cases, the spliceosome assembly is regulated at the stage of the E-complex formation and its subsequent transformation into the cross-intron A-complex (see section 4.2.2. for details).

Most splicing factors can recognize more than one splicing regulatory sequence and in turn, each regulatory sequence is bound by multiple splicing factors, giving rise to a complex regulatory network of RNA-protein interactions (Wang et al., 2012; Wang et al., 2013). Genome-wide analyses of splicing factors binding and RNA expression analyses detecting alternatively spliced isoforms together enabled the formulation of a putative so-called splicing code. The splicing code is able e. g. to predict whether an exon is constitutive or alternative (Gelfman et al., 2012) or to calculate tissue-specific alternative splicing patterns (Barash et al., 2010).

However, splicing code analysis is not able to predict the alternative splicing outcome with the absolute accuracy because there are other levels of regulation, mainly the coupling of splicing with transcription and the influence of epigenetic marks.

3.2 Coupling of transcription and splicing

Pre-mRNA splicing can occur co-transcriptionally (Beyer and Osheim, 1988; Bauren and Wieslander, 1994; Tennyson et al., 1995; Pandya-Jones and Black,

2009). Recruitment of splicing factors to the nascent transcript is dependent on the Pol II CTD which has to be specifically phosphorylated (Misteli and Spector, 1999; Bird et al., 2004). In some cases, the recruitment of splicing factors to the pre-mRNA is co-transcriptional but the splicing catalysis itself is executed post-transcriptionally (Denis et al., 2005; Moore et al., 2006; Girard et al., 2012). Even if the introns are spliced co-transcriptionally, they do not have to be removed in the

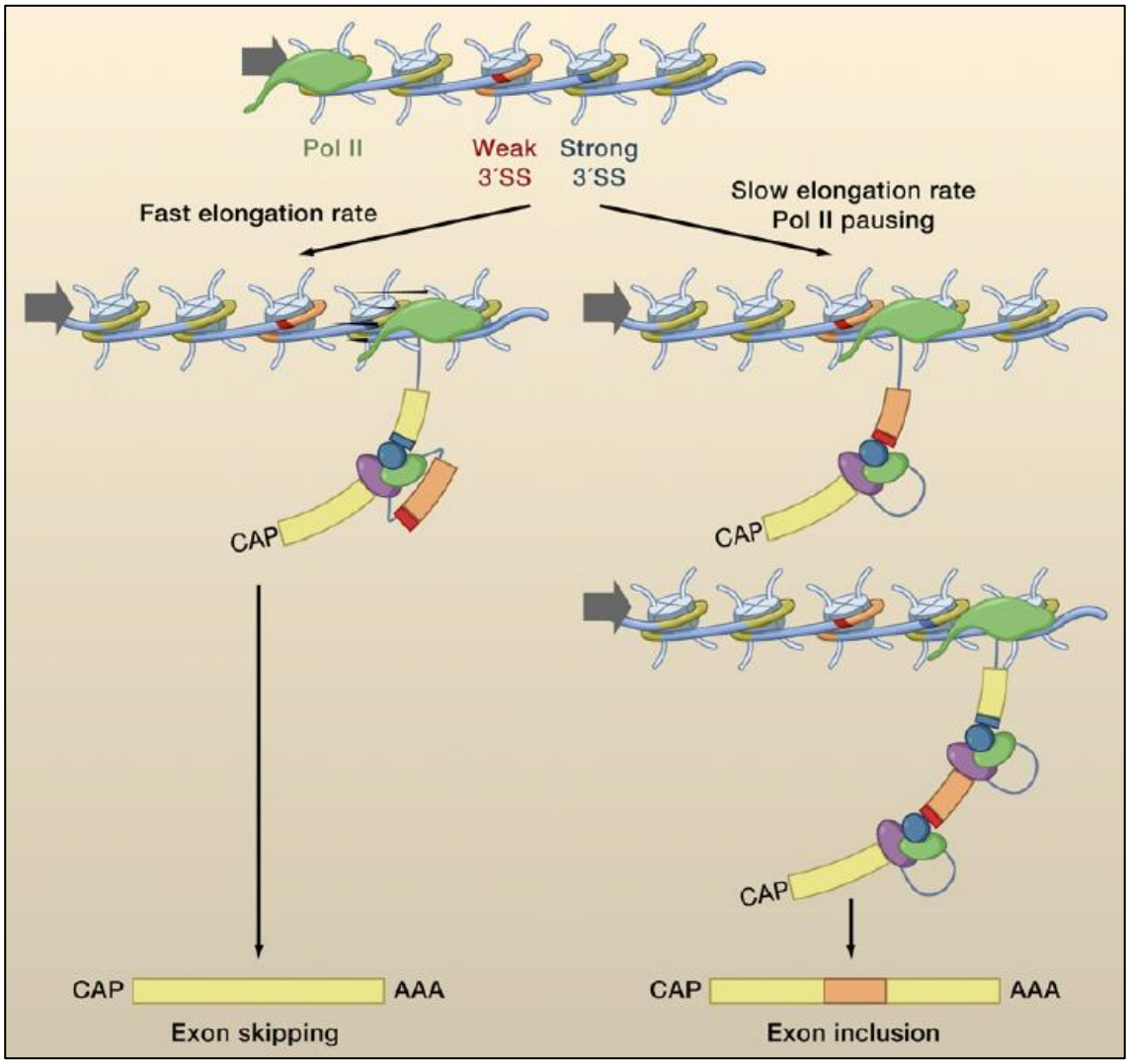

Fig. 14: Kinetic coupling model. Rapid elongation of Pol II leads to simultaneous availability of a weak and a strong splice site to the splicing machinery. Splice sites compete for the recruitment of splicing factors resulting in skipping of the weaker exon. Pausing or slowing down of the RNA Pol II favors the spliceosome assembly on the first transcribed weaker exon which is then included into mature mRNA. Adapted from (Luco et al., 2011).

exact order of transcription (Kessler et al., 1993; Attanasio et al., 2003).

The coupling of transcription and splicing means more than splicing occurring at the same time as ongoing transcription (Lazarev and Manley, 2007). Transcription and splicing are coupled functionally, meaning that these two processes intertwine and influence each other (Maniatis and Reed, 2002; Montes et al., 2012a). Alternative splicing patterns are thus influenced by transcription regulatory factors, such as promoters (Cramer et al., 1997; Cramer et al., 1999; Pagani et al., 2003; Duskova et al., 2014), transcriptional enhancers (Kadener et al., 2002), transcription factors and co-activators (Kadener et al., 2001; Nogues et al., 2002; Auboeuf et al., 2004) and chromatin remodeling events (Batsche et al., 2006; Allo et al., 2009; Luco et al., 2010).

Currently, there are two models explaining how the transcription/splicing coupling works – the kinetic model and the chromatin adaptor model.

Pol II kinetic model of alternative splicing regulation

The transcription elongation rate influences the splicing outcome (Fig. 14). When Pol II elongates slowly or pauses, there is enough time even for the weak splice sites to be recognized. This promotes cassette exons inclusion (Roberts et al., 1998; Nogues et al., 2003; Ip et al., 2011). On the other hand, if the elongation rate is high, the weak and strong splice sites emerge rapidly and side-by-side to compete for the splicing factors recruitment, resulting in the skipping of the weaker exon (Nogues et al., 2002; Schor et al., 2009). This mechanistic model was supported by studies with slow mutants of Pol II (Pol II with mutations in the

catalytic domain which slows its elongation rate both *in vitro* and *in vivo* (Chen et al., 1996; Boireau et al., 2007)). Alternative splicing changes modulated by transcription with these mutants were shown in human (Montes et al., 2012b), fruitfly (de la Mata et al., 2003) and yeast cells (Howe et al., 2003).

Chromatin adaptor model of alternative splicing

Histone modifications along the gene influence the alternative splicing outcome via recruiting adaptor proteins which in turn recruit splicing factors (Luco et al., 2010). For example, histone H3 lysine 36 trimethylation (H3K36me3) is a histone mark generally enriched at exons (Kolasinska-Zwierz et al., 2009). It has been shown to regulate alternative splicing by recruiting the polypyrimidine tract

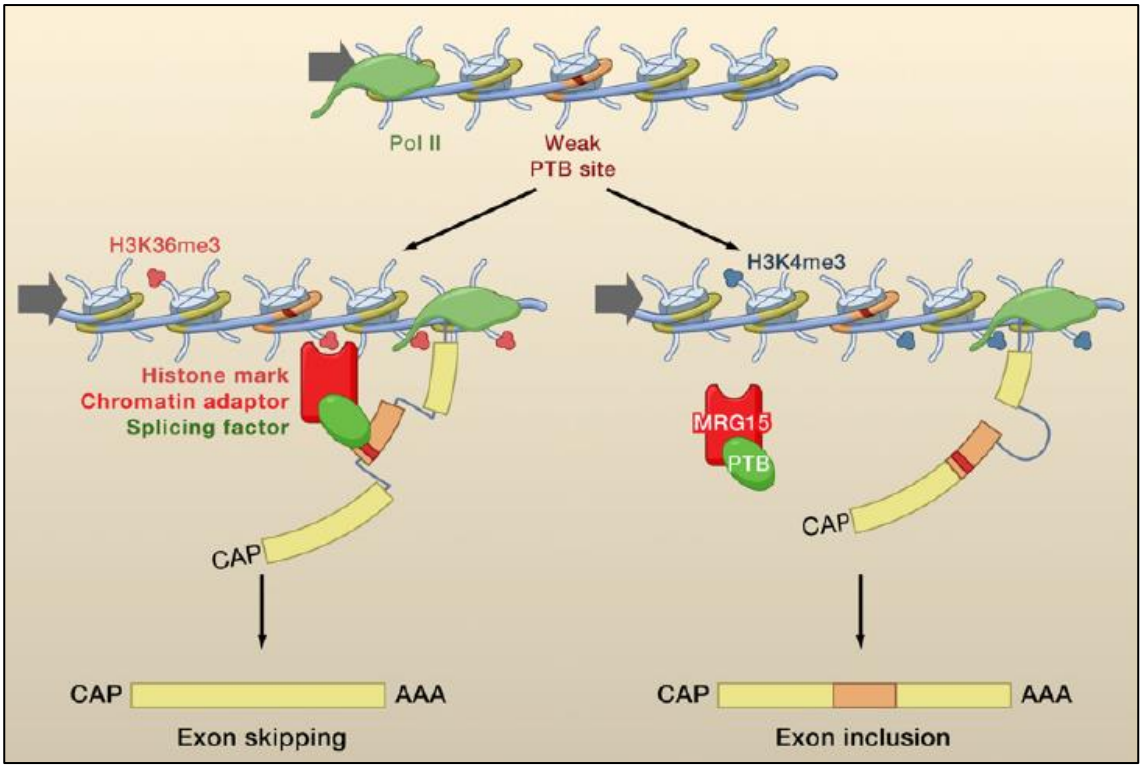

Fig. 15: Chromatin adaptor model. Chromatin-binding protein MRG15 binds to the H3K36me3 histone mark and helps to recruit splicing factor PTB to its binding site in the pre-mRNA inducing exon skipping. If the PTB binding is not promoted by chromatin adaptor, the PTB-dependent alternative exon is included. Adapted from (Luco et al., 2011).

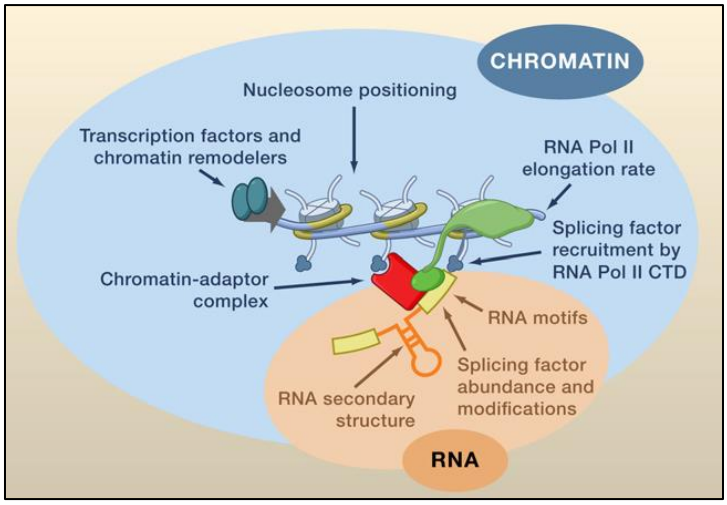

Fig. 16: Integrated model for the alternative splicing regulation. Alternative splicing outcome is determined by a combination of parameters including RNA regulatory elements and structure, state of chromatin and transcriptional kinetics. Adapted from (Luco et al., 2011).

binding protein (PTB) to some alternative exons via chromatin adaptor protein MRG15 (Fig. 15). PTB binding then promotes alternative exon skipping (Luco et al., 2010). H3K36 can also modulate alternative splicing via recruitment of the SR protein SRSF1 via chromatin adaptor Psip1/Ledgf (Pradeepa et al., 2012).

Several other histone marks are able to recruit different splicing factors via the adaptor proteins, e.g. U2 snRNP is attracted to the nascent pre-mRNA by H3acetyl mark bound by Gcn5 (Gunderson and Johnson, 2009) or H3K4me3 bound by CHD1 (Sims et al., 2007).

It seems that histone modifications act as modifiers of alternative splicing rather than its sole determinants (Luco et al., 2011). Alternative splice sites selection is influenced by chromatin on more levels of complexity. The chromatin state influences Pol II elongation kinetics and its pausing during transcription (Listerman et al., 2006). Nucleosome positioning and specific histone marks can modulate the recruitment of splicing regulators (Schwartz et al., 2009; Spies et al., 2009). Alternative splicing regulation is thus a complex process determined by a synergy of many parameters (Fig. 16).

3.3 BET proteins and alternative splicing regulation

Histone acetylation was shown to regulate alternative splicing (Hnilicova et al., 2011), however, not much is known about the role of histone acetylation reader proteins in this process. One group of such readers, proteins of the bromodomain extra-terminal (BET) family are involved in regulation of transcription and possibly splicing (LeRoy et al., 2008). They contain a highly conserved extra-terminal (ET) protein interaction domain (Rahman et al., 2011) and two conserved bromodomains (BDs) which recognize histone acetylation marks (Fig. 17, (Kanno et al., 2004)).

One of the BET family proteins, Brd2, is an essential gene and its deletion leads to severe defects in brain development in mice (Gyuris et al., 2009; Shang et al., 2009). Brd2 was linked to several human diseases, such as epilepsy, obesity and cancer (Pal et al., 2003; Belkina and Denis, 2012).

Brd2 is a part of multiple protein complexes – it associates for example with

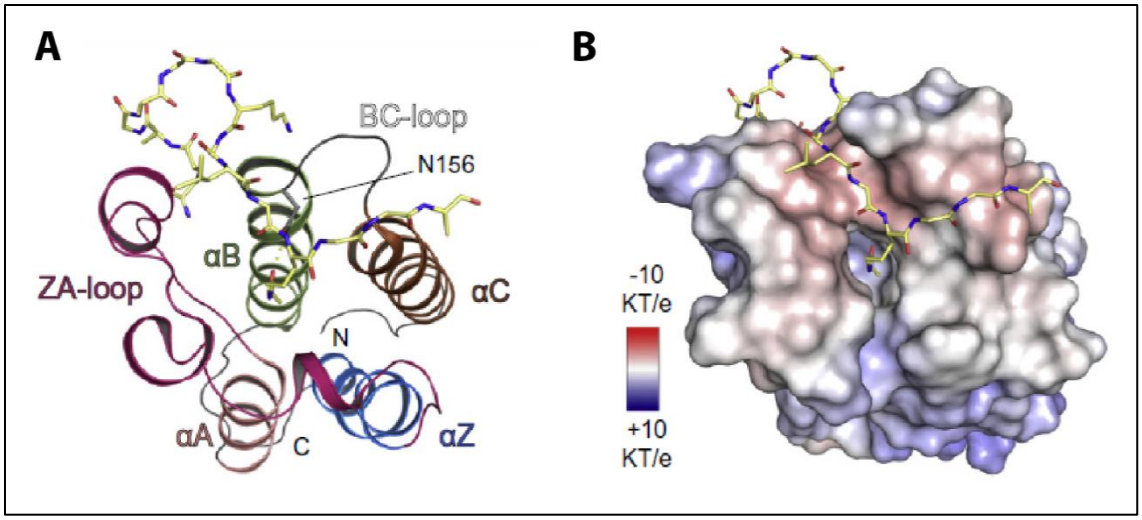

Fig. 17: Bromodomain structure. Overall structure of the Brd2 bromodomain 1 with H4K12ac bound to the central cavity (A) and its surface representation color-coded according to its electrostatic potential (indicated in the inset, B). Adapted from (Filippakopoulos and Knapp, 2012).

Pol II, histone acetylases and chromatin remodeling factors (Denis et al., 2006). It stays attached to the chromatin even during mitosis, suggesting its role in post-mitotic transcription activation (Garcia-Gutierrez et al., 2012). Brd2 associates with E2F transcription factors and participates on recruiting the TATA-box binding protein to promoters (Peng et al., 2007). It was also shown that Brd2 promotes the passage of Pol II through acetylated chromatin *in vitro* (LeRoy et al., 2008).

Based on the available data, we have chosen Brd2 as a putative alternative splicing regulator and characterized its chromatin-binding properties (see Results and Discussion, Project 3).

MATERIAL AND METHODS

1 Cell culture and treatments

All cells used in this study were maintained in DMEM supplemented with 10% fetal calf serum and penicillin/streptomycin (Invitrogen, Carlsbad, CA, USA). Unless stated otherwise, I worked with the HeLa KN cell line (Hebert et al., 2002).

For plasmid transfections, cells were grown to 60% confluence and then transfected with 1 μg of appropriate plasmid per 1 ml of DMEM using Lipofectamine LTX transfection reagent (Invitrogen, Carlsbad, CA, USA) according to manufacturer's instructions. Cells were harvested for IP or fixed for imaging after 24 hrs.

For RNA interference experiments, HeLa cells were grown to 40% confluence and transfected with appropriate siRNA using Oligofectamine transfection reagent (Invitrogen, Carlsbad, CA, USA) according to manufacturer's instructions.

2 Cloning and reagents

Plasmids

U1-70K-GFP-FL was described in (Huranova et al., 2010). Briefly, human U1-70K EST was cloned into pEGFP-N1 vector (Clontech) using BamHI and EcoRI restriction sites. U1-70K-CFP was generated by recloning U1-70K sequence from U1-70K-GFP-FL into pECFP-N1 using EcoRI/BamHI restriction sites. U1-70K GFP-

tagged mutants were generated by PCR-amplifying desired sequences from U1-70K-GFP-FL and subsequent cloning into pEGFP-N1 using EcoRI/BamHI restriction sites. Two silent point mutations G414A and G417T were introduced into siRNA binding site of U1-70K by site-directed mutagenesis to generate siRNA-resistant constructs for rescue experiments.

U1A-GFP and U1C-GFP were amplified from cDNA and inserted into pEGFP-N1 using EcoRI/BamHI and XhoI/EcoRI restriction sites, respectively. SMN-CFP-C1 was a gift from M. Dundr (Dundr et al., 2004).

RBM39-CFP described in (Ellis et al., 2008) was a gift from Javier Caceres. RBM39-GFP was generated by recloning RBM39 sequence into pEGFP-C1 (Clontech) using BglII/BamHI restriction sites. RBM39 GFP-tagged mutants were generated by PCR-amplifying desired sequences from RBM39-GFP and subsequent cloning into pEGFP-C1 using BglII/BamHI restriction sites giving rise to mutants ΔRS (aa 138-525 of RBM39), ΔUHM (aa 1-407) and ΔΔ (aa 138-407).

Brd2-wt was obtained by cloning human Brd2 cDNA into pEGFP-C1 vector using EcoRI/KpnI restriction sites. Brd2 mutant constructs were then prepared by site-directed mutagenesis of Brd2-wt. Tyrosines 113 or 386 or both were replaced by phenylalanine in Brd2-mut1, Brd2-mut2 and Brd2-mut1+2, respectively. Bromodomains (aa 1-472) were isolated by PCR from Brd2-wt and Brd2-mut1+2 and subsequently cloned to pEGFP-C1 using EcoRI/KpnI restriction sites, generating BD-wt and BD-mut1+2 constructs.

siRNAs

Cells were treated with the appropriate siRNA for 48 hrs. Knock-down efficiency was assayed by western-blotting and analyzed in ImageJ.

siRNA	Sequence	Catalogue number	Working conc.
U1-70K #1	GGUCUACAGUAAGCGGUCAtt	SilencerSelect s13211	20 nM
U1-70K #2	CGGACCUAUCAAAAGAAUAtt	SilencerSelect s13212	20 nM
FUS	AGCCCAUGAUUAAUUUGUAtt	Silencer Select s5401	50 nM
RBM39	GGACAGUCUUCUGUAUGCAtt	Silencer Select s18416	20 nM
NC	SilencerSelect Negative Control #5		20 nM

Tab. 1: List of siRNAs purchased from Ambion, Austin, TX, USA used in this study.

In addition to siRNAs listed in Tab. 1, 35 nM SMN esiRNA (EHU148811, Sigma Aldrich, St. Louis, MO, USA) was used.

Primers

For the analysis of alternative splicing of the vascular endothelial growth factor (VEGF) gene we used these custom-designed primers according to the (Wellmann et al., 2001) purchased from Sigma Aldrich:

$VEGF_{total}$ F CCCTGATGAGATCGAGTACATCTT

$VEGF_{total}$ R ACCGCCTCGGCTTGTCAC

Antibodies

Primary antibodies listed below were used for western blotting (WB) and/or immunofluorescence (IF) and/or immunoprecipitation (IP):

- anti-SMN1 (mouse monoclonal, clones 2B1 (IF, IP) and 2B11 (WB), Sigma Aldrich, St. Louis, MO, USA)
- anti-Gemin 2 (WB/IF, mouse monoclonal, clone 3F8, Santa Cruz Biotechnology, Santa Cruz, CA, USA)
- anti-Gemin 3 (WB, rabbit polyclonal, Sigma Aldrich, St. Louis, MO, USA)
- anti-Gemin 4 (WB, mouse monoclonal, clone 3E1, Sigma Aldrich, St. Louis, MO, USA)
- anti-Gemin 5 (WB, mouse monoclonal, clone 10G11, Millipore, Temecula, CA, USA)
- anti-Gemin 6 (WB, mouse polyclonal, Sigma Aldrich, St. Louis, MO, USA)
- anti-Gemin 8 (WB, rabbit polyclonal, Sigma Aldrich, St. Louis, MO, USA)
- anti-unrip (WB, rabbit polyclonal, Sigma Aldrich, St. Louis, MO, USA)
- anti-U1-70K (WB/IF, rabbit polyclonal, Sigma Aldrich, St. Louis, MO, USA; IP, goat polyclonal, Santa Cruz Biotechnology, Santa Cruz, CA, USA)
- anti-coilin (IF, mouse monoclonal, clone 5P10, was obtained from Maria Carmo-Fonseca, Instituto de Medicina Molecular, Lisbon, Portugal; and rabbit polyclonal, Sigma Aldrich, St. Louis, MO, USA)
- anti-FUS (WB, rabbit polyclonal, Sigma Aldrich, St. Louis, MO, USA)
- anti-beta actin (WB, rabbit polyclonal, abcam, Cambridge, UK)
- anti-SmB/B´ (WB, produced by the facility of IMG ASCR from hybridoma cell line obtained from Karla Neugebauer, Yale U., New Haven, CT)
- anti-FUS (WB, rabbit polyclonal, Sigma Aldrich, St. Louis, MO, USA)

- anti-RBM39 (WB, rabbit polyclonal, Sigma Aldrich, St. Louis, MO, USA)
- anti-U2AF35 (WB, rabbit polyclonal, abcam, Cambridge, UK)
- anti-GFP (WB, mouse monoclonal, clone B-2, Santa Cruz Biotechnology, Santa Cruz, CA, USA; IP, goat polyclonal obtained from David Drechsel, MPI-CBG, Dresden, Germany)

Anti-mouse and anti-rabbit secondary antibodies conjugated with DyLight488 or DyLight549 or Cy5 (Jackson ImmunoResearch Laboratories, West Grove, PA, USA) were used for immunofluorescence staining. Anti-mouse and anti-rabbit secondary antibodies conjugated with horse-radish peroxidase (Jackson ImmunoResearch Laboratories, West Grove, PA, USA) were used for western blotting.

4 Molecular Biology techniques

RNA isolation and RT-PCR

Total RNA was purified with TRIzol (Invitrogen) and reverse-transcribed using SuperScript III (Invitrogen) with random hexanucleotides (East Port Praha, Czech Republic) as primers. cDNA was amplified with specific primers using Taq polymerase (Fermentas) and the PCR products were resolved on agarose gels and quantified by densitometry in the ImageJ software.

Immunoprecipitation (IP) experiments

Cells were grown on a 15 cm Petri dish and harvested at minimal 90% confluency. Transfections were done as described above. Cells were harvested into NET2 buffer (50 mM Tris-HCl pH 7.5, 150 mM NaCl, 0.05% Nonidet P-40, all from Sigma Aldrich) supplemented with a complete mix of protease inhibitors (Calbiochem, Merck KGaA, Darmstadt, Germany) and pulse-sonicated for 90 s on ice. Cell extracts were incubated for 2 hrs with Protein-G agarose beads (GE Healthcare, Fairfield, CT, USA) covered with the appropriate antibody.

Co-immunoprecipitated proteins were extracted into the protein sample buffer (4% SDS, 20% glycerol, 10% 2-mercaptoethanol, 0.004% bromophenol blue, 0.125 M Tris HCl, pH approx. 6.8, Sigma Aldrich) by 10 min incubation at 95 °C. RNA was extracted using phenol/chloroform, resolved on a 7 M urea denaturing polyacrylamide gel and silver stained (all used chemicals from Sigma Aldrich). Proteins were resolved on SDS-PAGE gels and detected by western blotting with appropriate antibodies.

5 Fixed cells staining and image acquisition

Indirect immunofluorescence

Forty-eight hours after siRNA transfection or 24 hrs after plasmid transfection, cells planted on the surface of a coverslip were fixed in 4% paraformaldehyde in 0,1 M piperazine-N,N′-bis(2-ethanesulfonic acid), pH 6.9, for 10 min and then permeabilized for 5 min with 0.2% Triton X-100 (Sigma Aldrich). Coverslips were

blocked with 5% normal goat serum in PBS (Jackson ImmunoResearch Laboratories). Indirect immunofluorescence staining was performed for 1 hr with a primary antibody, followed by washes and 1 hr incubation with the appropriate secondary antibody.

RNA fluorescence *in situ* hybridization

The U1 snRNA was visualized by fluorescent *in situ* hybridization using Cy3-labelled oligodeoxynucelotide probe (sequence according to (Schaffert et al., 2004): CCTTCGTGATCATGGTATCTCCCCTGCCAGGTAAGTAT).

Briefly, cells grown on coverslips were fixed and permeabilized as described above and treated with 0.1M glycin in 0.2M TRIS, pH 7.4, for 10 min. They were then washed with 4x concentrated saline-sodium citrate buffer (4xSSC, 0.6M NaCl in 0.06M sodium citrate, pH 7.0) and incubated with the probe dissolved in 2x SSC with 50% formamide for 1 hr at 37°C followed by several washing steps.

Fluorescent microscopy

Images were acquired using the DeltaVision microscopic system (Applied Precision, Issaquah, WA, USA) coupled to the Olympus IX70 microscope equipped with an oil immersion objective (60x/1.4NA). Each image was reconstructed from stacks of 20 optical sections with 200-nm z step and restored using a measured point spread function (SoftWorx; Applied Precision).

High-content microscopy

Samples were scanned using automated acquisition driven by Acquisition Scan^R program using Scan^R system (Olympus, Hamburg, Germany) equipped with an oil immersion objective (60x/1.35NA). 225 images were taken per sample. Each image was reconstructed from stacks of 10 optical sections with 300-nm z step and automatically restored using a measured point spread function implemented in the Analysis Scan^R software (Olympus). Cellular compartments were automatically identified based on fluorescence intensity combined with compartment edge detection. Cell nuclei were visualized using 4',6-diamidino-2-phenylindole (DAPI) staining, gems were visualized by anti-SMN antibody. Gems were counted in each nucleus using the Analysis Scan^R software.

Structured illumination microscopy

For super-resolution microscopy, samples were stained as described above and mounted in anti-fade mounting media (5% (w/v) n-propyl gallate in 20 mM TRIS pH 8.5 in 86% glycerol optical grade). Acquisition was performed on the Delta Vision OMX (Applied Precision) super-resolution imaging system equipped with 3D structured illumination (3D-SIM) and a 60x1.42NA objective. 0.125 µm optical sections were acquired. For the image reconstruction we used the SoftWorx software implemented with the 3D SI Reconstruction function. Reconstructed images were processed and analyzed using ImageJ software.

Förster resonance energy transfer (FRET) measurements

Cells fixed as described above were embedded in glycerol containing 1,4-diaza-bicyclo[2.2.2]octane (DABCO). FRET was measured by the acceptor photobleaching method as described in (Staněk and Neugebauer, 2004) using Leica SP5 confocal microscope. Briefly, before the acceptor photobleaching, donor and acceptor fluorescence intensities were measured. Donor fluorophore (CFP) was excited by 405-nm laser and acceptor fluorophore (YFP) was excited by 514-nm laser line set to 5% of maximum power. Then, YFP was bleached in a region of interest with two intensive (50% maximum power) pulses of a 514-nm laser line, and CFP and YFP fluorescence was measured again.

FRET efficiency was calculated from CFP fluorescence intensities *I(CFP)* in bleached regions according to Eq. 1. Unbleached regions in the same cell were used as a negative control. Cells (10–20) were measured for each FRET pair and the mean and standard deviation were calculated.

$$FRET = \frac{I(CFP)_{after} - I(CFP)_{before}}{I(CFP)_{after}} \cdot 100\% \qquad \text{Eq. 1}$$

6 Live-cell microscopy

Raster image correlation spectroscopy (RICS) measurements

HeLa cells were plated on glass-bottomed Petri dishes and transfected as described above. 24 hrs post-transfection, RICS was performed as described in (Norris et al., 2011). Briefly, confocal images for the RICS experiments were acquired on Olympus Fluoview 1000 microscope equipped with a water immersion

objective (60×1.2NA). A 15 μW 470 nm diode laser in continuous wave mode was used for excitation. For every RICS experiment 100 frames consisting of 256×256 pixels were collected. The scanner step corresponding to one pixel was 50 nm and the speed along the fast scanning axis was 10 μs/pixel and along slow scanning axis 3.68 ms/line.

The correlation functions were calculated by Jana Humpolíčková (J. Heyrovsky Institute of Physical Chemistry, Prague) using a home-made script in Matlab via means of fast Fourier transform as described in (Hebert et al., 2005). Before the correlation, an average image was calculated from consecutive pairs of images and the obtained images were pixel-by-pixel subtracted from the individual two images used for the calculation of the particular average image. For data evaluation, two mathematical models were used, a model considering free diffusing proteins in the 3D (Norris et al., 2011) or a model considering binding (Digman and Gratton, 2009). In the cases where the two ways of motion occurred simultaneously, a combination of the two models was applied.

Fluorescence recovery after photobleaching (FRAP)

FRAP experiments were performed on the DeltaVision microscope system equipped with an oil immersion objective (60x1.4NA) and an environmental chamber with controlled temperature (37°C) and CO_2 level (5%). Photobleaching of a spot in the nucleoplasm was achieved by a 40 ms laser pulse at 488 nm (100 % of laser power). Fluorescence recovery in a circular spot with 2 μm radius was

monitored in a series of 65 images in 512x512 pixels format until reaching a plateau of recovery or for 5 mins.

FRAP curves were double normalized to background and whole cell fluorescence loss during acquisition. 12-15 separate FRAP measurements were performed for each experiment. Normalized FRAP curves were fitted with full model equations according to (Sprague et al., 2004) using home-made Matlab scripts as in (Huranova et al., 2010). To reduce the number of fitted parameters we used the diffusion constant determined by RICS and fitted only the parameters describing the rates of binding (k^*_{on}) and dissociation (k_{off}). Because k^*_{on} also depends on the concentration of binding sites, which could not be easily determined in live cells, only k_{off} values were used to describe the interactions.

RESULTS

This section is composed of our published and unpublished results divided into three projects:

Project 1: **"Splicing factor U1-70K interacts with the SMN complex and is required for nuclear gem integrity"** was published in the Journal of the Cell Science (IF: 5.325) and I performed all the experiments presented in this study.

> **Stejskalova, E. and Stanek, D.** (2014). Splicing factor U1-70K interacts with the SMN complex and is required for nuclear gem integrity. *J. Cell Sci.* **127**, 3909-3915.

Project 2: **"Possible role of RBM39 in the process of exon definition"** has not been published yet. I performed all the experiments presented here.

Project 3: **"The C-terminal domain of Brd2 is important for chromatin interaction and regulation of transcription and alternative splicing"** was published in the Molecular Biology of the Cell journal (IF: 4.548) and I participated in this project by preparing GFP-tagged Brd2 mutants and performing live-cell microscopy (RICS, FRAP) to characterize their interactions with chromatin *in vivo*.

> **Hnilicova, J., Hozeifi, S., Stejskalova, E., Duskova, E., Poser, I., Humpolickova, J., Hof, M. and Stanek, D.** (2013). The C-terminal domain of Brd2 is important for chromatin interaction and regulation of transcription and alternative splicing. *Mol. Biol. Cell* **24**, 3557-3568.

In addition to the projects listed above I participated in the project **"Sequestration of incomplete spliceosomal snRNPs in Cajal bodies"** which is currently under review in Cell Reports. For this paper, I analyzed snRNP dynamics in CBs using FRAP.

> **Novotny, I., Malinova, A., Stejskalova, E., Mateju, D., Klimesova, K., Roithova, A., Sveda, M., Knejzlik, Z. and Stanek, D.** (2014). Sequestration of incomplete spliceosomal snRNPs in Cajal bodies. *Cell Rep.*, under review

I also participated in writing the review **"Probing Nucleic Acid Interactions and Pre-mRNA Splicing by Förster Resonance Energy Transfer (FRET) Microscopy"** which was published in International Journal of Molecular Sciences (IF: 2.339) and for which I prepared the manuscript draft and all the Figures and participated in the final editing.

> **Simkova, E. and Stanek, D.** (2012). Probing Nucleic Acid Interactions and Pre-mRNA Splicing by Forster Resonance Energy Transfer (FRET) Microscopy. *Int. J. Mol. Sci.* **13**, 14929-14945.

Finally, I collaborated on the article **"Dynamics of Mitochondrial RNA-Binding Protein Complex in *Trypanosoma brucei* and Its Petite Mutant under Optimized Immobilization Conditions."** which was published in Eukaryotic Cell (IF: 3.179) and in which I participated in the FRAP measurements, their analysis and interpretation.

Huang, Z., Kaltenbrunner, S., Simkova, E., Stanek, D., Lukes, J., Hashimi, H. (2014). Dynamics of Mitochondrial RNA-Binding Protein Complex in *Trypanosoma brucei* and Its Petite Mutant under Optimized Immobilization Conditions. *Eukaryot. Cell* **13**, 1232-1240.

1 Splicing factor U1-70K interacts with the SMN complex and is required for nuclear gem integrity

SMN protein was recently detected in early spliceosome complexes (Makarov et al., 2012) and it was suggested that it is possibly involved in *in vitro* pre-mRNA splicing or recycling of post-spliceosomal complexes (Meister et al., 2000). We wanted to characterize interactions of SMN within the spliceosomal E-complex and decided to analyze association of SMN with the U1 snRNP.

The U1 snRNP protein U1-70K interacts with the SMN complex

We expressed U1 snRNP proteins U1-70K, U1A and U1C tagged with GFP and immunoprecipitated them using anti-GFP antibodies. SMN complex proteins co-precipitated specifically with the U1-70K-GFP (Fig. 18A). Next we found that endogenous U1-70K as well as ectopically expressed U1-70K-GFP co-precipitated with all major components of the SMN complex (Fig. 18B,C), except for unrip which is known to reside mainly in the cytoplasm (Grimmler et al., 2005). The interaction between U1-70K and the SMN complex was RNA independent (Fig. 18D), suggesting that U1-70K associated with the SMN complex via protein-protein interactions independently of the U1 snRNA.

It was recently shown that the protein Fused in sarcoma (FUS) interacted with both the SMN protein and the U1 snRNP. FUS was proposed to bridge the SMN complex with the U1 snRNP but the binding between the SMN complex and the U1 snRNP has not been directly tested (Yamazaki et al., 2012). Here we showed that

FUS depletion by RNAi did not interfere with the association between U1-70K and the SMN complex (Fig. 19).

U1-70K localizes in nuclear gems

It is known that the nuclear population of the SMN complex resides in the nuclear gems which sometimes co-localize with CBs. We wanted to determine whether U1-70K protein is also present in these structures. We expressed U1-70K

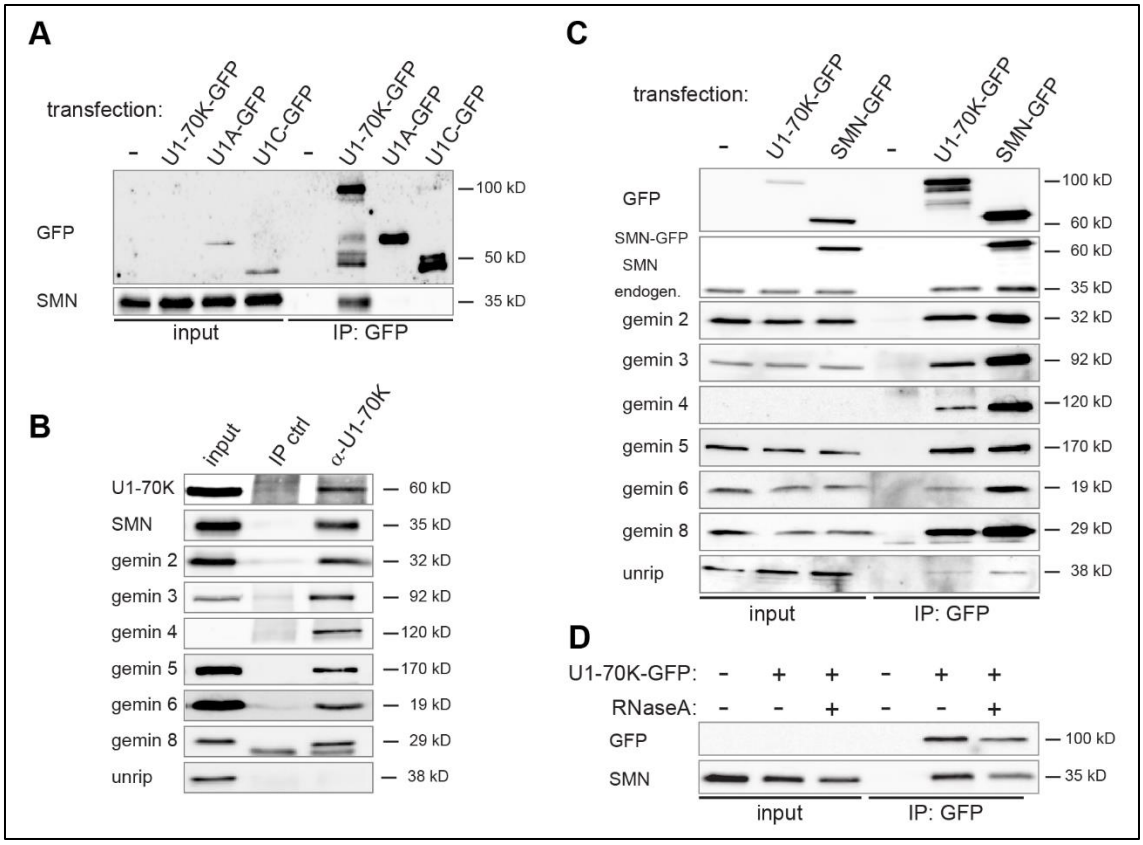

Fig. 18: U1-70K interacts with the SMN complex. (A) GFP-tagged U1 snRNP proteins were transiently expressed in HeLa cells, immunoprecipitated by anti-GFP antibodies and co-precipitated proteins assayed by western blotting. Non-transfected cells were used as a negative control. (B) Endogenous U1-70K was immunoprecipitated from cell lysates and co-precipitated proteins assayed by western blotting. Immunoprecipitation with unrelated antibody (goat anti-GFP) was used as a negative control. (C) GFP tag on U1-70K or SMN does not change their ability to incorporate into the SMN complex. GFP-tagged SMN or U1-70K proteins were transiently expressed in HeLa cells, immunoprecipitated by anti-GFP antibodies and co-precipitated proteins assayed by western blotting. Non-transfected cells were used as a negative control. (D) U1-70K interaction with the SMN protein is RNA independent. GFP-tagged U1-70K was immunoprecipitated by anti-GFP antibodies from RNase A treated cell lysate and co-precipitated proteins were assayed by western blotting.

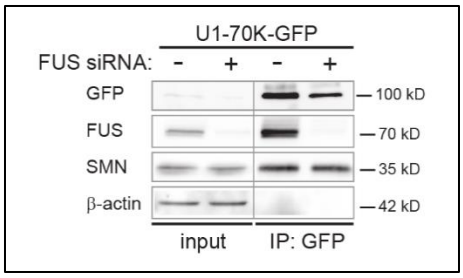

Fig. 19: U1-70K interaction with the SMN complex is not mediated by FUS. FUS or negative control siRNA treated HeLa cells were transiently transfected with U1-70K-GFP, immunoprecipitated by anti-GFP antibodies and co-precipitating proteins assayed by western blotting.

tagged with GFP in three different cell lines and analyzed its localization with respect to gems and CBs (Fig. 20). In addition, we used Kyoto HeLa cells stably expressing U1-70K-GFP from bacterial artificial chromosome, which preserves the endogenous U1-70K promoter and the exon-intron structure.

In all cell lines, the U1-70K protein localized into the nucleus and accumulated in sharp well-defined foci, which in most cases did not co-localize with the CB marker coilin, consistently with previous findings that U1 snRNP does not accumulate in CBs (Carmo-Fonseca et al., 1991; Matera and Ward, 1993). However, the U1-70K-GFP foci always co-localized with nuclear SMN.

To avoid possible artifacts of ectopic expression of U1-70K-GFP, we performed a super-resolution microscopy on the immunofluorescently labelled endogenous U1-70K which also showed accumulation in the nuclear gems (Fig. 21). In addition, U1 snRNA was also present in gems. We then tested the gem localization of U1A and U1C tagged with fluorescent proteins. Both proteins showed speckled localization pattern typical for splicing factors and although they were not excluded from gems, neither specifically accumulated there (Fig. 22). To our knowledge, U1-70K is the first example of a snRNP protein accumulating in gems.

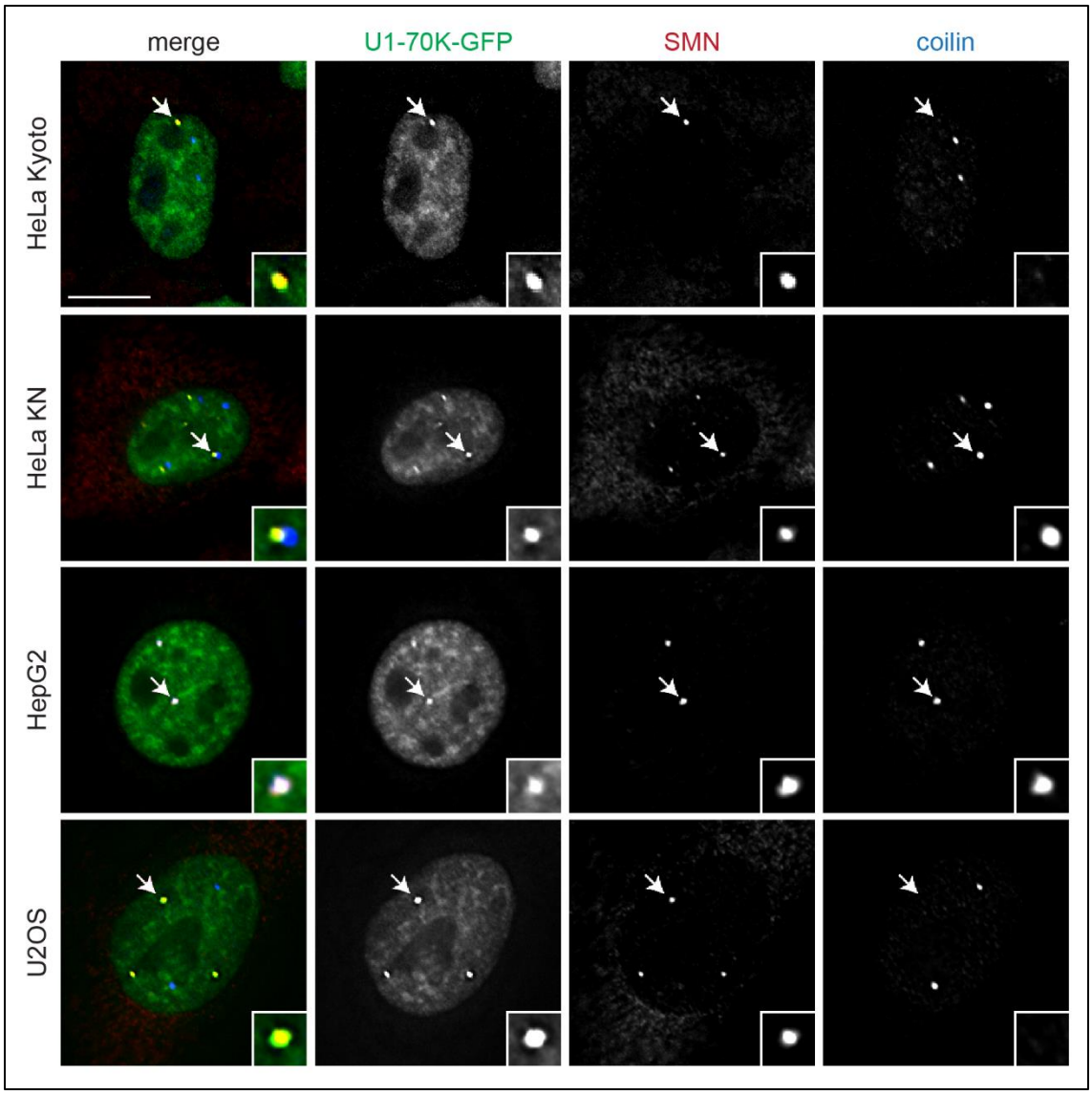

Fig. 20: U1-70K-GFP localizes to nuclear gems. Cells expressing GFP-tagged U1-70K (green) were stained with the anti-SMN antibody (red) marking nuclear gems and anti-coilin antibodies (blue) marking Cajal bodies. Details of selected gems (marked by arrows) are shown in insets. Scale bar: 10 μm, insets magnified 3x.

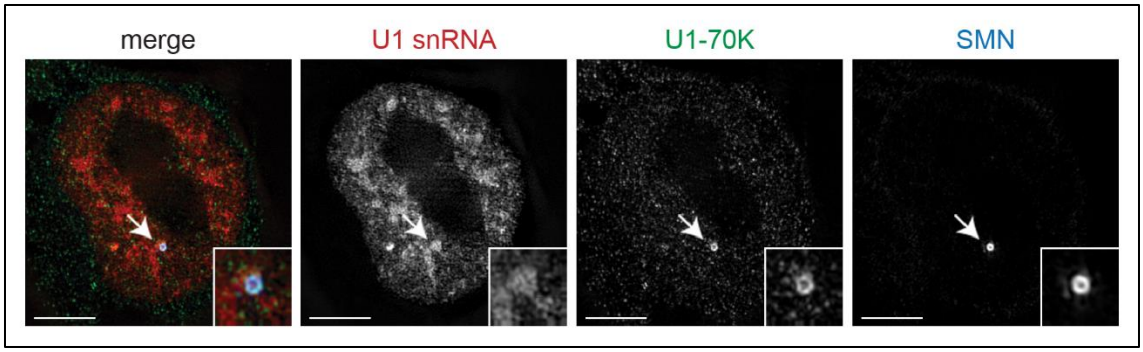

Fig. 21: Super-resolution image of nuclear gems containing SMN protein (blue), U1 snRNA (red) and U1-70K protein (green). Gem marked by arrow was magnified 2.5x in insets. Scale bar 5 μm.

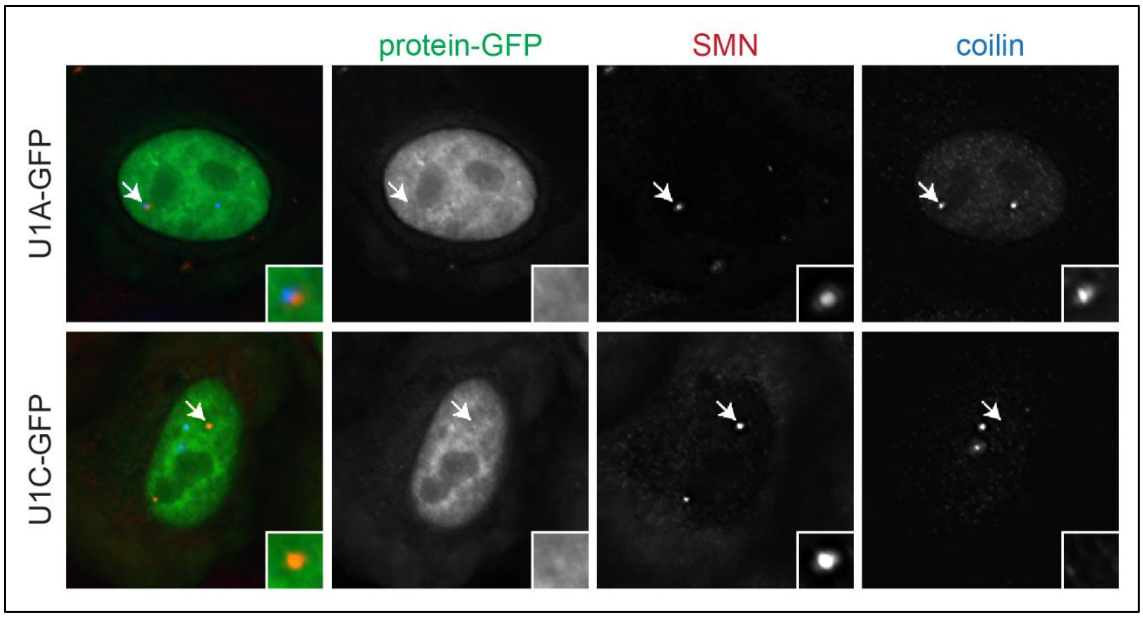

Fig. 22: U1A and U1C do not accumulate in gems. Cells expressing GFP-tagged U1A or U1C (green) were stained with the anti-SMN antibody (red) marking nuclear gems and anti-coilin antibodies (blue) marking Cajal bodies. Details of selected gems (marked by arrows) are shown in insets. Scale bar: 10 μm, insets magnified 3x.

U1-70K interacts with the SMN complex in gems

To probe whether U1-70K residing in gems interacts with the SMN complex, we employed Förster resonance energy transfer (FRET), which has been previously utilized to detect snRNP interaction partners in Cajal bodies (Staněk and Neugebauer, 2004; Huranova et al., 2009). We expressed YFP-tagged SMN protein together with CFP-tagged U1-70K and measured for increases of CFP fluorescence after YFP bleaching (Fig. 23A). FRET efficiency between U1-70K and SMN in gems was comparable to FRET detected between SMN-SMN (Dundr et al., 2004), which was used as a positive control, whereas FRET between SMN and non-interacting U1C was on the background level (Fig. 23B). These data show that U1-70K associates with the SMN complex in nuclear gems.

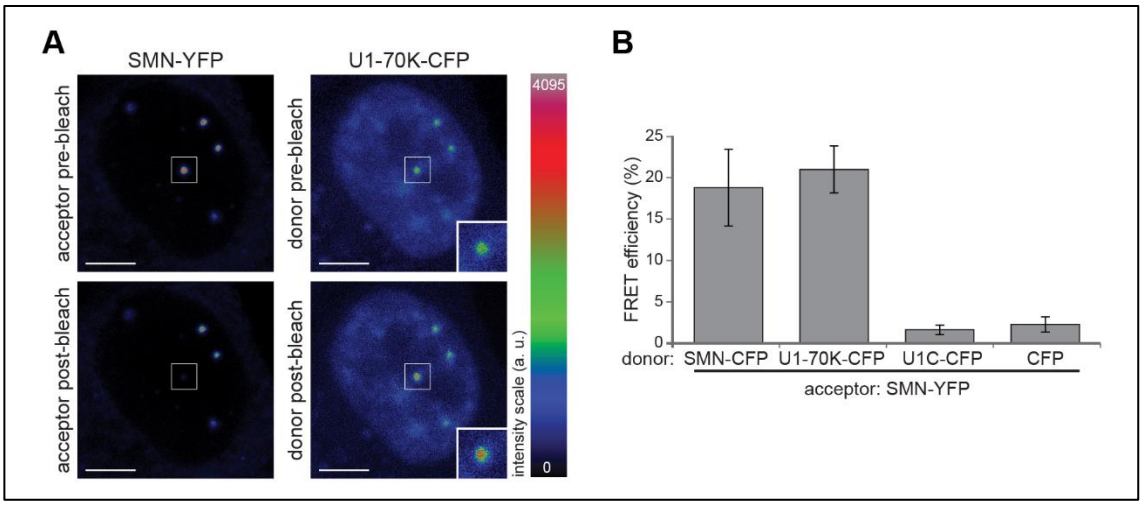

Fig. 23: U1-70K interacts with the SMN complex in gems. (A) Cells were transiently co-transfected with U1-70K-CFP and SMN-YFP. YFP was bleached specifically in gems and CFP fluorescence measured before and after bleaching. Scale bar 5 µm, insets magnified 2x. (B) FRET efficiency was measured in three independent biological replicas each containing at least 10 cells and the average is shown together with standard error of the mean. Self-interaction between SMN was used as a positive control and CFP with SMN-YFP served as a negative control.

Interaction between U1-70K and the SMN complex is mediated by the unstructured N-terminal part of U1-70K

Next we addressed which part of U1-70K interacts with the SMN complex. We found that the SMN complex interaction domain lies in the N-terminal half (aa 1-200) of U1-70K (Fig. 24 and data not shown). Aa 1-200 of U1-70K comprise an RNA recognition motif (RRM), which together with the alpha-helical region binds U1 snRNA stem-loop 1 (Fig. 24A) (Stark et al., 2001; Pomeranz Krummel et al., 2009). The very N-terminus (aa 1 to 60) forms a long unstructured tail and interacts with the Sm ring proteins (Pomeranz Krummel et al., 2009). To further narrow the SMN-interacting domain, we tagged four different parts of the N-terminal half with GFP (Fig. 24B), expressed them in HeLa cells and immunoprecipitated them using anti-GFP antibodies. The co-precipitated SMN protein as a marker of the SMN complex was detected by western blotting (Fig. 24C).

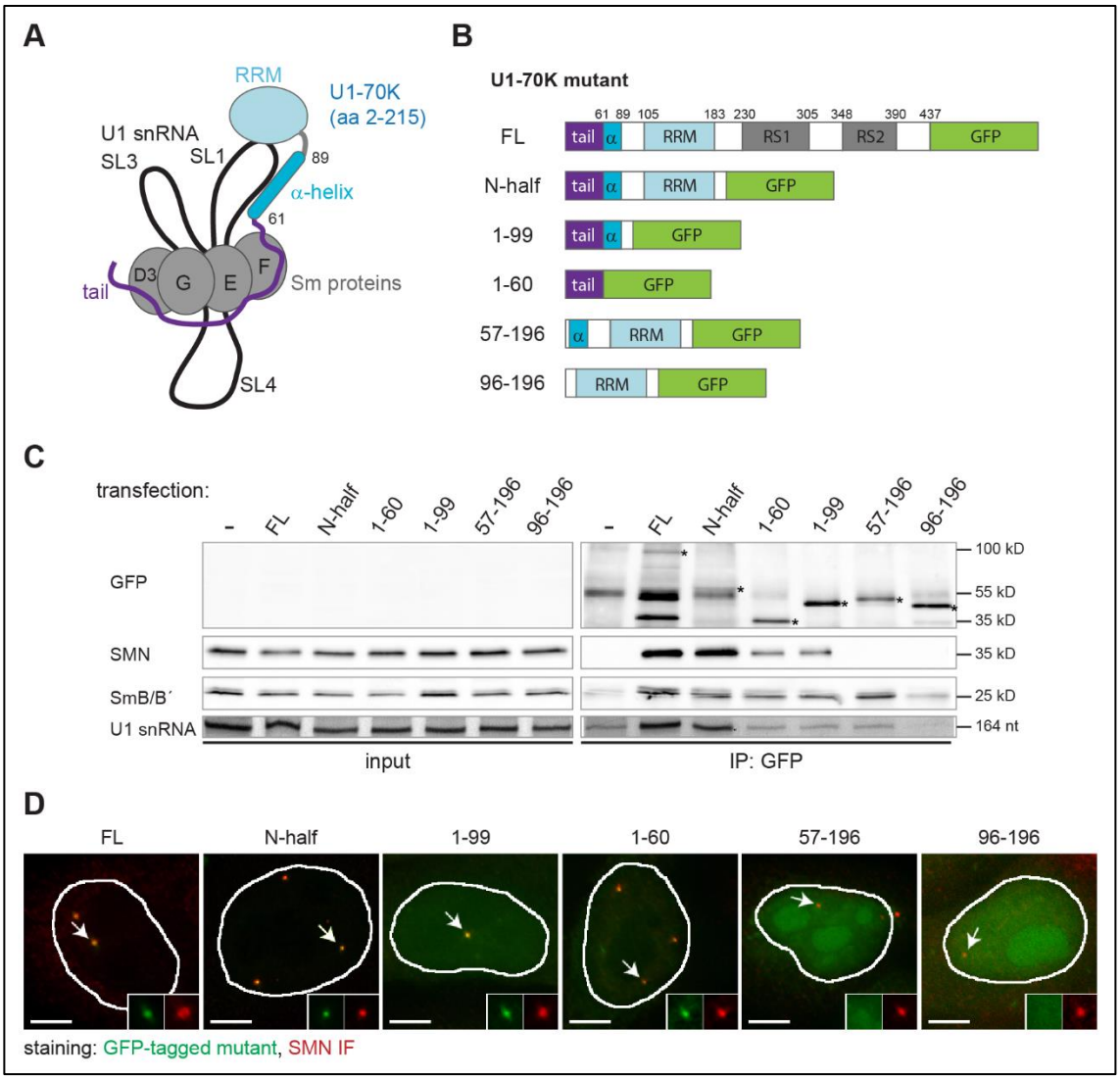

Fig. 24: The N-terminal tail of U1-70K interacts with SMN. (A) A schematic representation of the U1-70K N-terminal half within the U1 snRNP, based on (Pomeranz Krummel et al., 2009). (B) A schematic representation of U1-70K deletion constructs used in this study. (C) Transiently transfected GFP-tagged U1-70K mutants were immunoprecipitated using anti-GFP antibodies and co-precipitated proteins and the U1 snRNA were visualized by western blotting and silver staining, respectively. Non-transfected HeLa cells served as a negative control. Protein bands with correct size are marked by asterisks. The band around 55 kD corresponds to antibody heavy chains. (D) HeLa cells expressing GFP-tagged U1-70K mutants (green) stained with the anti-SMN antibody (red) marking nuclear gems. Details of selected gems (marked by arrows) are shown in insets. Scale bar: 5 µm, insets magnified 2.5x. Nuclear outlines are shown in white.

The minimal domain of U1-70K that interacts with the SMN complex consisted of the first 60 aa and correlated with the gem-targeting domain (Fig. 24D). In contrast, the mutant lacking the first 60 aa and containing the alpha-helix and RRM was not able to co-precipitate the SMN complex and did not accumulate in gems.

However, the alpha-helix and RRM domain still interacted with the U1 snRNP, as indicated by co-precipitation of the Sm proteins and the U1 snRNA (Fig. 24C, bottom lines). These results suggest that U1-70K incorporation into the U1 snRNP is not necessary for its interaction with the SMN complex.

U1-70K is important for gem integrity

Our data showed U1-70K association with the SMN complex and co-localization and FRET between U1-70K and SMN in gems. To test whether U1-70K is important for gems integrity, we depleted U1-70K from HeLa cells by RNA

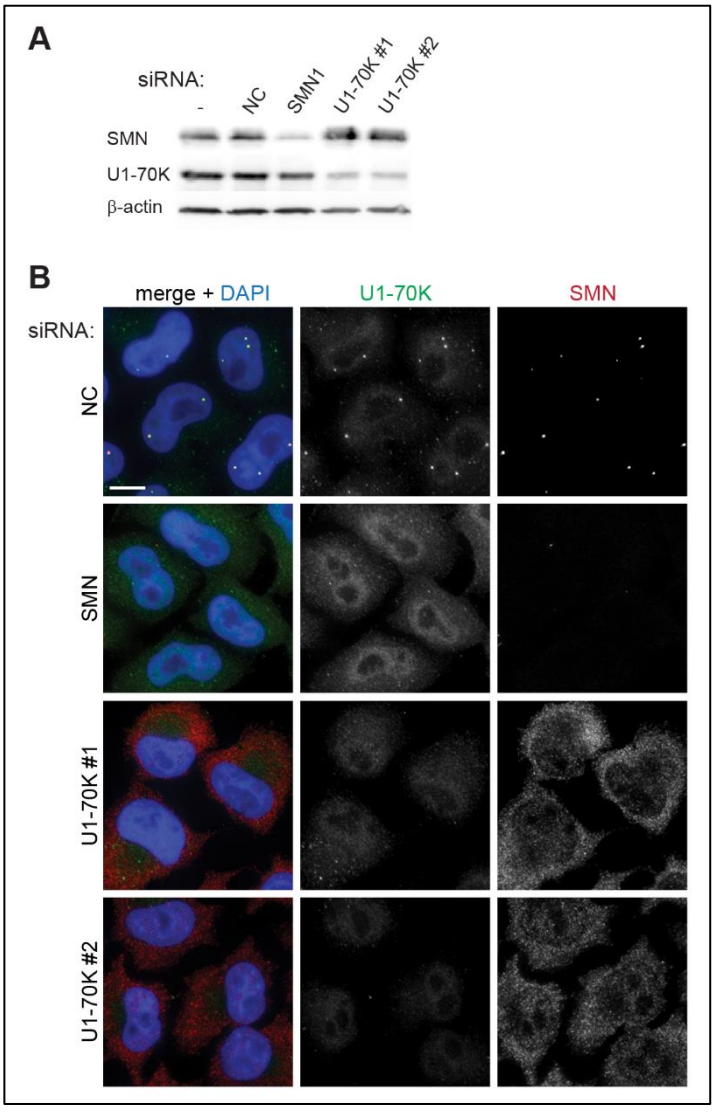

Fig. 25: U1-70K knockdown causes loss of nuclear gems. (A) Knockdown efficiency of SMN or U1-70K assayed by western blotting. (B) U1-70K depletion caused loss of nuclear gems (marked by SMN staining, red). Two different siRNAs against U1-70K showed the same phenotype, SMN knockdown served as a positive control. Scale bar 10 µm.

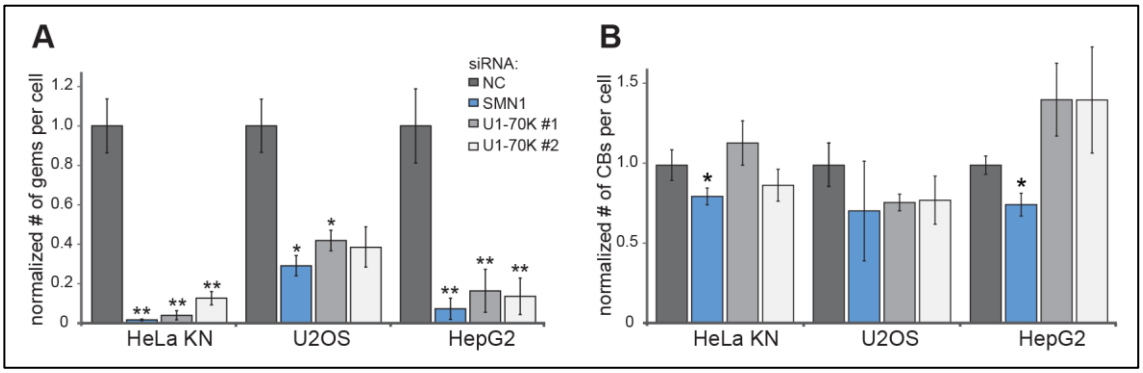

Fig. 26: Quantification of the U1-70K knockdown phenotype by high-content microscopy using three different cell lines. Anti-SMN antibody was used to mark gems (A) and anti-coilin antibody was used to mark CBs (B). The average of three experiments (each containing hundreds of cells) is shown together with the standard error of the mean. The significance was assayed by T-test, *p≤0.05, **p≤0.01 against negative control siRNA treated cells.

interference (Fig. 25A). Indeed, nuclear gems disappeared after U1-70K knockdown and SMN localized diffusely in the cytoplasm and the nucleus (Fig. 25B). We tested two different siRNAs against U1-70K in three different cell lines and in all cases gems decreased after the siRNA treatment. To quantify the phenotype we employed high-content microscopy, which revealed that U1-70K depletion reduced the average number of gems per cell in HeLa KN, U2OS and HepG2 cells, while CB number was not significantly affected (Fig. 26). The expression of the SMN protein was not reduced (Fig. 25A), indicating that the gem loss was not due to SMN protein downregulation.

To test whether U1-70K is important for integrity of the SMN complex, we knocked down U1-70K and assayed for Gemins co-precipitating with SMN (Fig. 27). All the tested components of SMN complex co-purified with the SMN protein to a similar extent as in negative control siRNA treated cells, which suggests that gem loss is not due to the disintegration of the SMN complex.

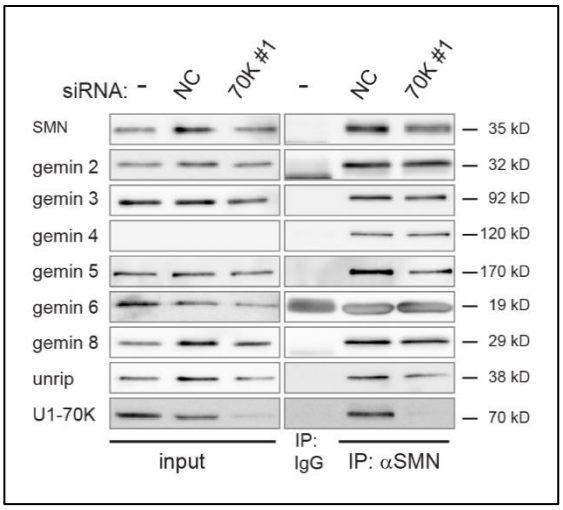

Fig. 27: SMN complex integrity after U1-70K depletion. Endogenous SMN protein was immunoprecipitated from HeLa cells treated with anti-U1-70K siRNA and co-precipitated proteins assayed by western blotting.

The loss of gems is rescued by expression of U1-70K N-terminal tail or SMN

To confirm the role of U1-70K in gem formation, we expressed siRNA resistant U1-70K mutants and analyzed gem formation after U1-70K downregulation (Fig. 28). The expression of the full-length protein, its N-terminal half or the first 1-60 aa, all of which interact with SMN complex (see above Fig. 24), rescued average number of gems to almost 70% of original value in HeLa cells. Contrary, the mutant 57-196, which did not bind SMN complex, was unable to rescue the phenotype above the empty GFP control. These results suggest that the N-terminal fragment of the U1-70K protein, which interacts with the SMN complex, is important for the nuclear gem integrity.

To analyze the relationship between U1-70K and SMN protein in the process of gems formation, we decided to test whether loss of gems after U1-70K depletion can be rescued via the overexpression of the SMN protein. The ectopic overexpression of SMN-GFP rescued the formation of gems very efficiently (Fig. 29). This result suggests that U1-70K induces gems indirectly, e. g. by increasing a local concentration of SMN or by enhancing SMN oligomerization properties.

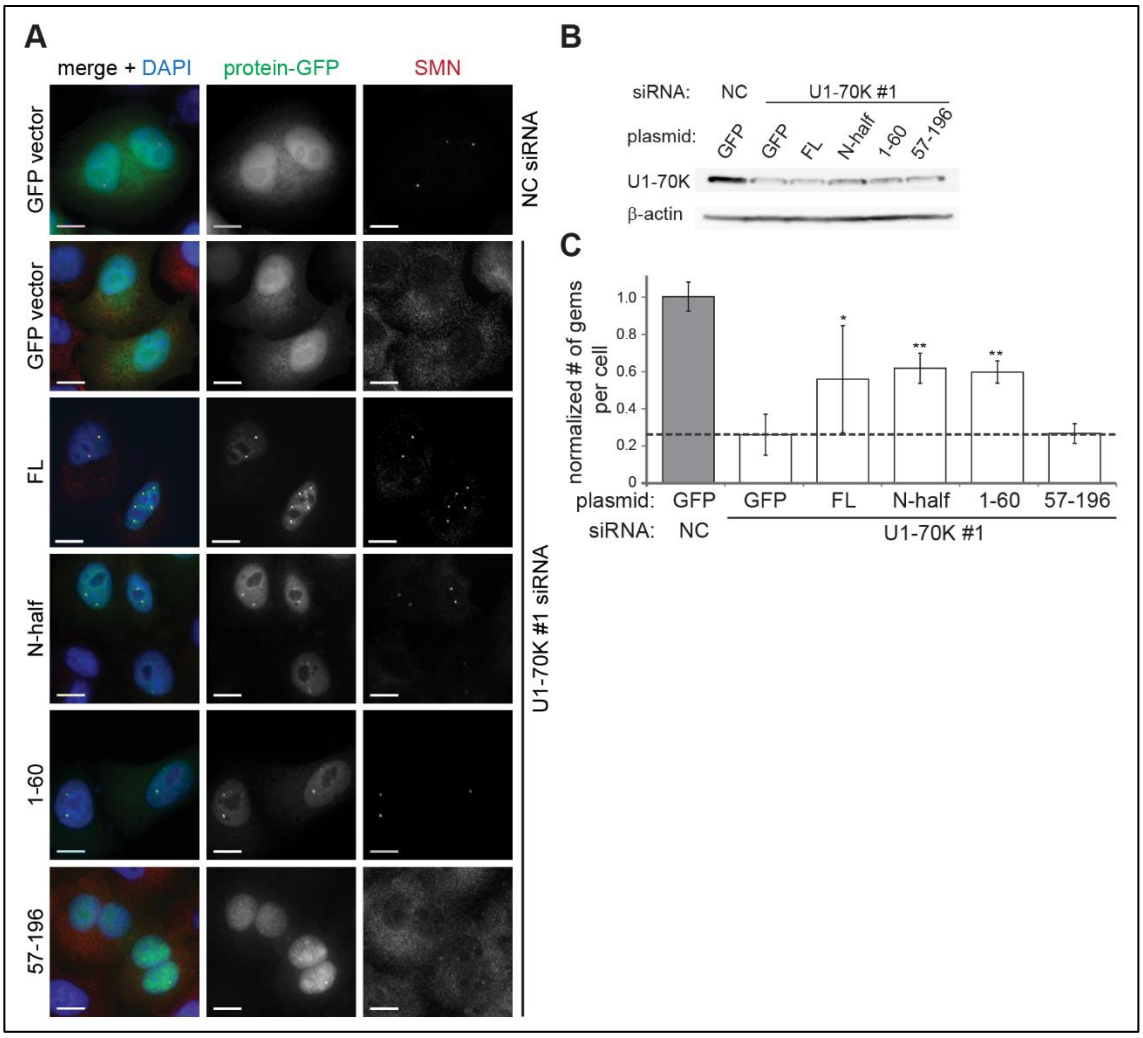

Fig. 28: Nuclear gems are rescued by ectopic expression of the U1-70K N-terminal tail.
(A) U1-70K or negative control siRNA treated cells were transiently transfected with GFP-tagged U1-70K mutant constructs (green) and stained with the anti-SMN antibody (red) to mark gems. Scale bar 10 μm. All U1-70K-GFP constructs were resistant to siRNA used. (B) Knockdown efficiency of U1-70K assayed by western blotting. Transient transfection with plasmids does not change the knockdown efficiency. (C) Gems were quantified by high-content microscopy. Only cells expressing similar levels of fluorescent proteins were taken into analysis. The average of three experiments (each containing at least 100 cells) is shown together with the standard error of the mean. The significance was assayed by T-test, *p≤0.05, **p≤0.01 against the empty GFP vector.

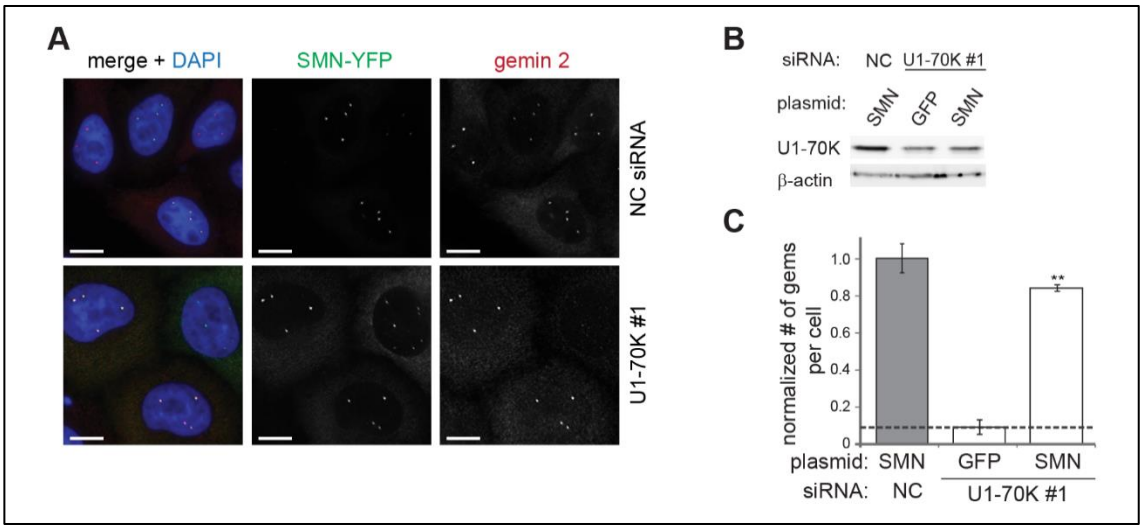

Fig. 29: Nuclear gems are rescued by ectopic expression of the SMN protein.
(A) U1-70K or negative control siRNA treated cells were transiently transfected with YFP-tagged SMN (green) and stained with the anti-Gemin2 antibody (red) to mark gems. Scale bar 10 µm. (B) Knockdown efficiency of U1-70K assayed by western blotting. Transient transfection with plasmids does not change the knockdown efficiency. (C) Gems were quantified by high-content microscopy. Only cells expressing similar levels of fluorescent proteins were taken into analysis. The average of three experiments (each containing at least 100 cells) is shown together with the standard error of the mean. The significance was assayed by T-test, *p≤0.05, **p≤0.01 against the empty GFP vector.

2 Possible role of RBM39 in the process of exon definition

RBM39 regulates alternative splicing of VEGF

It was shown that RBM39 regulates alternative splicing of vascular endothelial growth factor (VEGF) gene in cancer cells (Dowhan et al., 2005; Huang et al., 2012). We confirmed this in two different cancer cell lines – HeLa and U2OS cells. We depleted RBM39 by RNAi and tested VEGF alternative splicing pattern by RT-PCR. Two isoforms of VEGF, $VEGF_{165}$ and $VEGF_{121}$ (Fig. 30A), were expressed in both cell lines and the expression of the 165 isoform was predominant (Fig 30B). After the RBM39 depletion the isoforms ratio shifted more towards the 121 isoform (Fig. 30B,C).

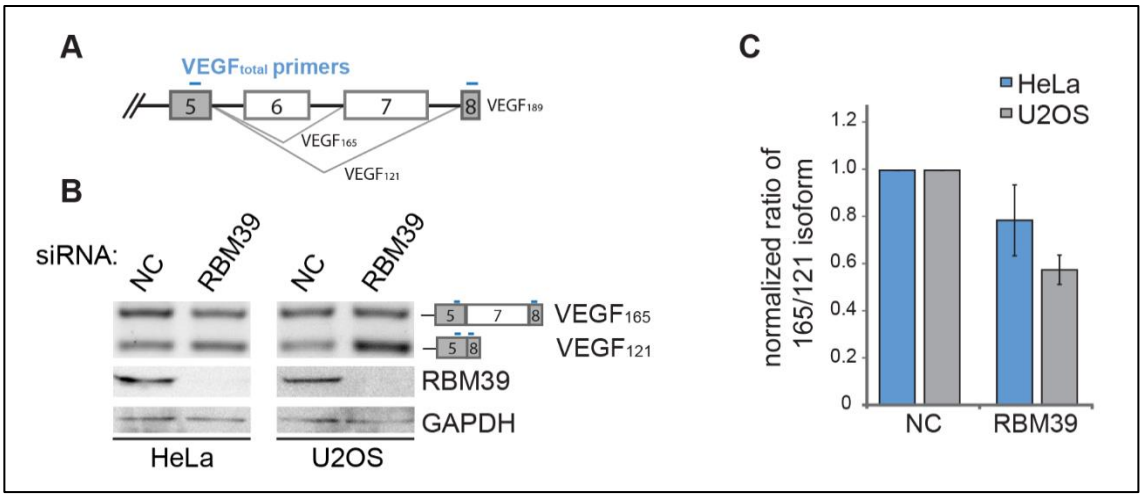

Fig. 30: RBM39 regulates alternative splicing of VEGF. (A) Schematic representation of the VEGF gene and its alternative splicing isoforms (Dowhan et al., 2005) showing the position of primers used for isoform detection by RT-PCR. (B) The ratio of expression of VEGF isoforms 165/121 detected by RT-PCR (top lines) changes upon RBM39 depletion (knock down efficiency shown by western blotting in the bottom lines). (C) Densitometric quantification of RT-PCR results (average of three independent biological replicas is shown together with the standard error of the mean).

RBM39 is a part of the spliceosomal E-complex

To gain more insight into the possible mechanism of this regulation, we decided to pull-down RBM39 by immunoprecipitation and assay for spliceosomal components. For the lack of a suitable antibody to immunoprecipitate endogenous RBM39, we expressed GFP-tagged RBM39 in HeLa cells and performed IP with a very efficient anti-GFP antibody. We detected small amounts of U1 and U2 snRNPs in the co-precipitate (Fig. 31A), suggesting that RBM39 associates with the snRNAs only transiently and likely in the spliceosomal E or A complex. To confirm this, we expressed GFP-tagged spliceosomal components and assayed for endogenous RBM39 in their co-immunoprecipitates. We selected U1-70K-GFP as a marker of U1 snRNP, U2AF35-GFP represents the E-complex and U2A' represents the A-complex. Endogenous RBM39 was pulled down by both U1-70K and U2AF35 but not by U2A' (Fig. 31B) which suggests that RBM39 interacts primarily with the E-complex.

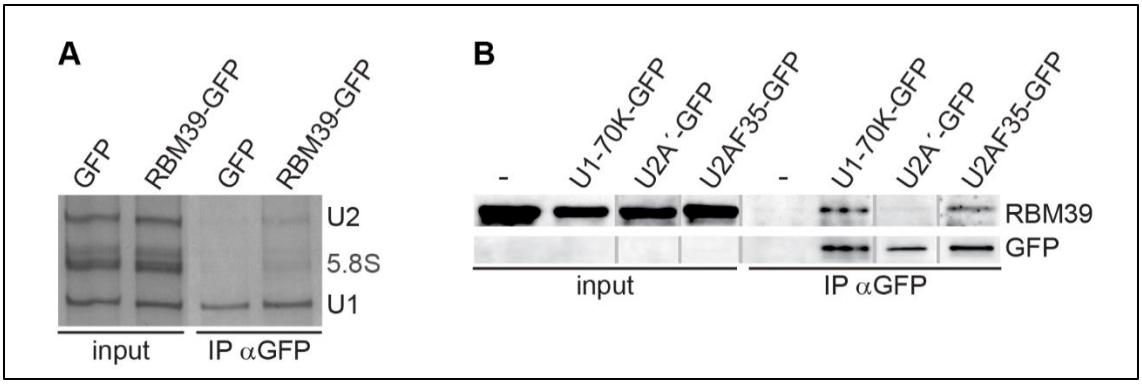

Fig. 31: RBM39 is a part of the spliceosomal E-complex. (A) RBM39-GFP was expressed in cells, immunoprecipitated with anti-GFP antibody and the pulled-down RNAs analyzed by gel electrophoresis followed by silver-staining. (B) GFP-tagged spliceosomal proteins were expressed in cells, immunoprecipitated with anti-GFP antibody and the pull-downs analyzed by gel electrophoresis followed by western blotting.

RBM39 associates with U1 snRNP via interaction with U1-70K

We decided to probe interactions between the U1 snRNP and RBM39 directly *in situ* in fixed cells by FRET microscopy (Fig. 32). For this, we utilized CFP-tagged RBM39 as a FRET donor and an array of YFP-tagged U1 snRNP proteins as FRET acceptors. We used U2AF35-YFP as a positive control for FRET, according to the (Ellis et al., 2008). We detected a positive FRET between RBM39-CFP and U1-70K tagged with YFP at its C-terminus (U1-70K-C, Fig. 32A). When we switched to the N-terminally tagged U1-70K (U1-70K-N), the FRET efficiency decreased almost to a half (Fig. 32B). FRET efficiency depends not only on the distance of the two fluorophores but also on their orientation (Simkova and Stanek, 2012). When we used U1-70K tagged on the other end, we changed either the distance or mutual

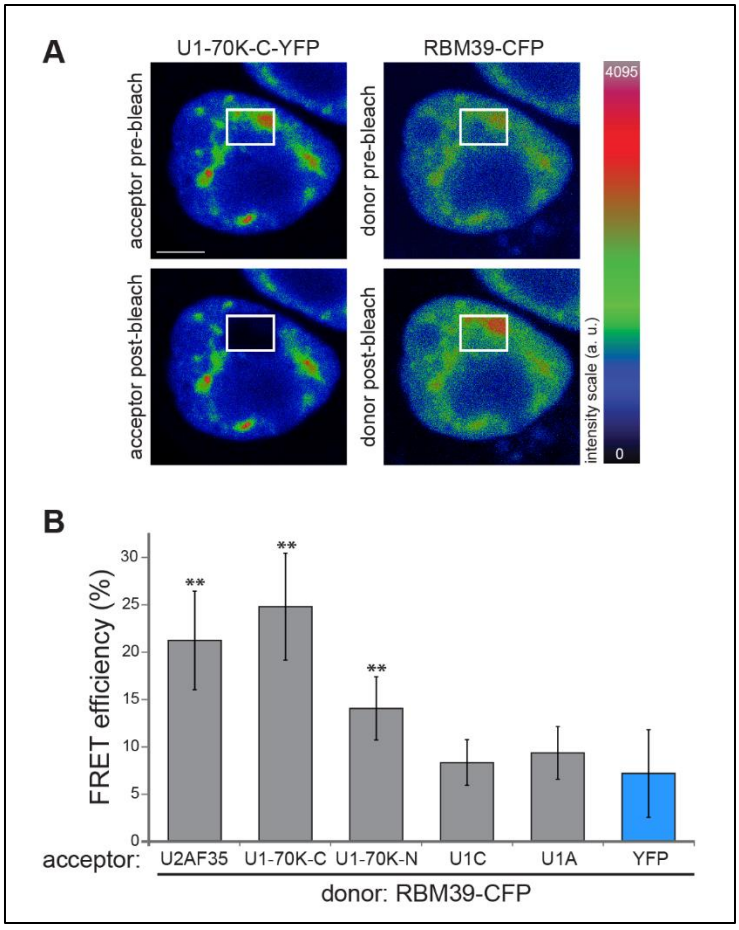

Fig. 32: RBM39 interactions monitored by FRET. (A) Cells were transiently co-transfected with RBM39-CFP and C-terminally YFP-tagged U1-70K. YFP was bleached in a small region comprising nucleoplasm as well as a part of a nuclear speckle and CFP fluorescence was measured before and after bleaching. Scale bar 5 μm. (B) FRET efficiency was measured in three independent biological replicas containing at least 10 cells each and the average is shown together with standard error of the mean. Interaction between RBM39-CFP and U2AF-35-YFP was used as a positive control and YFP with RBM39-CFP served as a negative control.

orientation of the donor and acceptor fluorophores and the FRET efficiency decreased, which would not happen in case of unspecific FRET detection. This result suggests that we are indeed detecting a specific interaction between RBM39 and U1-70K. FRET efficiency measured for RBM39 and U1A or U1C was comparable to the empty YFP negative control level. Taken together, we showed that RBM39 is a part of the spliceosomal E-complex where it interacts with both the U2AF35 and U1-70K, which suggests a potential role in bridging the two splice sites together.

RBM39 RS-domain is responsible for its interactions with the E-complex

Next we addressed which part of RBM39 is important for its interactions with the E-complex. RBM39 consists of a serine/arginine rich domain (RS) in the N-terminal part of the protein, two RNA-recognition motifs (RRMs) in the middle region and a U2AF homology motif (UHM) at the C-terminus (Fig. 33A, (Kielkopf et al., 2004)). It was shown that UHM domains involved in interactions between the splicing proteins SPF45, U2AF65, SF1 and SF3b155 play a role in the alternative splicing regulation (Corsini et al., 2007). It is known that RS domains also serve as mediators of protein-protein interactions (Graveley, 2000). Therefore we decided to prepare GFP-tagged UHM- and RS-deletion mutants of RBM39 (Fig. 33A) and assay for their interactions by IPs.

First, we determined the cellular localization of the mutants (Fig. 33B). Mutants lacking the RS domain show a diffused nucleo-cytoplasmic localization pattern, showing that this domain is essential for RBM39 targeting into the nucleus

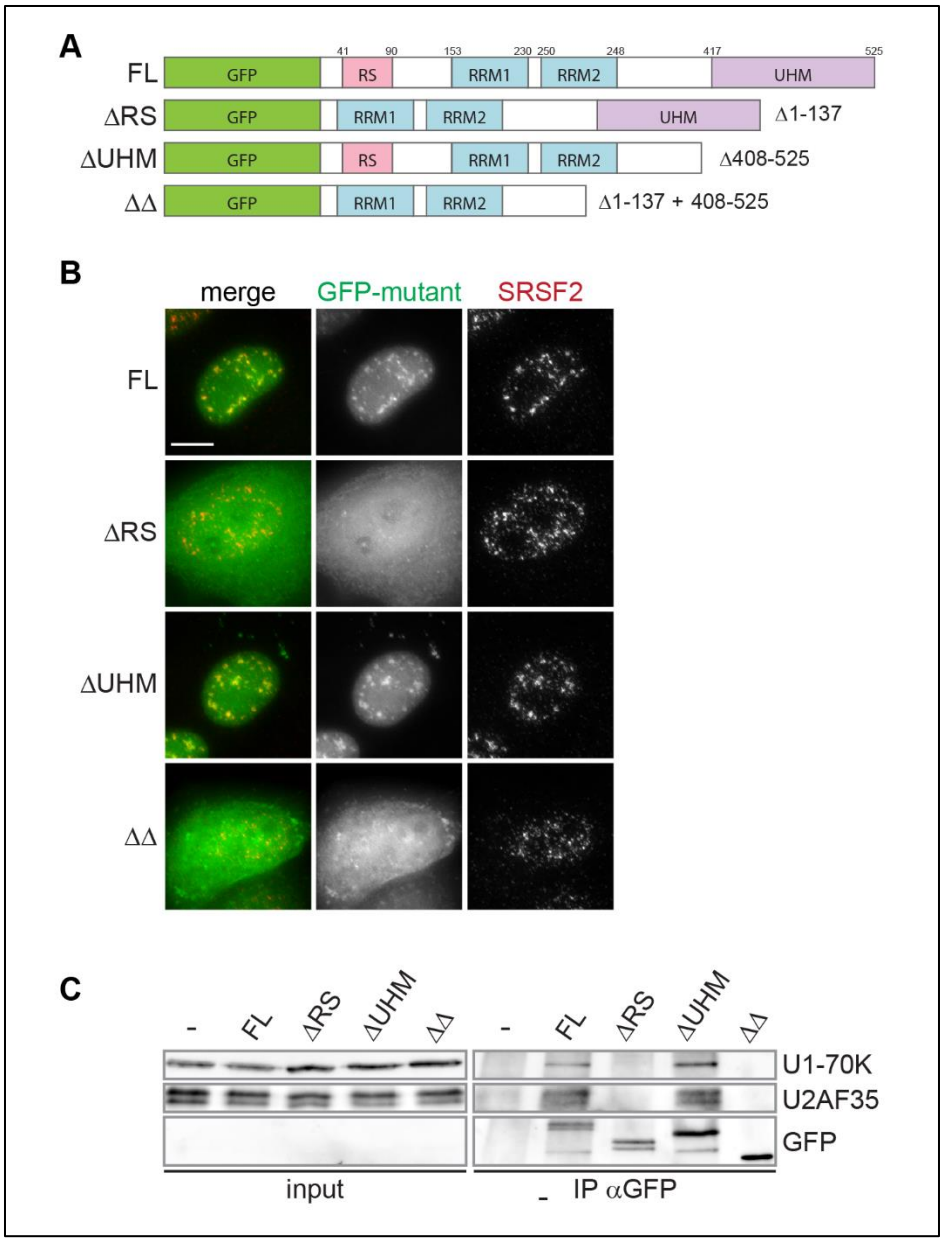

Fig 33: RBM39 RS domain is responsible for its interactions with the E-complex.
(A) A schematic representation of the RBM39 domain structure, based on (Kielkopf et al., 2004; Corsini et al., 2007), and the RBM39 deletion constructs used in this study. (B) HeLa cells expressing GFP-tagged RBM39 mutants (green) stained with the anti-SRSF2 antibody (red) marking nuclear speckles. Scale bar: 10 μm. (C) Transiently transfected GFP-tagged RBM39 mutants were immuno-precipitated using anti-GFP antibodies and co-precipitated proteins visualized by western blotting. Non-transfected HeLa cells served as a negative control.

and nuclear speckles. Next, we analyzed the interactions of the mutants. We show that the mutants lacking the RS domain are not able to co-precipitate neither U1-70K nor U2AF35 (Fig. 33C). Taken together, we showed that the RS domain of

RBM39 is responsible for both its correct cellular localization and its ability to associate with the spliceosomal E-complex.

RBM39 depletion does not influence E-complex formation kinetics

To test the overall physiological function of RBM39 in the spliceosome assembly we employed FRAP analysis of the E-complex components. As was previously shown, recovery curves of splicing factors in the nucleus reflect the interaction of snRNPs with pre-mRNA molecules and thus spliceosome assembly kinetics (Huranova et al., 2010).

We utilized GFP-tagged RBM39-interacting proteins U1-70K and U2AF35 and measured their dynamics in the nucleoplasm where most of the splicing events take place (Girard et al., 2012). We expected that if RBM39 serves as a universal bridge in the E-complex assembly, we should detect changes in the splicing factor kinetics upon its depletion. We observed slower recovery of U1-70K after RBM39 knock-down, while the kinetics of U2AF35 remained unchanged (Fig. 34). This could suggest that RBM39 helps with releasing of the U1 snRNP from spliceosomal complexes. However, even though the recovery of U1-70K protein is visibly slower, the change in the recovery curve after RBM39 depletion compared to the negative control was not statistically significant on the 95% confidence level. We also observed no change in splicing efficiency measured for two different house-keeping genes, GAPDH and LDHA, after RBM39 knock-down (data not shown).

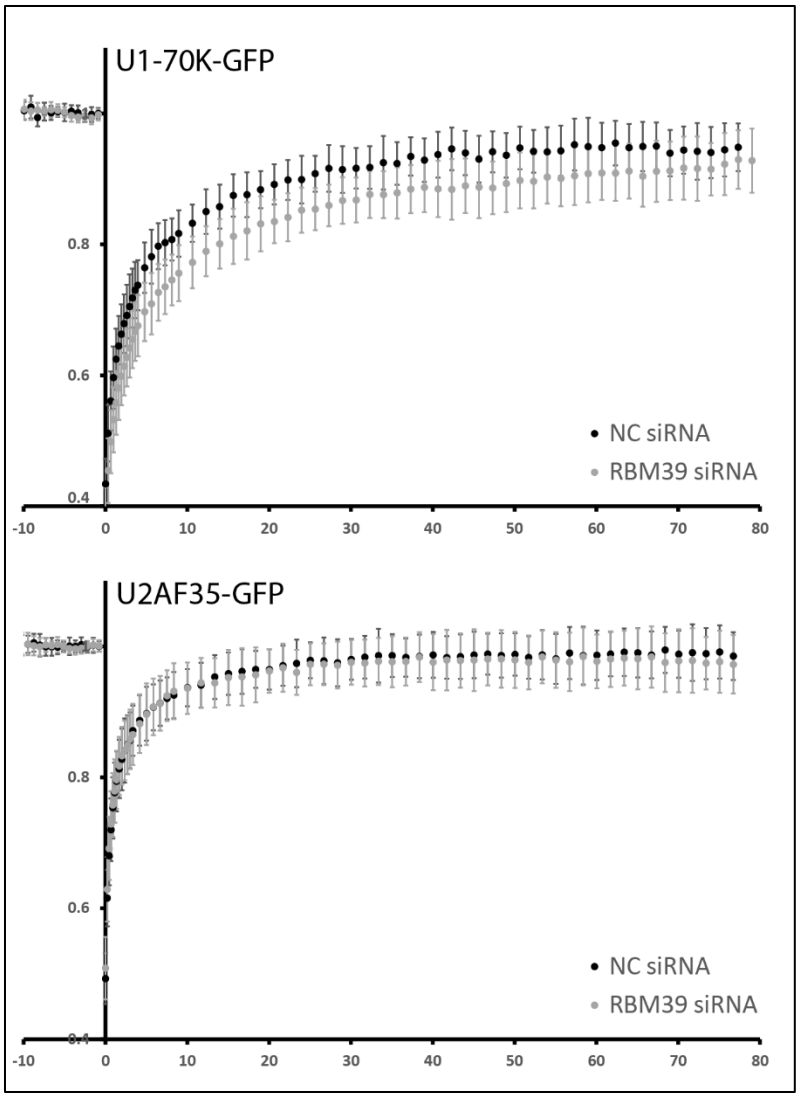

Fig. 34: RBM39 depletion does not change dynamics of the E-complex assembly. Cells were transiently transfected with the GFP-tagged splicing factor and treated with the appropriate siRNA. GFP-tagged protein dynamics was measured by FRAP in the nucleoplasm. The recovery curves represent an average of 10 to 15 measurements shown together with the standard deviation.

Taken together, our data show that RBM39 is not an essential factor in the E-complex assembly in general. We suggest that RBM39 function is rather gene-specific. To test this, it would be interesting to monitor spliceosome assembly dynamics upon RBM39 depletion directly on a reporter gene, the splicing of which is influenced by changes in RBM39 expression, such as VEGF.

3 Characterization of the dynamics of Brd2 interactions with chromatin

As splicing can occur co-transcriptionally in a close proximity of chromatin, its outcome can be influenced by the chromatin landscape. It was shown that chromatin marks, such as histone acetylation, regulate alternative splicing (Hnilicova et al., 2011). However, the role of acetylated chromatin binding proteins in this process is still unclear. We were interested in the essential histone acetylation reader protein Brd2 and its putative function in regulation of alternative splicing. For this, Samira Hozeifi and Jarmila Hnilicova from our laboratory monitored how Brd2 influences splicing outcomes genome-wide. I aimed to characterize interactions of Brd2 with acetylated chromatin and to map contributions of individual Brd2 domains to the overall chromatin binding.

To assess the role of individual Brd2 domains, I prepared several GFP-tagged Brd2 constructs bearing a mutation in the conserved residues inside either of the bromodomains (Fig. 35). These mutations inhibit Brd2 association with acetylated histone H4, both *in vivo* and *in vitro* (Kanno et al., 2004; Ito et al., 2011). I also prepared mutants lacking the self-interacting mB domain (Garcia-Gutierrez et al., 2012) and the ET domain which binds several factors involved in gene expression (Rahman et al., 2011).

Brd2 diffusion parameters

First of all, we needed to determine the diffusion parameters of Brd2, to be able to analyze the kinetic parameters of its binding to chromatin. For diffusion

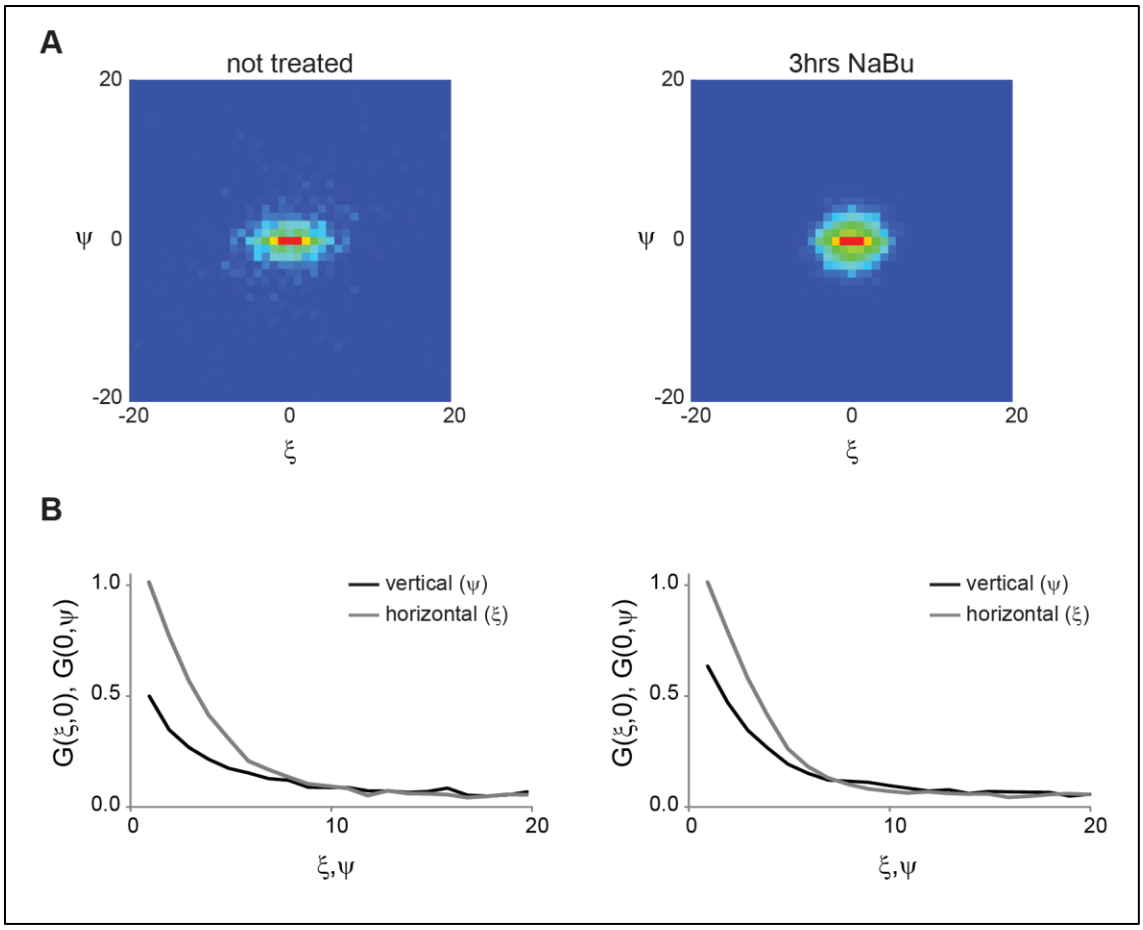

Fig. 35: Dynamic behavior of Brd2 bromodomains analyzed by measuring RICS of BD-mut1+2. Representative two-dimensional autocorrelation functions (A) and their corresponding cross-sections (B) obtained by RICS. RICS of BD-mut1+2 was measured before (left pannel) and after (right pannel) 3 hours of treatment with 5 mM NaBu. Note the increase in the vertical cross-section after NaBu treatment, indicating stronger interaction with chromatin.

properties analysis we used raster image correlation spectroscopy (RICS). RICS can be utilized to measure the diffusion together with binding, in case the binding time does not exceed 20 ms (Brown et al., 2008). To determine the effective diffusion of the Brd2, we utilized the construct containing mutations in both of the bromodomains (BD-mut1+2) and monitored its movement in live cells by RICS. In collaboration with Jana Humpolíčková (J. Heyrovský Institute of Physical Chemistry, Prague) we calculated the two-dimensional spatial auto-correlation function (G(ξ,ψ), ACF, Fig. 36A). The horizontal cross-section of the ACF (G(ξ,0))

Brd2 mutant	NaBu	D ($\mu m \cdot s^{-1}$)	Diffusing fraction	Binding time (ms)
BD-wt	-	3.17	0.60 ± 0.17	> 20
	+	3.17	0.16 ± 0.09	> 20
BD-mut1+2	-	3.17	1.00	n.a.
	+	3.17	0.68 ± 0.07	> 20

Tab. 2: RICS analysis. The RICS curves of BD-mut1+2 were fitted for pure diffusion and the diffusion coefficient D was determined. D was then fixed and the fraction of diffusing molecules and binding time was determined.

reflects the diffusion and the vertical cross-section ($G(0,\psi)$) corresponds to the binding (Fig. 36B). The ACF can be then fitted with equations describing the movement with diffusion and binding parameters (Hebert et al., 2005).

In non-treated cells the ACF of the mutant BD-mut1+2 fitted perfectly the pure-diffusion model according to (Norris et al., 2011), showing that BD-mut1+2 did not exhibit any binding. The diffusion coefficient obtained from the fitting had a value of 3.17 $\mu m \cdot s^{-1}$ (Tab. 2) which was then used as a fixed value for fitting the ACF of BD-wt with the model describing both diffusion and binding according to the (Digman and Gratton, 2009). This model provides the binding time and the diffusing and unbound fractions that contribute to the overall ACF. Thus, it is possible to get a good estimate of the ratio of bound and diffusing proteins. Our data reveal that 60% of the BD-wt molecules were freely diffusing and only 40% of the population was bound to chromatin at a given time, with binding times exceeding 20 ms.

Next we treated cells with sodium butyrate (NaBu) which is a potent inhibitor of human histone deacetylases. This treatment increases overall histone acetylation in the chromatin. We then tested whether additional binding sites will affect the movement of the Brd2. The wild-type bromodomains strongly interacted

with overacetylated chromatin and the ratio changed to over 80% of the population bound to the chromatin with binding time exceeding 20 ms. To our surprise, even the mutated bromodomains, which did not interact with chromatin in non-treated cells, interacted with overacetylated chromatin with almost 30% of the population bound at a given time (Tab.2). These data show that mutations previously published as abolishing the association of Brd2 with acetylated H4 (Kanno et al., 2004) do not completely prevent the interaction of BDs with acetylated chromatin but instead significantly reduce its binding potential. It is possible that the conserved amino acid residues increase the affinity of BDs towards acetylated histones and/or stabilize the interaction between BDs and chromatin.

Dynamics of Brd2 interaction with chromatin

We determined by RICS that BDs associated with chromatin for longer than 20 ms. Such interactions can be analyzed by fluorescence recovery after photo-bleaching (FRAP, (Mueller et al., 2010)). We measured FRAP curves for the constructs analyzed by RICS, BD-wt and BD-mut1+2 (Fig. 36A,B), and fitted them with a model considering both diffusion and binding (so called full model according to (Sprague et al., 2004)). BD-wt curves were accurately fitted with the full model, providing us with the disassociation constant k_{off} which we then converted to the binding time τ (Tab. 3, τ corresponds to the inverse value of the k_{off}). The binding time of the BD-wt construct was approximately 1 s and it increased approx. three-fold upon the histone overacetylation caused by the NaBu treatment, showing that

Brd2 mutant	NaBu	k_{off} (s^{-1})	Binding time τ (s)
Brd2-wt	-	0.62 ± 0.24	1.61 ± 0.62
	+	0.07 ± 0.09	14.29 ± 16.50
Brd2-mut1	-	1.22 ± 0.47	0.82 ± 0.32
	+	0.71 ± 0.72	1.41 ± 1.43
Brd2-mut2	-	1.42 ± 0.70	0.70 ± 0.35
	+	0.15 ± 0.26	6.67 ± 11.53
Brd2-mut1+2	-	0.77 ± 0.34	1.30 ± 0.58
	+	0.64 ± 0.27	1.56 ± 0.68
BD-wt	-	1.07 ± 0.33	0.93 ± 0.29
	+	0.32 ± 0.26	3.13 ± 2.63
BD-mut1+2	-	n. a.	n. a.
	+	3.94 ± 2.40	0.25 ± 0.15

Tab. 3: Full model fitting of the FRAP curves. FRAP curves were fitted with the full model equations according to (Sprague et al., 2004) and the binding time was calculated as an inverse value of the k_{off}. The average of 10 to 15 curves fitting is shown together with the standard deviation.

bromodomains indeed interact with the acetylated chromatin (Fig. 36A and Tab. 3).

We were not able to properly fit the recovery curve of BD-mut1+2 constructs neither with the full model, nor with the pure diffusion model. Currently we have no explanation for this. However, even though the construct BD-mut1+2 did not show any apparent changes in the fluorescence recovery curves upon the HDAC inhibition, we were able to fit the curves with the full model equations and in this case we got a binding time of approx. 250 ms. However, such a short binding time is close to the detection limit of FRAP and should be therefore interpreted cautiously. A reasonable explanation would be that the conserved residues mutated in the BD-mut1+2 are important for stabilization of the interaction between BDs and acetylated lysines.

We then analyzed the behavior of the full-length constructs. Brd2-wt showed slower recovery than the BD-wt mutant (Fig. 36C, Tab. 3), suggesting that the C-terminal domain contributes to the overall interaction of Brd2 with chromatin. The

interaction time of the Brd2-wt and Brd2-mut1+2 differed only very slightly in the non-treated cells. This suggests that the C-terminal part of the protein determines the overall dynamic behavior of the Brd2 in the nuclear environment. The influence of the bromodomains conserved residues became apparent only after the HDAC inhibition. Brd2-mut1+2 was insensitive to the NaBu treatment (Fig. 36D), whereas the single-mutation constructs interactions with chromatin increased upon histone overacetylation as demonstrated by the fluorescent recovery slow-down (Fig. 36E,F). Recovery of both mutants Brd2mut1 and 2 was faster than the recovery of Brd2-wt (Fig. 36B,E,F), indicating that both bromodomains are important for the stable association of Brd2 with acetylated chromatin. However, there is a difference between BD1 and 2 – the binding time of a protein bearing mutation in the BD1 was almost five times shorter than in case of the mutation in BD2 (Tab. 3), suggesting that the BD1 contributes more to the overall interaction of Brd2 with the acetylated chromatin.

To sum up, the RICS and FRAP analysis showed that under normal conditions, the dynamic behavior of the Brd2 protein is driven mainly by the C-terminal domain interactions, which also contribute to the chromatin binding. Normally, only about 40% of the bromodomains are associated with chromatin, leaving the rest 60% to be diffusing freely in the nucleus. In case of the histone hyperacetylation, the bound fraction increases almost to 85% and the binding time is prolonged approx. 7-times. In addition, BD1 and 2 interact with the acetylated chromatin independently and the interaction is stronger for BD1.

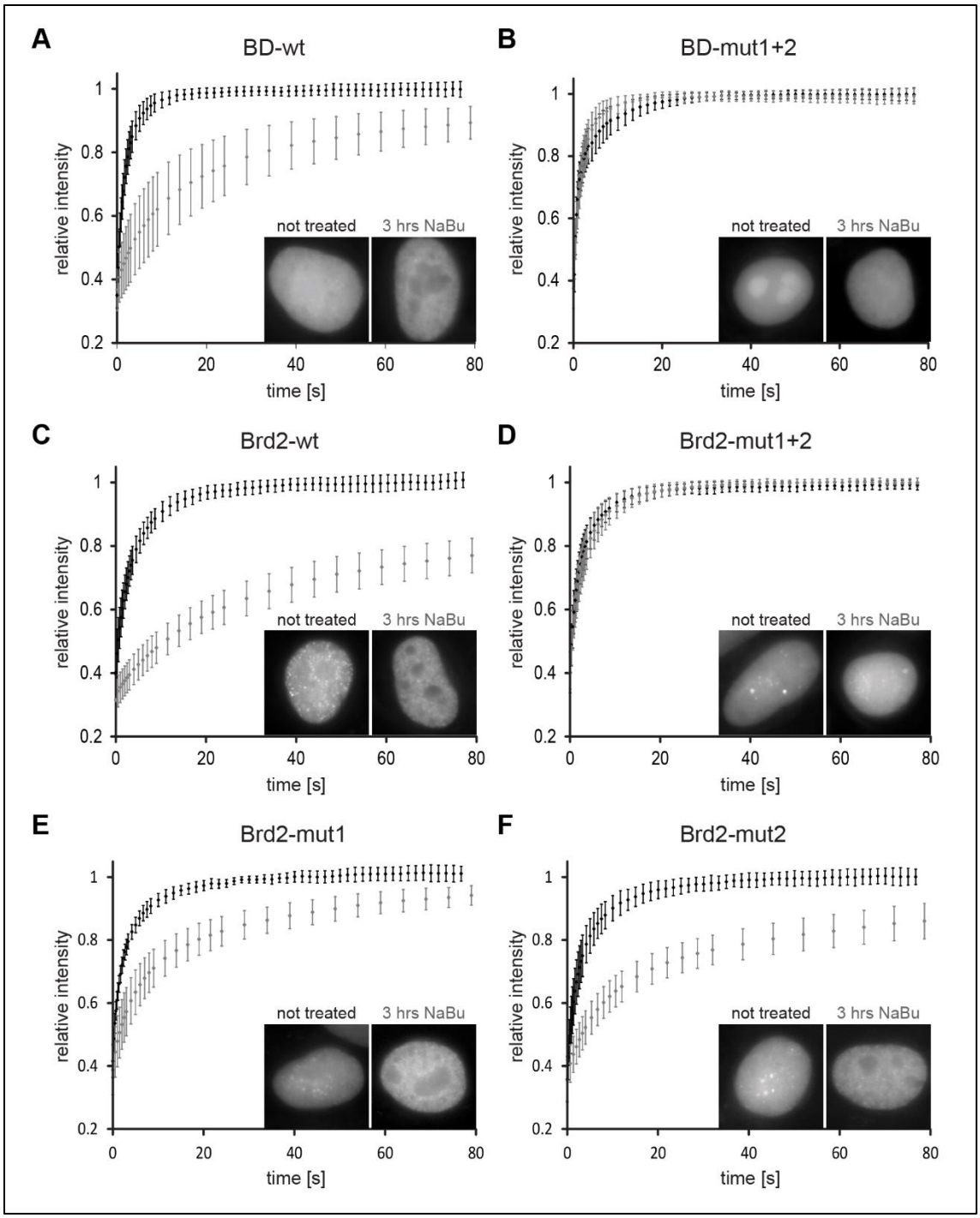

Fig. 36: Mutations in both BDs abolish stable interaction of Brd2 with the acetylated chromatin. Cells were transiently transfected with the indicated Brd2-GFP constructs and treated for 3 hrs with 5 mM NaBu, if appropriate. Dynamics of the constructs was measured by FRAP before (black) or after (grey) histone overacetylation. FRAP curves represent the average of 10 to 15 measurements shown together with the standard deviation. Representative wide-field fluorescence images of transfected cells are shown as 15x15 µm insets.

DISCUSSION

1 Unexpected connection between the SMN complex and splicing factor U1-70K

Primary transcripts of the majority of protein higher eukaryotes coding genes contain many introns which are not included in the mature mRNA. The splicing of introns is accomplished by the dynamic network of spliceosomal snRNPs generated via a complex assembly pathway. The key player in the snRNP assembly pathway is the SMN complex, a multiprotein complex with SMN protein in its center.

SMN, or survival of motor neurons, got its name owing to its connection with a neurodegenerative disease called spinal muscular atrophy (SMA). SMA manifests itself by a progressive loss of alpha motor neurons within the anterior horns of the spinal cords. Motor neurons start dying and the muscles they innervate atrophy, leading to progressive loss of muscle tonus resulting in the paralysis of breathing muscles. SMA is in most cases an early-onset disease which leads to death in infancy. Currently it is not clear what causes the tissue-specific phenotype of the disease. It is possible that the disrupted formation of snRNPs affects splicing of a subset of genes which are particularly important for the correct function and survival of motor neurons (Burghes and Beattie, 2009).

On the cellular level, the number of nuclear gems is an established indicator of SMN levels in SMA patients' cells and the loss of gems correlates with SMA severity

(Lefebvre et al., 1997). Interestingly, it was recently revealed that depletion of gems is also a cellular hallmark of another neurodegenerative disease, amyotrophic lateral sclerosis (ALS). ALS is mostly sporadic and is linked to various mutations in several genes. It was demonstrated that SMN levels are significantly reduced in patients with sporadic ALS bearing SOD1 mutations (Turner et al., 2014). Loss of nuclear gems initiates before the disease onset and is progressive during the disease evolution (Gertz et al., 2012; Kariya et al., 2012). These results are in agreement with evidence showing an association between disrupted SMN genes copy numbers and the increased severity of ALS (Veldink et al., 2005; Blauw et al., 2012).

However, a significant subset of ALS cases is caused by mutations in genes linked to RNA processing. It was recently shown that the total number of gems is altered in cells derived from ALS patients with disrupted levels or mutant forms of RNA-binding proteins TDP43 or FUS, even though the intracellular SMN levels are normal (Shan et al., 2010; Yamazaki et al., 2012; Ishihara et al., 2013; Tsuiji et al., 2013).

We showed that the splicing factor U1-70K is a gem resident protein and its depletion leads to the loss of gems. To our knowledge, no mutation of U1-70K was identified in amyotrophic lateral sclerosis patients to date (Finsterer and Burgunder, 2014). However, our findings link U1-70K to proteins important for gem integrity and potentially to the etiology of neurodegenerative diseases. U1-70K mutations can thus pose an interesting target for screening the sporadic

amyotrophic lateral sclerosis patients with yet unidentified genetic background of the disease.

We also revealed that U1-70K is a novel SMN complex interaction partner. The SMN complex was recently identified in the early spliceosomal complexes (Makarov et al., 2012) and it was suggested to be directly involved in *in vitro* pre-mRNA splicing or recycling of post-spliceosomal complexes (Meister et al., 2000). U1-70K is a core splicing protein, found specifically in early splicing complexes, which leaves the spliceosome during its activation (Will and Luhrmann, 2011). Our data provide a direct link between the SMN complex and early spliceosomes and could explain how the SMN complex associates with the spliceosome.

2 Alternative splicing regulation and spliceosome assembly

The spliceosome is a complex macromolecular machine which is assembled step by step on the pre-mRNA. Spliceosome assembly needs to be carefully orchestrated and tightly controlled because usage of correct splice sites is essential for survival. Proteins resulting from translation of non-accurately spliced transcripts would be functionally aberrant. Thus the spliceosome must be able to splice introns both rapidly and accurately. This pose quite a difficult accomplishment given that introns are usually much longer than exons and there is a huge amount of the cryptic splice site consensus sequences throughout the genome.

At the beginning of the genomic era it was thought that introns belong to a group of a so-called "junk" DNA. Therefore it was quite puzzling why the cell would keep sequences which must be replicated, transcribed and then excised and degraded at great metabolic costs in its genome. Then it became evident that complex organisms evolutionary profited from the possibility of the alternative splicing which allows the expression of multiple functionally distinct protein isoforms from a single gene. Alternative splicing thus allows the enrichment of transcriptome and proteome without the need of genome expansion. It also enables a protein expression regulatory network depending on the cell type, developmental stage and other signaling in complex organisms.

We showed that an SR-like protein RBM39 regulates alternative splicing of the vascular endothelial growth factor in tumor-derived cell lines. Expression of RBM39 shifts the isoform ratio towards the expression of the $VEGF_{165}$ isoform which is less angiogenic than the isoform $VEGF_{121}$ (Neufeld et al., 1999) expressed in the absence of RBM39. Our results corroborate the study of (Huang et al., 2012) who showed that RBM39 overexpression reduce vascularization and growth in tumors derived from Ewing sarcoma cells.

RBM39 has been detected in human pre- and early spliceosome complexes (Hartmuth et al., 2002; Behzadnia et al., 2007; Bessonov et al., 2008) and it was shown to function in pre-mRNA splicing of fission yeast (Shao et al., 2012), *Drosophila* (Park et al., 2004) and human (Dowhan et al., 2005). It was shown that the fission yeast homolog of RBM39, a small SR-like protein Rsd1, connects the U1 snRNP with the U2 via an interaction network consisting of the U1A, Rsd1, SpPrp5

and the SF3b protein subunit (Shao et al., 2012). Human RBM39 was shown to interact with the U2AF heterodimer (Ellis et al., 2008) and the SF3b155 splicing factor (Loerch et al., 2014). However, the interaction partners of RBM39 in the U1 snRNP remained elusive.

Using immunoprecipitation and advanced fluorescence microscopy techniques, we showed that RBM39 interacts with splicing factor U1-70K and that this interaction is mediated by the C-terminal RS domain of RBM39 (Fig. 31-33). It was recently shown that the N-terminal UHM domain of RBM39 is essential for its binding to the U2 snRNP protein SF3b155 (Loerch et al., 2014). It is tempting to speculate that RBM39 interacts with both U1-70K and SF3b155 at the same time, thus posing as a bridge between U1 and U2 snRNPs in the emerging spliceosome. However, we weren't able to detect U2 snRNP marked by the U2A´ protein in our IPs, suggesting that this putative interaction is probably transient or weak.

The transition from cross-exon interactions to cross-intron assembly is still poorly understood and it often involves additional cis-acting sequences and factors (De Conti et al., 2013). RBM39 might be such a factor able to recognize weak splice sites and regulate the spliceosome assembly on them. However, the putative coordination of RBM39 interactions with U1 and U2 snRNP in time and space needs to be addressed by further experiments.

In a wider biological context, the exact mechanism of the gene-specific regulation of spliceosome assembly by various cis-acting splicing factors remains open. It is probable that these factors form a large regulatory network. Cooperation between multiple RNA-binding proteins would enable recognition of longer

cognate pre-mRNA sites. Moreover, a sigmoidal response resulting from subtle changes in splicing factors levels in such a cooperative network would enable nearly digital regulation of alternative splicing.

It was shown that at least two RBM39 molecules simultaneously bind one SF3b155 protein via their UHM motifs (Loerch et al., 2014). In addition, SF3b155 was shown to interact with several UHM-containing splicing factors, such as U2AF65 (Cass and Berglund, 2006; Thickman et al., 2006), SPF45 (Corsini et al., 2007) and Puf60 (Corsini et al., 2009). Therefore it was hypothesized that a tightly controlled network of UHM domains interactions recognize multiple weak SF3b155 binding sites in a coordinated manner, thus selectively enhancing or disrupting recognition of specific splice sites (Loerch et al., 2014).

3 Epigenetics of alternative splicing

As most of the pre-mRNA splicing is achieved co-transcriptionaly, the splicing outcome is driven not only by the regulatory elements in the pre-mRNA sequence, but also by the chromatin environment. Recent studies show a close connection between histone modification and alternative splicing regulation (Hnilicova and Stanek, 2011). So far, only a few chromatin-binding proteins, such as MRG15, CHD1 and BS69 were shown to directly influence splicing (Sims et al., 2007; Luco et al., 2010; Guo et al., 2014).

Histone acetylation was shown to regulate alternative splicing (Hnilicova et al., 2011), however, not much is known about the role of histone acetylation reader

proteins in this process. We have chosen to characterize a putative alternative splicing regulator – Brd2 protein, a BET family member.

Brd2 is a histone-acetylation reader protein which associates with multiple protein complexes such as Pol II, transcription factors, histone acetylases and chromatin remodeling factors (Denis et al., 2006; Peng et al., 2007; LeRoy et al., 2008). Brd2 bromodomains are able to selectively distinguish specific acetylated lysines on histone H4. BD1 preferentially interacts with H4K5ac/K8ac whereas the BD2 recognizes specifically H4K12ac or H4K5ac/K12ac (Huang et al., 2007; Umehara et al., 2010; Filippakopoulos and Knapp, 2012). In addition, the bromodomains have much higher affinity to H4K5ac/K8ac/K12ac/K16ac tetra-acetylated peptides than to single acetylation marks (Filippakopoulos et al., 2012; LeRoy et al., 2012). The C-terminal ET domain of BET family members interacts with chromatin remodelers, such as NSD3 methyltransferase or JMJD6 hydroxylase (Webby et al., 2009; Rahman et al., 2011). The mB motif was recently shown to self-interact (Garcia-Gutierrez et al., 2012).

Here we utilized live-cell microscopy techniques to characterize interactions of Brd2 with chromatin *in vivo*. We showed that under normal conditions the movement of Brd2 is mainly driven by interactions mediated by the C-terminal domain (Fig. 35,36) and that mutations previously shown to abolish the association of Brd2 with acetylated H4 (Kanno et al., 2004) do not completely prevent binding to the acetylated chromatin but significantly reduce the bromodomains binding potential. Moreover, we show that the interactions of bromodomains with

acetylated chromatin are independent on each other and supported by the C-terminal domain.

Our data showing the prolonged interaction time after chromatin hyperacetylation are in accordance with *in vitro* data showing stronger association of the bromodomains with the tetraacetylated H4 peptides than with monoacetylated ones (Filippakopoulos et al., 2012; LeRoy et al., 2012).

Taken together, we showed that Brd2 association with chromatin is not driven solely by the bromodomains but it is modulated by the C-terminal domain. This modulation can be either direct via its interaction with chromatin, or indirect via the C-terminal domain association with other chromatin-binding proteins which would synergize with the Brd2-BDs. However, when chromatin is hyperacetylated, the interaction of the bromodomains with acetylated histones overcomes other interactions and becomes dominant. To sum up, Brd2 is targeted to chromatin via cooperative action of BDs and the C-terminal domain.

Work of Jarmila Hnilicova and Samira Hozeifi from our laboratory revealed that Brd2 regulates alternative splicing of almost 300 genes and it is specifically localized at the promoters of its target genes (Hnilicova et al., 2013). It was shown that promoters and their usage plays a role in alternative splicing (Kornblihtt, 2005), however, a molecular mechanism that couples promoters and splicing regulation is unknown. Recently, it was suggested that alternative exons contact promoters in the three-dimensional space (Mercer et al., 2013). This would enable the proteins associating with promoters to contact the alternative elements and directly influence the spliceosome assembly. However, our chromatin

immunoprecipitation analyses have not proven Brd2 association with the alternative exons it regulates.

Another possible explanation of Brd2 influence upon the alternative splicing might be its interaction with JMJD6, an enzyme which hydroxylates the general splicing factor U2AF65 and thus modifies alternative splicing of several minigene reporters (Webby et al., 2009). Brd2 might possibly recruit JMJD6 to specific genes where it would regulate the splicing outcome.

It becomes increasingly obvious that the chromatin landscape, transcription and splicing are functionally coupled but so far only a few factors were identified explaining this cross-talk. Brd2 protein interacts with chromatin and affects both transcription and alternative splicing. Brd2 is an essential gene which was linked to epilepsy in humans (Pal et al., 2003; Cavalleri et al., 2007). Neurons are heavily regulated by alternative splicing. Thus changes in alternative splicing of proteins important for cell communication can explain the link between Brd2 expression and human epilepsy.

CONCLUSION

In this work we focused on the formation of splicing machinery in the context of the cell nucleus from several points of view.

In the first project we described an interaction between U1 snRNP core protein U1-70K and the SMN complex. We mapped this interaction to the N-terminal tail domain of U1-70K and showed that this interaction is important for targeting of U1-70K into the nuclear gems. Moreover, we showed that after U1-70K depletion gems disappear from the nucleus. Exogenous expression of the U1-70K N-terminal tail rescued gem formation. These findings show U1-70K as an SMN complex associating protein and suggest a new function for U1-70K in gem formation.

In the second project we confirmed that SR-like protein RBM39 regulates alternative splicing of the VEGF gene. We analyzed RBM39 interactions and revealed that it associates with U2AF and U1-70K splicing factors in the early spliceosomal complex. We mapped both of these interactions to the RS domain of RBM39. We suggest that RBM39 is able to regulate alternative splicing processes via its association with the E-complex.

In the third project we further explored alternative splicing regulation. We characterized interactions of the histone acetylation reader protein Brd2 with chromatin. We showed that under normal conditions the movement of Brd2 is mainly driven by interactions mediated by the C-terminal domain and that mutations previously shown to abolish the association of Brd2 with acetylated H4

do not completely prevent binding to the acetylated chromatin but significantly reduce the bromodomains binding potential. Moreover, we showed that bromodomains 1 and 2 interact with the acetylated chromatin independently and the interaction is stronger for BD1.

REFERENCES

Allo, M., Buggiano, V., Fededa, J. P., Petrillo, E., Schor, I., de la Mata, M., Agirre, E., Plass, M., Eyras, E., Elela, S. A. et al. (2009). Control of alternative splicing through siRNA-mediated transcriptional gene silencing. *Nat Struct Mol Biol* **16**, 717-724.

Ast, G. (2004). How did alternative splicing evolve? *Nat Rev Genet* **5**, 773-782.

Attanasio, C., David, A. and Neerman-Arbez, M. (2003). Outcome of donor splice site mutations accounting for congenital afibrinogenemia reflects order of intron removal in the fibrinogen alpha gene (FGA). *Blood* **101**, 1851-1856.

Auboeuf, D., Dowhan, D. H., Kang, Y. K., Larkin, K., Lee, J. W., Berget, S. M. and O'Malley, B. W. (2004). Differential recruitment of nuclear receptor coactivators may determine alternative RNA splice site choice in target genes. *Proc Natl Acad Sci U S A* **101**, 2270-2274.

Baccon, J., Pellizzoni, L., Rappsilber, J., Mann, M. and Dreyfuss, G. (2002). Identification and characterization of Gemin7, a novel component of the survival of motor neuron complex. *J Biol Chem* **277**, 31957-31962.

Baillat, D., Hakimi, M. A., Naar, A. M., Shilatifard, A., Cooch, N. and Shiekhattar, R. (2005). Integrator, a multiprotein mediator of small nuclear RNA processing, associates with the C-terminal repeat of RNA polymerase II. *Cell* **123**, 265-276.

Barash, Y., Calarco, J. A., Gao, W., Pan, Q., Wang, X., Shai, O., Blencowe, B. J. and Frey, B. J. (2010). Deciphering the splicing code. *Nature* **465**, 53-59.

Batsche, E., Yaniv, M. and Muchardt, C. (2006). The human SWI/SNF subunit Brm is a regulator of alternative splicing. *Nat Struct Mol Biol* **13**, 22-29.

Battle, D. J., Lau, C. K., Wan, L., Deng, H., Lotti, F. and Dreyfuss, G. (2006a). The Gemin5 protein of the SMN complex identifies snRNAs. *Molecular cell* **23**, 273-279.

Battle, D. J., Kasim, M., Yong, J., Lotti, F., Lau, C. K., Mouaikel, J., Zhang, Z., Han, K., Wan, L. and Dreyfuss, G. (2006b). The SMN complex: an assembly machine for RNPs. *Cold Spring Harb Symp Quant Biol* **71**, 313-320.

Bauren, G. and Wieslander, L. (1994). Splicing of Balbiani ring 1 gene pre-mRNA occurs simultaneously with transcription. *Cell* **76**, 183-192.

Behzadnia, N., Golas, M. M., Hartmuth, K., Sander, B., Kastner, B., Deckert, J., Dube, P., Will, C. L., Urlaub, H., Stark, H. et al. (2007). Composition and three-dimensional EM structure of double affinity-purified, human prespliceosomal A complexes. *Embo j* **26**, 1737-1748.

Belkina, A. C. and Denis, G. V. (2012). BET domain co-regulators in obesity, inflammation and cancer. *Nat Rev Cancer* **12**, 465-477.

Berget, S. M. (1995). Exon recognition in vertebrate splicing. *J Biol Chem* **270**, 2411-2414.

Berglund, J. A., Abovich, N. and Rosbash, M. (1998). A cooperative interaction between U2AF65 and mBBP/SF1 facilitates branchpoint region recognition. *Genes Dev* **12**, 858-867.

Bernues, J., Simmen, K. A., Lewis, J. D., Gunderson, S. I., Polycarpou-Schwarz, M., Moncollin, V., Egly, J. M. and Mattaj, I. W. (1993). Common and unique

transcription factor requirements of human U1 and U6 snRNA genes. *Embo j* **12**, 3573-3585.
Bessonov, S., Anokhina, M., Will, C. L., Urlaub, H. and Luhrmann, R. (2008). Isolation of an active step I spliceosome and composition of its RNP core. *Nature* **452**, 846-850.
Beyer, A. L. and Osheim, Y. N. (1988). Splice site selection, rate of splicing, and alternative splicing on nascent transcripts. *Genes Dev* **2**, 754-765.
Bindereif, A. and Green, M. R. (1987). An ordered pathway of snRNP binding during mammalian pre-mRNA splicing complex assembly. *Embo j* **6**, 2415-2424.
Bird, G., Zorio, D. A. and Bentley, D. L. (2004). RNA polymerase II carboxy-terminal domain phosphorylation is required for cotranscriptional pre-mRNA splicing and 3'-end formation. *Mol Cell Biol* **24**, 8963-8969.
Blauw, H. M., Barnes, C. P., van Vught, P. W., van Rheenen, W., Verheul, M., Cuppen, E., Veldink, J. H. and van den Berg, L. H. (2012). SMN1 gene duplications are associated with sporadic ALS. *Neurology* **78**, 776-780.
Boireau, S., Maiuri, P., Basyuk, E., de la Mata, M., Knezevich, A., Pradet-Balade, B., Backer, V., Kornblihtt, A., Marcello, A. and Bertrand, E. (2007). The transcriptional cycle of HIV-1 in real-time and live cells. *J Cell Biol* **179**, 291-304.
Bonnal, S., Martinez, C., Forch, P., Bachi, A., Wilm, M. and Valcarcel, J. (2008). RBM5/Luca-15/H37 regulates Fas alternative splice site pairing after exon definition. *Molecular cell* **32**, 81-95.
Branlant, C., Krol, A., Ebel, J. P., Lazar, E., Haendler, B. and Jacob, M. (1982). U2 RNA shares a structural domain with U1, U4, and U5 RNAs. *Embo j* **1**, 1259-1265.
Brody, E. and Abelson, J. (1985). The "spliceosome": yeast pre-messenger RNA associates with a 40S complex in a splicing-dependent reaction. *Science* **228**, 963-967.
Brown, C. M., Dalal, R. B., Hebert, B., Digman, M. A., Horwitz, A. R. and Gratton, E. (2008). Raster image correlation spectroscopy (RICS) for measuring fast protein dynamics and concentrations with a commercial laser scanning confocal microscope. *J Microsc* **229**, 78-91.
Burghes, A. H. and Beattie, C. E. (2009). Spinal muscular atrophy: why do low levels of survival motor neuron protein make motor neurons sick? *Nat Rev Neurosci* **10**, 597-609.
Busch, A. and Hertel, K. J. (2012). Evolution of SR protein and hnRNP splicing regulatory factors. *Wiley Interdiscip Rev RNA* **3**, 1-12.
Caceres, J. F., Stamm, S., Helfman, D. M. and Krainer, A. R. (1994). Regulation of alternative splicing in vivo by overexpression of antagonistic splicing factors. *Science* **265**, 1706-1709.
Carissimi, C., Baccon, J., Straccia, M., Chiarella, P., Maiolica, A., Sawyer, A., Rappsilber, J. and Pellizzoni, L. (2005). Unrip is a component of SMN complexes active in snRNP assembly. *FEBS Lett* **579**, 2348-2354.
Carissimi, C., Saieva, L., Baccon, J., Chiarella, P., Maiolica, A., Sawyer, A., Rappsilber, J. and Pellizzoni, L. (2006). Gemin8 is a novel component of the survival motor neuron complex and functions in small nuclear ribonucleoprotein assembly. *J Biol Chem* **281**, 8126-8134.

Carmo-Fonseca, M., Pepperkok, R., Sproat, B. S., Ansorge, W., Swanson, M. S. and Lamond, A. I. (1991). In vivo detection of snRNP-rich organelles in the nuclei of mammalian cells. *Embo j* **10**, 1863-1873.
Cass, D. M. and Berglund, J. A. (2006). The SF3b155 N-terminal domain is a scaffold important for splicing. *Biochemistry* **45**, 10092-10101.
Cavalleri, G. L., Walley, N. M., Soranzo, N., Mulley, J., Doherty, C. P., Kapoor, A., Depondt, C., Lynch, J. M., Scheffer, I. E., Heils, A. et al. (2007). A multicenter study of BRD2 as a risk factor for juvenile myoclonic epilepsy. *Epilepsia* **48**, 706-712.
Corsini, L., Bonnal, S., Basquin, J., Hothorn, M., Scheffzek, K., Valcarcel, J. and Sattler, M. (2007). U2AF-homology motif interactions are required for alternative splicing regulation by SPF45. *Nat Struct Mol Biol* **14**, 620-629.
Corsini, L., Hothorn, M., Stier, G., Rybin, V., Scheffzek, K., Gibson, T. J. and Sattler, M. (2009). Dimerization and protein binding specificity of the U2AF homology motif of the splicing factor Puf60. *J. Biol. Chem.* **284**, 630-639.
Cramer, P., Pesce, C. G., Baralle, F. E. and Kornblihtt, A. R. (1997). Functional association between promoter structure and transcript alternative splicing. *Proc Natl Acad Sci U S A* **94**, 11456-11460.
Cramer, P., Caceres, J. F., Cazalla, D., Kadener, S., Muro, A. F., Baralle, F. E. and Kornblihtt, A. R. (1999). Coupling of transcription with alternative splicing: RNA pol II promoters modulate SF2/ASF and 9G8 effects on an exonic splicing enhancer. *Molecular cell* **4**, 251-258.
Cullen, B. R. (2003). Nuclear RNA export. *J Cell Sci* **116**, 587-597.
Dahlberg, J. E., Yang, H., Neuman de Vegvar, H. and Lund, E. (1990). Formation of the 3 end of U1 snRNA. *Mol Biol Rep* **14**, 161-162.
De Conti, L., Baralle, M. and Buratti, E. (2013). Exon and intron definition in pre-mRNA splicing. *Wiley interdisciplinary reviews. RNA* **4**, 49-60.
de la Mata, M., Alonso, C. R., Kadener, S., Fededa, J. P., Blaustein, M., Pelisch, F., Cramer, P., Bentley, D. and Kornblihtt, A. R. (2003). A slow RNA polymerase II affects alternative splicing in vivo. *Molecular cell* **12**, 525-532.
Deckert, J., Hartmuth, K., Boehringer, D., Behzadnia, N., Will, C. L., Kastner, B., Stark, H., Urlaub, H. and Luhrmann, R. (2006). Protein composition and electron microscopy structure of affinity-purified human spliceosomal B complexes isolated under physiological conditions. *Mol Cell Biol* **26**, 5528-5543.
Denis, G. V., McComb, M. E., Faller, D. V., Sinha, A., Romesser, P. B. and Costello, C. E. (2006). Identification of transcription complexes that contain the double bromodomain protein Brd2 and chromatin remodeling machines. *J Proteome Res* **5**, 502-511.
Denis, M. M., Tolley, N. D., Bunting, M., Schwertz, H., Jiang, H., Lindemann, S., Yost, C. C., Rubner, F. J., Albertine, K. H., Swoboda, K. J. et al. (2005). Escaping the nuclear confines: signal-dependent pre-mRNA splicing in anucleate platelets. *Cell* **122**, 379-391.
Deutsch, M. and Long, M. (1999). Intron-exon structures of eukaryotic model organisms. *Nucleic Acids Res* **27**, 3219-3228.
Digman, M. A. and Gratton, E. (2009). Analysis of diffusion and binding in cells using the RICS approach. *Microsc Res Tech* **72**, 323-332.

Dowhan, D. H., Hong, E. P., Auboeuf, D., Dennis, A. P., Wilson, M. M., Berget, S. M. and O'Malley, B. W. (2005). Steroid hormone receptor coactivation and alternative RNA splicing by U2AF65-related proteins CAPERalpha and CAPERbeta. *Molecular cell* **17**, 429-439.
Drivas, G. T., Shih, A., Coutavas, E., Rush, M. G. and D'Eustachio, P. (1990). Characterization of four novel ras-like genes expressed in a human teratocarcinoma cell line. *Mol Cell Biol* **10**, 1793-1798.
Du, H. and Rosbash, M. (2002). The U1 snRNP protein U1C recognizes the 5' splice site in the absence of base pairing. *Nature* **419**, 86-90.
Dundr, M., Hebert, M. D., Karpova, T. S., Stanek, D., Xu, H., Shpargel, K. B., Meier, U. T., Neugebauer, K. M., Matera, A. G. and Misteli, T. (2004). In vivo kinetics of Cajal body components. *J Cell Biol* **164**, 831-842.
Duskova, E., Hnilicova, J. and Stanek, D. (2014). CRE promoter sites modulate alternative splicing via p300-mediated histone acetylation. *RNA biology* **11**.
Egloff, S., O'Reilly, D. and Murphy, S. (2008). Expression of human snRNA genes from beginning to end. *Biochem Soc Trans* **36**, 590-594.
Egloff, S., O'Reilly, D., Chapman, R. D., Taylor, A., Tanzhaus, K., Pitts, L., Eick, D. and Murphy, S. (2007). Serine-7 of the RNA polymerase II CTD is specifically required for snRNA gene expression. *Science* **318**, 1777-1779.
Ellis, J. D., Lleres, D., Denegri, M., Lamond, A. I. and Caceres, J. F. (2008). Spatial mapping of splicing factor complexes involved in exon and intron definition. *J Cell Biol* **181**, 921-934.
Filippakopoulos, P. and Knapp, S. (2012). The bromodomain interaction module. *FEBS Lett* **586**, 2692-2704.
Filippakopoulos, P., Picaud, S., Mangos, M., Keates, T., Lambert, J. P., Barsyte-Lovejoy, D., Felletar, I., Volkmer, R., Muller, S., Pawson, T. et al. (2012). Histone recognition and large-scale structural analysis of the human bromodomain family. *Cell* **149**, 214-231.
Finsterer, J. and Burgunder, J. M. (2014). Recent progress in the genetics of motor neuron disease. *Eur J Med Genet* **57**, 103-112.
Fischer, U. and Luhrmann, R. (1990). An essential signaling role for the m3G cap in the transport of U1 snRNP to the nucleus. *Science* **249**, 786-790.
Fischer, U., Liu, Q. and Dreyfuss, G. (1997). The SMN-SIP1 complex has an essential role in spliceosomal snRNP biogenesis. *Cell* **90**, 1023-1029.
Fischer, U., Englbrecht, C. and Chari, A. (2011). Biogenesis of spliceosomal small nuclear ribonucleoproteins. *Wiley Interdisciplinary Reviews: RNA* **2**, 718-731.
Fischer, U., Sumpter, V., Sekine, M., Satoh, T. and Luhrmann, R. (1993). Nucleo-cytoplasmic transport of U snRNPs: definition of a nuclear location signal in the Sm core domain that binds a transport receptor independently of the m3G cap. *Embo j* **12**, 573-583.
Fornerod, M., Ohno, M., Yoshida, M. and Mattaj, I. W. (1997). CRM1 is an export receptor for leucine-rich nuclear export signals. *Cell* **90**, 1051-1060.
Fourmann, J. B., Schmitzova, J., Christian, H., Urlaub, H., Ficner, R., Boon, K. L., Fabrizio, P. and Luhrmann, R. (2013). Dissection of the factor requirements for spliceosome disassembly and the elucidation of its dissociation products using a purified splicing system. *Genes Dev* **27**, 413-428.

Fox-Walsh, K. L., Dou, Y., Lam, B. J., Hung, S. P., Baldi, P. F. and Hertel, K. J. (2005). The architecture of pre-mRNAs affects mechanisms of splice-site pairing. *Proc Natl Acad Sci U S A* **102**, 16176-16181.
Friesen, W. J. and Dreyfuss, G. (2000). Specific sequences of the Sm and Sm-like (Lsm) proteins mediate their interaction with the spinal muscular atrophy disease gene product (SMN). *J Biol Chem* **275**, 26370-26375.
Friesen, W. J., Paushkin, S., Wyce, A., Massenet, S., Pesiridis, G. S., Van Duyne, G., Rappsilber, J., Mann, M. and Dreyfuss, G. (2001). The methylosome, a 20S complex containing JBP1 and pICln, produces dimethylarginine-modified Sm proteins. *Mol Cell Biol* **21**, 8289-8300.
Garcia-Gutierrez, P., Mundi, M. and Garcia-Dominguez, M. (2012). Association of bromodomain BET proteins with chromatin requires dimerization through the conserved motif B. *J Cell Sci* **125**, 3671-3680.
Gelfman, S., Burstein, D., Penn, O., Savchenko, A., Amit, M., Schwartz, S., Pupko, T. and Ast, G. (2012). Changes in exon-intron structure during vertebrate evolution affect the splicing pattern of exons. *Genome Res* **22**, 35-50.
Gertz, B., Wong, M. and Martin, L. J. (2012). Nuclear localization of human SOD1 and mutant SOD1-specific disruption of survival motor neuron protein complex in transgenic amyotrophic lateral sclerosis mice. *J. Neuropathol. Exp. Neurol.* **71**, 162-177.
Girard, C., Will, C. L., Peng, J., Makarov, E. M., Kastner, B., Lemm, I., Urlaub, H., Hartmuth, K. and Luhrmann, R. (2012). Post-transcriptional spliceosomes are retained in nuclear speckles until splicing completion. *Nat Commun* **3**, 994.
Gozani, O., Feld, R. and Reed, R. (1996). Evidence that sequence-independent binding of highly conserved U2 snRNP proteins upstream of the branch site is required for assembly of spliceosomal complex A. *Genes Dev* **10**, 233-243.
Graveley, B. R. (2000). Sorting out the complexity of SR protein functions. *Rna* **6**, 1197-1211.
Grimm, C., Chari, A., Pelz, J. P., Kuper, J., Kisker, C., Diederichs, K., Stark, H., Schindelin, H. and Fischer, U. (2013). Structural basis of assembly chaperone-mediated snRNP formation. *Molecular cell* **49**, 692-703.
Grimmler, M., Otter, S., Peter, C., Muller, F., Chari, A. and Fischer, U. (2005). Unrip, a factor implicated in cap-independent translation, associates with the cytosolic SMN complex and influences its intracellular localization. *Hum Mol Genet* **14**, 3099-3111.
Gubitz, A. K., Mourelatos, Z., Abel, L., Rappsilber, J., Mann, M. and Dreyfuss, G. (2002). Gemin5, a novel WD repeat protein component of the SMN complex that binds Sm proteins. *J Biol Chem* **277**, 5631-5636.
Gunderson, F. Q. and Johnson, T. L. (2009). Acetylation by the transcriptional coactivator Gcn5 plays a novel role in co-transcriptional spliceosome assembly. *PLoS Genet* **5**, e1000682.
Guo, R., Zheng, L., Park, J. W., Lv, R., Chen, H., Jiao, F., Xu, W., Mu, S., Wen, H., Qiu, J. et al. (2014). BS69/ZMYND11 Reads and Connects Histone H3.3 Lysine 36 Trimethylation-Decorated Chromatin to Regulated Pre-mRNA Processing. *Molecular cell*.

Gupta, S., Singh, R. and Reddy, R. (1990). Capping of U6 small nuclear RNA in vitro can be uncoupled from transcription. *J Biol Chem* **265**, 9491-9495.
Gyuris, A., Donovan, D. J., Seymour, K. A., Lovasco, L. A., Smilowitz, N. R., Halperin, A. L., Klysik, J. E. and Freiman, R. N. (2009). The chromatin-targeting protein Brd2 is required for neural tube closure and embryogenesis. *Biochim Biophys Acta* **1789**, 413-421.
Hall, L. L., Smith, K. P., Byron, M. and Lawrence, J. B. (2006). Molecular anatomy of a speckle. *Anat Rec A Discov Mol Cell Evol Biol* **288**, 664-675.
Hamada, M., Sakulich, A. L., Koduru, S. B. and Maraia, R. J. (2000). Transcription termination by RNA polymerase III in fission yeast. A genetic and biochemically tractable model system. *J Biol Chem* **275**, 29076-29081.
Hartmuth, K., Urlaub, H., Vornlocher, H. P., Will, C. L., Gentzel, M., Wilm, M. and Luhrmann, R. (2002). Protein composition of human prespliceosomes isolated by a tobramycin affinity-selection method. *Proc Natl Acad Sci U S A* **99**, 16719-16724.
Hebert, B., Costantino, S. and Wiseman, P. W. (2005). Spatiotemporal image correlation spectroscopy (STICS) theory, verification, and application to protein velocity mapping in living CHO cells. *Biophys J* **88**, 3601-3614.
Hebert, M. D., Shpargel, K. B., Ospina, J. K., Tucker, K. E. and Matera, A. G. (2002). Coilin methylation regulates nuclear body formation. *Dev Cell* **3**, 329-337.
Hernandez, N. (2001). Small nuclear RNA genes: a model system to study fundamental mechanisms of transcription. *J Biol Chem* **276**, 26733-26736.
Hnilicova, J. and Stanek, D. (2011). Where splicing joins chromatin. *Nucleus (Austin, Tex.)* **2**, 182-188.
Hnilicova, J., Hozeifi, S., Duskova, E., Icha, J., Tomankova, T. and Stanek, D. (2011). Histone deacetylase activity modulates alternative splicing. *PLoS One* **6**, e16727.
Hnilicova, J., Hozeifi, S., Stejskalova, E., Duskova, E., Poser, I., Humpolickova, J., Hof, M. and Stanek, D. (2013). The C-terminal domain of Brd2 is important for chromatin interaction and regulation of transcription and alternative splicing. *Mol Biol Cell* **24**, 3557-3568.
Hoffman, B. E. and Grabowski, P. J. (1992). U1 snRNP targets an essential splicing factor, U2AF65, to the 3' splice site by a network of interactions spanning the exon. *Genes Dev* **6**, 2554-2568.
House, A. E. and Lynch, K. W. (2006). An exonic splicing silencer represses spliceosome assembly after ATP-dependent exon recognition. *Nat Struct Mol Biol* **13**, 937-944.
Howe, K. J., Kane, C. M. and Ares, M., Jr. (2003). Perturbation of transcription elongation influences the fidelity of internal exon inclusion in Saccharomyces cerevisiae. *Rna* **9**, 993-1006.
Huang, G., Zhou, Z., Wang, H. and Kleinerman, E. S. (2012). CAPER-alpha alternative splicing regulates the expression of vascular endothelial growth factor(1)(6)(5) in Ewing sarcoma cells. *Cancer* **118**, 2106-2116.
Huang, H., Zhang, J., Shen, W., Wang, X., Wu, J., Wu, J. and Shi, Y. (2007). Solution structure of the second bromodomain of Brd2 and its specific interaction with acetylated histone tails. *BMC structural biology* **7**, 57.

Huang, Q., Jacobson, M. R. and Pederson, T. (1997). 3' processing of human pre-U2 small nuclear RNA: a base-pairing interaction between the 3' extension of the precursor and an internal region. *Mol Cell Biol* **17**, 7178-7185.
Huang, Y. and Maraia, R. J. (2001). Comparison of the RNA polymerase III transcription machinery in Schizosaccharomyces pombe, Saccharomyces cerevisiae and human. *Nucleic Acids Res* **29**, 2675-2690.
Huber, J., Dickmanns, A. and Luhrmann, R. (2002). The importin-beta binding domain of snurportin1 is responsible for the Ran- and energy-independent nuclear import of spliceosomal U snRNPs in vitro. *J Cell Biol* **156**, 467-479.
Huber, J., Cronshagen, U., Kadokura, M., Marshallsay, C., Wada, T., Sekine, M. and Luhrmann, R. (1998). Snurportin1, an m3G-cap-specific nuclear import receptor with a novel domain structure. *Embo j* **17**, 4114-4126.
Huranova, M., Hnilicova, J., Fleischer, B., Cvackova, Z. and Stanek, D. (2009). A mutation linked to retinitis pigmentosa in HPRP31 causes protein instability and impairs its interactions with spliceosomal snRNPs. *Hum Mol Genet* **18**, 2014-2023.
Huranova, M., Ivani, I., Benda, A., Poser, I., Brody, Y., Hof, M., Shav-Tal, Y., Neugebauer, K. M. and Stanek, D. (2010). The differential interaction of snRNPs with pre-mRNA reveals splicing kinetics in living cells. *Journal of Cell Biology* **191**, 75-86.
Chari, A., Golas, M. M., Klingenhager, M., Neuenkirchen, N., Sander, B., Englbrecht, C., Sickmann, A., Stark, H. and Fischer, U. (2008). An assembly chaperone collaborates with the SMN complex to generate spliceosomal SnRNPs. *Cell* **135**, 497-509.
Charroux, B., Pellizzoni, L., Perkinson, R. A., Shevchenko, A., Mann, M. and Dreyfuss, G. (1999). Gemin3: A novel DEAD box protein that interacts with SMN, the spinal muscular atrophy gene product, and is a component of gems. *Journal of Cell Biology* **147**, 1181-1193.
Charroux, B., Pellizzoni, L., Perkinson, R. A., Yong, J., Shevchenko, A., Mann, M. and Dreyfuss, G. (2000). Gemin4: A novel component of the SMN complex that is found in both gems and nucleoli. *Journal of Cell Biology* **148**, 1177-1186.
Chen, Y., Chafin, D., Price, D. H. and Greenleaf, A. L. (1996). Drosophila RNA polymerase II mutants that affect transcription elongation. *J Biol Chem* **271**, 5993-5999.
Cho, S., Hoang, A., Sinha, R., Zhong, X. Y., Fu, X. D., Krainer, A. R. and Ghosh, G. (2011). Interaction between the RNA binding domains of Ser-Arg splicing factor 1 and U1-70K snRNP protein determines early spliceosome assembly. *Proc Natl Acad Sci U S A* **108**, 8233-8238.
Ilagan, J. O., Chalkley, R. J., Burlingame, A. L. and Jurica, M. S. (2013). Rearrangements within human spliceosomes captured after exon ligation. *Rna* **19**, 400-412.
Imai, H., Chan, E. K., Kiyosawa, K., Fu, X. D. and Tan, E. M. (1993). Novel nuclear autoantigen with splicing factor motifs identified with antibody from hepatocellular carcinoma. *J Clin Invest* **92**, 2419-2426.
Ip, J. Y., Schmidt, D., Pan, Q., Ramani, A. K., Fraser, A. G., Odom, D. T. and Blencowe, B. J. (2011). Global impact of RNA polymerase II elongation inhibition on alternative splicing regulation. *Genome Res* **21**, 390-401.

Ishihara, T., Ariizumi, Y., Shiga, A., Kato, T., Tan, C.-F., Sato, T., Miki, Y., Yokoo, M., Fujino, T., Koyama, A. et al. (2013). Decreased number of Gemini of coiled bodies and U12 snRNA level in amyotrophic lateral sclerosis. *Human Molecular Genetics* **22**, 4136-4147.

Ito, T., Umehara, T., Sasaki, K., Nakamura, Y., Nishino, N., Terada, T., Shirouzu, M., Padmanabhan, B., Yokoyama, S., Ito, A. et al. (2011). Real-time imaging of histone H4K12-specific acetylation determines the modes of action of histone deacetylase and bromodomain inhibitors. *Chem Biol* **18**, 495-507.

Izaurralde, E., Stepinski, J., Darzynkiewicz, E. and Mattaj, I. W. (1992). A cap binding protein that may mediate nuclear export of RNA polymerase II-transcribed RNAs. *J Cell Biol* **118**, 1287-1295.

Jady, B. E. and Kiss, T. (2001). A small nucleolar guide RNA functions both in 2'-O-ribose methylation and pseudouridylation of the U5 spliceosomal RNA. *Embo j* **20**, 541-551.

Jady, B. E., Darzacq, X., Tucker, K. E., Matera, A. G., Bertrand, E. and Kiss, T. (2003). Modification of Sm small nuclear RNAs occurs in the nucleoplasmic Cajal body following import from the cytoplasm. *Embo j* **22**, 1878-1888.

Jung, D. J., Na, S. Y., Na, D. S. and Lee, J. W. (2002). Molecular cloning and characterization of CAPER, a novel coactivator of activating protein-1 and estrogen receptors. *J Biol Chem* **277**, 1229-1234.

Jurica, M. S., Licklider, L. J., Gygi, S. R., Grigorieff, N. and Moore, M. J. (2002). Purification and characterization of native spliceosomes suitable for three-dimensional structural analysis. *Rna* **8**, 426-439.

Kadener, S., Fededa, J. P., Rosbash, M. and Kornblihtt, A. R. (2002). Regulation of alternative splicing by a transcriptional enhancer through RNA pol II elongation. *Proc Natl Acad Sci U S A* **99**, 8185-8190.

Kadener, S., Cramer, P., Nogues, G., Cazalla, D., de la Mata, M., Fededa, J. P., Werbajh, S. E., Srebrow, A. and Kornblihtt, A. R. (2001). Antagonistic effects of T-Ag and VP16 reveal a role for RNA pol II elongation on alternative splicing. *Embo j* **20**, 5759-5768.

Kambach, C., Walke, S., Young, R., Avis, J. M., de la Fortelle, E., Raker, V. A., Luhrmann, R., Li, J. and Nagai, K. (1999). Crystal structures of two Sm protein complexes and their implications for the assembly of the spliceosomal snRNPs. *Cell* **96**, 375-387.

Kanno, T., Kanno, Y., Siegel, R. M., Jang, M. K., Lenardo, M. J. and Ozato, K. (2004). Selective recognition of acetylated histones by bromodomain proteins visualized in living cells. *Molecular cell* **13**, 33-43.

Kariya, S., Re, D. B., Jacquier, A., Nelson, K., Przedborski, S. and Monani, U. R. (2012). Mutant superoxide dismutase 1 (SOD1), a cause of amyotrophic lateral sclerosis, disrupts the recruitment of SMN, the spinal muscular atrophy protein to nuclear Cajal bodies. *Human molecular genetics* **21**, 3421-3434.

Kessler, O., Jiang, Y. and Chasin, L. A. (1993). Order of intron removal during splicing of endogenous adenine phosphoribosyltransferase and dihydrofolate reductase pre-mRNA. *Mol Cell Biol* **13**, 6211-6222.

Kielkopf, C. L., Lucke, S. and Green, M. R. (2004). U2AF homology motifs: protein recognition in the RRM world. *Genes Dev* **18**, 1513-1526.

Kitao, S., Segref, A., Kast, J., Wilm, M., Mattaj, I. W. and Ohno, M. (2008). A compartmentalized phosphorylation/dephosphorylation system that regulates U snRNA export from the nucleus. *Mol Cell Biol* **28**, 487-497.
Klingauf, M., Stanek, D. and Neugebauer, K. M. (2006). Enhancement of U4/U6 small nuclear ribonucleoprotein particle association in Cajal bodies predicted by mathematical modeling. *Mol Biol Cell* **17**, 4972-4981.
Kolasinska-Zwierz, P., Down, T., Latorre, I., Liu, T., Liu, X. S. and Ahringer, J. (2009). Differential chromatin marking of introns and expressed exons by H3K36me3. *Nat Genet* **41**, 376-381.
Konarska, M. M., Vilardell, J. and Query, C. C. (2006). Repositioning of the reaction intermediate within the catalytic center of the spliceosome. *Molecular cell* **21**, 543-553.
Kornblihtt, A. R. (2005). Promoter usage and alternative splicing. *Curr. Opin. Cell Biol.* **17**, 262-268.
Kornblihtt, A. R., Schor, I. E., Allo, M., Dujardin, G., Petrillo, E. and Munoz, M. J. (2013). Alternative splicing: a pivotal step between eukaryotic transcription and translation. *Nat Rev Mol Cell Biol* **14**, 153-165.
Kuhlman, T. C., Cho, H., Reinberg, D. and Hernandez, N. (1999). The general transcription factors IIA, IIB, IIF, and IIE are required for RNA polymerase II transcription from the human U1 small nuclear RNA promoter. *Mol Cell Biol* **19**, 2130-2141.
Lamond, A. I. and Spector, D. L. (2003). Nuclear speckles: a model for nuclear organelles. *Nat Rev Mol Cell Biol* **4**, 605-612.
Lazarev, D. and Manley, J. L. (2007). Concurrent splicing and transcription are not sufficient to enhance splicing efficiency. *Rna* **13**, 1546-1557.
Lefebvre, S., Burlet, P., Liu, Q., Bertrandy, S., Clermont, O., Munnich, A., Dreyfuss, G. and Melki, J. (1997). Correlation between severity and SMN protein level in spinal muscular atrophy. *Nat Genet* **16**, 265-269.
Lefebvre, S., Burglen, L., Reboullet, S., Clermont, O., Burlet, P., Viollet, L., Benichou, B., Cruaud, C., Millasseau, P., Zeviani, M. et al. (1995). Identification and characterization of a spinal muscular atrophy-determining gene. *Cell* **80**, 155-165.
LeRoy, G., Rickards, B. and Flint, S. J. (2008). The double bromodomain proteins Brd2 and Brd3 couple histone acetylation to transcription. *Molecular cell* **30**, 51-60.
LeRoy, G., Chepelev, I., DiMaggio, P. A., Blanco, M. A., Zee, B. M., Zhao, K. and Garcia, B. A. (2012). Proteogenomic characterization and mapping of nucleosomes decoded by Brd and HP1 proteins. *Genome biology* **13**, R68.
Leung, A. K., Nagai, K. and Li, J. (2011). Structure of the spliceosomal U4 snRNP core domain and its implication for snRNP biogenesis. *Nature* **473**, 536-539.
Listerman, I., Sapra, A. K. and Neugebauer, K. M. (2006). Cotranscriptional coupling of splicing factor recruitment and precursor messenger RNA splicing in mammalian cells. *Nat Struct Mol Biol* **13**, 815-822.
Liu, Q. and Dreyfuss, G. (1996). A novel nuclear structure containing the survival of motor neurons protein. *Embo j* **15**, 3555-3565.
Loerch, S., Maucuer, A., Manceau, V., Green, M. R. and Kielkopf, C. L. (2014). Cancer-relevant Splicing Factor CAPERα Engages the Essential Splicing Factor

SF3b155 in a Specific Ternary Complex. *Journal of Biological Chemistry* **289**, 17325-17337.
Luco, R. F., Allo, M., Schor, I. E., Kornblihtt, A. R. and Misteli, T. (2011). Epigenetics in alternative pre-mRNA splicing. *Cell* **144**, 16-26.
Luco, R. F., Pan, Q., Tominaga, K., Blencowe, B. J., Pereira-Smith, O. M. and Misteli, T. (2010). Regulation of alternative splicing by histone modifications. *Science* **327**, 996-1000.
Madhani, H. D. and Guthrie, C. (1992). A novel base-pairing interaction between U2 and U6 snRNAs suggests a mechanism for the catalytic activation of the spliceosome. *Cell* **71**, 803-817.
Machyna, M., Heyn, P. and Neugebauer, K. M. (2013). Cajal bodies: where form meets function. *Wiley Interdiscip Rev RNA* **4**, 17-34.
Makarov, E. M., Owen, N., Bottrill, A. and Makarova, O. V. (2012). Functional mammalian spliceosomal complex E contains SMN complex proteins in addition to U1 and U2 snRNPs. *Nucleic Acids Res* **40**, 2639-2652.
Makarov, E. M., Makarova, O. V., Urlaub, H., Gentzel, M., Will, C. L., Wilm, M. and Luhrmann, R. (2002). Small nuclear ribonucleoprotein remodeling during catalytic activation of the spliceosome. *Science* **298**, 2205-2208.
Makarova, O. V., Makarov, E. M., Urlaub, H., Will, C. L., Gentzel, M., Wilm, M. and Luhrmann, R. (2004). A subset of human 35S U5 proteins, including Prp19, function prior to catalytic step 1 of splicing. *Embo j* **23**, 2381-2391.
Malatesta, M., Scassellati, C., Meister, G., Plöttner, O., Bühler, D., Sowa, G., Martin, T. E., Keidel, E., Fischer, U. and Fakan, S. (2004). Ultrastructural characterisation of a nuclear domain highly enriched in survival of motor neuron (SMN) protein. *Experimental Cell Research* **292**, 312-321.
Maniatis, T. and Reed, R. (2002). An extensive network of coupling among gene expression machines. *Nature* **416**, 499-506.
Matera, A. G. and Ward, D. C. (1993). Nucleoplasmic organization of small nuclear ribonucleoproteins in cultured human cells. *J Cell Biol* **121**, 715-727.
Matera, A. G. and Wang, Z. (2014). A day in the life of the spliceosome. *Nat Rev Mol Cell Biol* **15**, 108-121.
Matlin, A. J., Clark, F. and Smith, C. W. (2005). Understanding alternative splicing: towards a cellular code. *Nat Rev Mol Cell Biol* **6**, 386-398.
Mattaj, I. W. (1986). Cap trimethylation of U snRNA is cytoplasmic and dependent on U snRNP protein binding. *Cell* **46**, 905-911.
Mattaj, I. W. and De Robertis, E. M. (1985). Nuclear segregation of U2 snRNA requires binding of specific snRNP proteins. *Cell* **40**, 111-118.
Meister, G. and Fischer, U. (2002). Assisted RNP assembly: SMN and PRMT5 complexes cooperate in the formation of spliceosomal UsnRNPs. *Embo j* **21**, 5853-5863.
Meister, G., Buhler, D., Pillai, R., Lottspeich, F. and Fischer, U. (2001a). A multiprotein complex mediates the ATP-dependent assembly of spliceosomal U snRNPs. *Nat Cell Biol* **3**, 945-949.
Meister, G., Buhler, D., Laggerbauer, B., Zobawa, M., Lottspeich, F. and Fischer, U. (2000). Characterization of a nuclear 20S complex containing the survival of

motor neurons (SMN) protein and a specific subset of spliceosomal Sm proteins. *Hum Mol Genet* **9**, 1977-1986.
Meister, G., Eggert, C., Buhler, D., Brahms, H., Kambach, C. and Fischer, U. (2001b). Methylation of Sm proteins by a complex containing PRMT5 and the putative U snRNP assembly factor pICln. *Curr Biol* **11**, 1990-1994.
Mercer, T. R., Edwards, S. L., Clark, M. B., Neph, S. J., Wang, H., Stergachis, A. B., John, S., Sandstrom, R., Li, G., Sandhu, K. S. et al. (2013). DNase I-hypersensitive exons colocalize with promoters and distal regulatory elements. *Nat. Genet.* **45**, 852-859.
Misteli, T. and Spector, D. L. (1999). RNA polymerase II targets pre-mRNA splicing factors to transcription sites in vivo. *Molecular cell* **3**, 697-705.
Montes, M., Becerra, S., Sanchez-Alvarez, M. and Sune, C. (2012a). Functional coupling of transcription and splicing. *Gene* **501**, 104-117.
Montes, M., Cloutier, A., Sanchez-Hernandez, N., Michelle, L., Lemieux, B., Blanchette, M., Hernandez-Munain, C., Chabot, B. and Sune, C. (2012b). TCERG1 regulates alternative splicing of the Bcl-x gene by modulating the rate of RNA polymerase II transcription. *Mol Cell Biol* **32**, 751-762.
Moore, M. J., Schwartzfarb, E. M., Silver, P. A. and Yu, M. C. (2006). Differential recruitment of the splicing machinery during transcription predicts genome-wide patterns of mRNA splicing. *Molecular cell* **24**, 903-915.
Moore, M. S. (1998). Ran and nuclear transport. *J Biol Chem* **273**, 22857-22860.
Mouaikel, J., Narayanan, U., Verheggen, C., Matera, A. G., Bertrand, E., Tazi, J. and Bordonne, R. (2003). Interaction between the small-nuclear-RNA cap hypermethylase and the spinal muscular atrophy protein, survival of motor neuron. *EMBO Rep* **4**, 616-622.
Mougin, A., Torterotot, F., Branlant, C., Jacobson, M. R., Huang, Q. and Pederson, T. (2002). A 3'-terminal minihelix in the precursor of human spliceosomal U2 small nuclear RNA. *J Biol Chem* **277**, 23137-23142.
Mueller, F., Mazza, D., Stasevich, T. J. and McNally, J. G. (2010). FRAP and kinetic modeling in the analysis of nuclear protein dynamics: what do we really know? *Curr Opin Cell Biol* **22**, 403-411.
Murphy, S. (1997). Differential in vivo activation of the class II and class III snRNA genes by the POU-specific domain of Oct-1. *Nucleic Acids Res* **25**, 2068-2076.
Murphy, S., Yoon, J. B., Gerster, T. and Roeder, R. G. (1992). Oct-1 and Oct-2 potentiate functional interactions of a transcription factor with the proximal sequence element of small nuclear RNA genes. *Mol Cell Biol* **12**, 3247-3261.
Narayanan, U., Achsel, T., Lührmann, R. and Matera, a. G. (2004). Coupled in vitro import of U snRNPs and SMN, the spinal muscular atrophy protein. *Molecular cell* **16**, 223-234.
Narayanan, U., Ospina, J. K., Frey, M. R., Hebert, M. D. and Matera, A. G. (2002). SMN, the spinal muscular atrophy protein, forms a pre-import snRNP complex with snurportin1 and importin beta. *Hum Mol Genet* **11**, 1785-1795.
Nesic, D., Tanackovic, G. and Kramer, A. (2004). A role for Cajal bodies in the final steps of U2 snRNP biogenesis. *J Cell Sci* **117**, 4423-4433.
Neufeld, G., Cohen, T., Gengrinovitch, S. and Poltorak, Z. (1999). Vascular endothelial growth factor (VEGF) and its receptors. *FASEB J.* **13**, 9-22.

Nogues, G., Munoz, M. J. and Kornblihtt, A. R. (2003). Influence of polymerase II processivity on alternative splicing depends on splice site strength. *J Biol Chem* **278**, 52166-52171.
Nogues, G., Kadener, S., Cramer, P., Bentley, D. and Kornblihtt, A. R. (2002). Transcriptional activators differ in their abilities to control alternative splicing. *J Biol Chem* **277**, 43110-43114.
Norris, S. C., Humpolickova, J., Amler, E., Huranova, M., Buzgo, M., Machan, R., Lukas, D. and Hof, M. (2011). Raster image correlation spectroscopy as a novel tool to study interactions of macromolecules with nanofiber scaffolds. *Acta Biomater* **7**, 4195-4203.
Novotný, I., Blažíková, M., Staněk, D., Herman, P. and Malinsky, J. (2011). In vivo kinetics of U4/U6·U5 tri-snRNP formation in Cajal bodies. *Molecular biology of the cell* **22**, 513-523.
Ohno, M., Segref, A., Bachi, A., Wilm, M. and Mattaj, I. W. (2000). PHAX, a mediator of U snRNA nuclear export whose activity is regulated by phosphorylation. *Cell* **101**, 187-198.
Otter, S., Grimmler, M., Neuenkirchen, N., Chari, A., Sickmann, A. and Fischer, U. (2007). A Comprehensive Interaction Map of the Human Survival of Motor Neuron (SMN) Complex. *Journal of Biological Chemistry* **282**, 5825-5833.
Pagani, F., Stuani, C., Zuccato, E., Kornblihtt, A. R. and Baralle, F. E. (2003). Promoter architecture modulates CFTR exon 9 skipping. *J Biol Chem* **278**, 1511-1517.
Pal, D. K., Evgrafov, O. V., Tabares, P., Zhang, F., Durner, M. and Greenberg, D. A. (2003). BRD2 (RING3) is a probable major susceptibility gene for common juvenile myoclonic epilepsy. *Am J Hum Genet* **73**, 261-270.
Palacios, I., Hetzer, M., Adam, S. A. and Mattaj, I. W. (1997). Nuclear import of U snRNPs requires importin beta. *Embo j* **16**, 6783-6792.
Pan, Q., Shai, O., Lee, L. J., Frey, B. J. and Blencowe, B. J. (2008). Deep surveying of alternative splicing complexity in the human transcriptome by high-throughput sequencing. *Nat Genet* **40**, 1413-1415.
Pandya-Jones, A. and Black, D. L. (2009). Co-transcriptional splicing of constitutive and alternative exons. *Rna* **15**, 1896-1908.
Park, J. W., Parisky, K., Celotto, A. M., Reenan, R. A. and Graveley, B. R. (2004). Identification of alternative splicing regulators by RNA interference in Drosophila. *Proc Natl Acad Sci U S A* **101**, 15974-15979.
Pellizzoni, L., Yong, J. and Dreyfuss, G. (2002a). Essential role for the SMN complex in the specificity of snRNP assembly. *Science* **298**, 1775-1779.
Pellizzoni, L., Baccon, J., Rappsilber, J., Mann, M. and Dreyfuss, G. (2002b). Purification of native survival of motor neurons complexes and identification of Gemin6 as a novel component. *J Biol Chem* **277**, 7540-7545.
Peng, J., Dong, W., Chen, L., Zou, T., Qi, Y. and Liu, Y. (2007). Brd2 is a TBP-associated protein and recruits TBP into E2F-1 transcriptional complex in response to serum stimulation. *Mol Cell Biochem* **294**, 45-54.
Pomeranz Krummel, D. A., Oubridge, C., Leung, A. K. W., Li, J. and Nagai, K. (2009). Crystal structure of human spliceosomal U1 snRNP at 5.5 A resolution. *Nature* **458**, 475-480.

Pradeepa, M. M., Sutherland, H. G., Ule, J., Grimes, G. R. and Bickmore, W. A. (2012). Psip1/Ledgf p52 binds methylated histone H3K36 and splicing factors and contributes to the regulation of alternative splicing. *PLoS Genet* **8**, e1002717.
Raghunathan, P. L. and Guthrie, C. (1998). RNA unwinding in U4/U6 snRNPs requires ATP hydrolysis and the DEIH-box splicing factor Brr2. *Curr Biol* **8**, 847-855.
Rahman, S., Sowa, M. E., Ottinger, M., Smith, J. A., Shi, Y., Harper, J. W. and Howley, P. M. (2011). The Brd4 extraterminal domain confers transcription activation independent of pTEFb by recruiting multiple proteins, including NSD3. *Mol Cell Biol* **31**, 2641-2652.
Raker, V. A., Plessel, G. and Luhrmann, R. (1996). The snRNP core assembly pathway: identification of stable core protein heteromeric complexes and an snRNP subcore particle in vitro. *Embo j* **15**, 2256-2269.
Rappsilber, J., Ryder, U., Lamond, A. I. and Mann, M. (2002). Large-scale proteomic analysis of the human spliceosome. *Genome Res* **12**, 1231-1245.
Reddy, R., Henning, D., Das, G., Harless, M. and Wright, D. (1987). The capped U6 small nuclear RNA is transcribed by RNA polymerase III. *J Biol Chem* **262**, 75-81.
Reed, R. (2000). Mechanisms of fidelity in pre-mRNA splicing. *Curr Opin Cell Biol* **12**, 340-345.
Roberts, G. C., Gooding, C., Mak, H. Y., Proudfoot, N. J. and Smith, C. W. (1998). Co-transcriptional commitment to alternative splice site selection. *Nucleic Acids Res* **26**, 5568-5572.
Sadowski, C. L., Henry, R. W., Lobo, S. M. and Hernandez, N. (1993). Targeting TBP to a non-TATA box cis-regulatory element: a TBP-containing complex activates transcription from snRNA promoters through the PSE. *Genes Dev* **7**, 1535-1548.
Salditt-Georgieff, M., Harpold, M., Chen-Kiang, S. and Darnell, J. E., Jr. (1980). The addition of 5' cap structures occurs early in hnRNA synthesis and prematurely terminated molecules are capped. *Cell* **19**, 69-78.
Shan, X., Chiang, P. M., Price, D. L. and Wong, P. C. (2010). Altered distributions of Gemini of coiled bodies and mitochondria in motor neurons of TDP-43 transgenic mice. *Proc Natl Acad Sci U S A* **107**, 16325-16330.
Shang, E., Wang, X., Wen, D., Greenberg, D. A. and Wolgemuth, D. J. (2009). Double bromodomain-containing gene Brd2 is essential for embryonic development in mouse. *Dev Dyn* **238**, 908-917.
Shao, W., Kim, H. S., Cao, Y., Xu, Y. Z. and Query, C. C. (2012). A U1-U2 snRNP interaction network during intron definition. *Mol Cell Biol* **32**, 470-478.
Sharma, S., Kohlstaedt, L. A., Damianov, A., Rio, D. C. and Black, D. L. (2008). Polypyrimidine tract binding protein controls the transition from exon definition to an intron defined spliceosome. *Nat Struct Mol Biol* **15**, 183-191.
Schaffert, N., Hossbach, M., Heintzmann, R., Achsel, T. and Lührmann, R. (2004). RNAi knockdown of hPrp31 leads to an accumulation of U4/U6 di-snRNPs in Cajal bodies. *The EMBO journal* **23**, 3000-3009.
Schneider, M., Will, C. L., Anokhina, M., Tazi, J., Urlaub, H. and Luhrmann, R. (2010). Exon definition complexes contain the tri-snRNP and can be directly converted into B-like precatalytic splicing complexes. *Molecular cell* **38**, 223-235.

Schor, I. E., Rascovan, N., Pelisch, F., Allo, M. and Kornblihtt, A. R. (2009). Neuronal cell depolarization induces intragenic chromatin modifications affecting NCAM alternative splicing. *Proc Natl Acad Sci U S A* **106**, 4325-4330.
Schwartz, S., Meshorer, E. and Ast, G. (2009). Chromatin organization marks exon-intron structure. *Nat Struct Mol Biol* **16**, 990-995.
Schwer, B. and Gross, C. H. (1998). Prp22, a DExH-box RNA helicase, plays two distinct roles in yeast pre-mRNA splicing. *Embo j* **17**, 2086-2094.
Simkova, E. and Stanek, D. (2012). Probing Nucleic Acid Interactions and Pre-mRNA Splicing by Forster Resonance Energy Transfer (FRET) Microscopy. *Int J Mol Sci* **13**, 14929-14945.
Sims, R. J., 3rd, Millhouse, S., Chen, C. F., Lewis, B. A., Erdjument-Bromage, H., Tempst, P., Manley, J. L. and Reinberg, D. (2007). Recognition of trimethylated histone H3 lysine 4 facilitates the recruitment of transcription postinitiation factors and pre-mRNA splicing. *Molecular cell* **28**, 665-676.
Sleeman, J. E. and Lamond, A. I. (1999). Newly assembled snRNPs associate with coiled bodies before speckles, suggesting a nuclear snRNP maturation pathway. *Curr Biol* **9**, 1065-1074.
Sleeman, J. E. and Trinkle-Mulcahy, L. (2014). Nuclear bodies: new insights into assembly/dynamics and disease relevance. *Curr Opin Cell Biol* **28c**, 76-83.
Spies, N., Nielsen, C. B., Padgett, R. A. and Burge, C. B. (2009). Biased chromatin signatures around polyadenylation sites and exons. *Molecular cell* **36**, 245-254.
Sprague, B. L., Pego, R. L., Stavreva, D. A. and McNally, J. G. (2004). Analysis of binding reactions by fluorescence recovery after photobleaching. *Biophys J* **86**, 3473-3495.
Stade, K., Ford, C. S., Guthrie, C. and Weis, K. (1997). Exportin 1 (Crm1p) is an essential nuclear export factor. *Cell* **90**, 1041-1050.
Staknis, D. and Reed, R. (1994). SR proteins promote the first specific recognition of Pre-mRNA and are present together with the U1 small nuclear ribonucleoprotein particle in a general splicing enhancer complex. *Mol Cell Biol* **14**, 7670-7682.
Stanek, D. and Neugebauer, K. M. (2006). The Cajal body: a meeting place for spliceosomal snRNPs in the nuclear maze. *Chromosoma* **115**, 343-354.
Stanek, D., Rader, S. D., Klingauf, M. and Neugebauer, K. M. (2003). Targeting of U4/U6 small nuclear RNP assembly factor SART3/p110 to Cajal bodies. *J Cell Biol* **160**, 505-516.
Stanek, D., Pridalova-Hnilicova, J., Novotny, I., Huranova, M., Blazikova, M., Wen, X., Sapra, A. K. and Neugebauer, K. M. (2008). Spliceosomal small nuclear ribonucleoprotein particles repeatedly cycle through Cajal bodies. *Mol Biol Cell* **19**, 2534-2543.
Staněk, D. and Neugebauer, K. M. (2004). Detection of snRNP assembly intermediates in Cajal bodies by fluorescence resonance energy transfer. *The Journal of cell biology* **166**, 1015-1025.
Stark, H., Dube, P., Luhrmann, R. and Kastner, B. (2001). Arrangement of RNA and proteins in the spliceosomal U1 small nuclear ribonucleoprotein particle. *Nature* **409**, 539-542.

Strasser, A., Dickmanns, A., Luhrmann, R. and Ficner, R. (2005). Structural basis for m3G-cap-mediated nuclear import of spliceosomal UsnRNPs by snurportin1. *Embo j* **24**, 2235-2243.
Strzelecka, M., Trowitzsch, S., Weber, G., Luhrmann, R., Oates, A. C. and Neugebauer, K. M. (2010). Coilin-dependent snRNP assembly is essential for zebrafish embryogenesis. *Nat Struct Mol Biol* **17**, 403-409.
Sun, H. and Chasin, L. A. (2000). Multiple splicing defects in an intronic false exon. *Mol Cell Biol* **20**, 6414-6425.
Suzuki, T., Izumi, H. and Ohno, M. (2010). Cajal body surveillance of U snRNA export complex assembly. *J Cell Biol* **190**, 603-612.
Tennyson, C. N., Klamut, H. J. and Worton, R. G. (1995). The human dystrophin gene requires 16 hours to be transcribed and is cotranscriptionally spliced. *Nat Genet* **9**, 184-190.
Thickman, K. R., Swenson, M. C., Kabogo, J. M., Gryczynski, Z. and Kielkopf, C. L. (2006). Multiple U2AF65 binding sites within SF3b155: thermodynamic and spectroscopic characterization of protein-protein interactions among pre-mRNA splicing factors. *J Mol Biol* **356**, 664-683.
Tsuiji, H., Iguchi, Y., Furuya, A., Kataoka, A., Hatsuta, H., Atsuta, N., Tanaka, F., Hashizume, Y., Akatsu, H., Murayama, S. et al. (2013). Spliceosome integrity is defective in the motor neuron diseases ALS and SMA. *EMBO molecular medicine* **5**, 221-234.
Turner, B. J., Alfazema, N., Sheean, R. K., Sleigh, J. N., Davies, K. E., Horne, M. K. and Talbot, K. (2014). Overexpression of survival motor neuron improves neuromuscular function and motor neuron survival in mutant SOD1 mice. *Neurobiol. Aging* **35**, 906-915.
Umehara, T., Nakamura, Y., Wakamori, M., Ozato, K., Yokoyama, S. and Padmanabhan, B. (2010). Structural implications for K5/K12-di-acetylated histone H4 recognition by the second bromodomain of BRD2. *FEBS Lett.* **584**, 3901-3908.
Urlaub, H., Raker, V. A., Kostka, S. and Luhrmann, R. (2001). Sm protein-Sm site RNA interactions within the inner ring of the spliceosomal snRNP core structure. *Embo j* **20**, 187-196.
Valadkhan, S. (2010). Role of the snRNAs in spliceosomal active site. *RNA Biol* **7**, 345-353.
Valcarcel, J., Gaur, R. K., Singh, R. and Green, M. R. (1996). Interaction of U2AF65 RS region with pre-mRNA branch point and promotion of base pairing with U2 snRNA [corrected]. *Science* **273**, 1706-1709.
Veldink, J. H., Kalmijn, S., Van der Hout, A. H., Lemmink, H. H., Groeneveld, G. J., Lummen, C., Scheffer, H., Wokke, J. H. and Van den Berg, L. H. (2005). SMN genotypes producing less SMN protein increase susceptibility to and severity of sporadic ALS. *Neurology* **65**, 820-825.
Wahl, M. C., Will, C. L. and Luhrmann, R. (2009). The spliceosome: design principles of a dynamic RNP machine. *Cell* **136**, 701-718.
Wang, Y., Ma, M., Xiao, X. and Wang, Z. (2012). Intronic splicing enhancers, cognate splicing factors and context-dependent regulation rules. *Nat Struct Mol Biol* **19**, 1044-1052.

Wang, Y., Xiao, X., Zhang, J., Choudhury, R., Robertson, A., Li, K., Ma, M., Burge, C. B. and Wang, Z. (2013). A complex network of factors with overlapping affinities represses splicing through intronic elements. *Nat Struct Mol Biol* **20**, 36-45.

Webby, C. J., Wolf, A., Gromak, N., Dreger, M., Kramer, H., Kessler, B., Nielsen, M. L., Schmitz, C., Butler, D. S., Yates, J. R., 3rd et al. (2009). Jmjd6 catalyses lysyl-hydroxylation of U2AF65, a protein associated with RNA splicing. *Science* **325**, 90-93.

Wellmann, S., Taube, T., Paal, K., Graf, V. E. H., Geilen, W., Seifert, G., Eckert, C., Henze, G. and Seeger, K. (2001). Specific reverse transcription-PCR quantification of vascular endothelial growth factor (VEGF) splice variants by LightCycler technology. *Clin Chem* **47**, 654-660.

Will, C. L. and Luhrmann, R. (2011). Spliceosome structure and function. *Cold Spring Harb Perspect Biol* **3**.

Wohlwend, D., Strasser, A., Dickmanns, A. and Ficner, R. (2007). Structural basis for RanGTP independent entry of spliceosomal U snRNPs into the nucleus. *J Mol Biol* **374**, 1129-1138.

Wong, M. W., Henry, R. W., Ma, B., Kobayashi, R., Klages, N., Matthias, P., Strubin, M. and Hernandez, N. (1998). The large subunit of basal transcription factor SNAPc is a Myb domain protein that interacts with Oct-1. *Mol Cell Biol* **18**, 368-377.

Yamazaki, T., Chen, S., Yu, Y., Yan, B., Haertlein, Tyler C., Carrasco, Monica A., Tapia, Juan C., Zhai, B., Das, R., Lalancette-Hebert, M. et al. (2012). FUS-SMN Protein Interactions Link the Motor Neuron Diseases ALS and SMA. *Cell Reports* **2**, 799-806.

Yong, J., Pellizzoni, L. and Dreyfuss, G. (2002). Sequence-specific interaction of U1 snRNA with the SMN complex. *EMBO Journal* **21**, 1188-1196.

Yong, J., Kasim, M., Bachorik, J. L., Wan, L. and Dreyfuss, G. (2010). Gemin5 delivers snRNA precursors to the SMN complex for snRNP biogenesis. *Molecular cell* **38**, 551-562.

Yu, Y. T., Shu, M. D. and Steitz, J. A. (1998). Modifications of U2 snRNA are required for snRNP assembly and pre-mRNA splicing. *Embo j* **17**, 5783-5795.

Zhang, R., So, B. R., Li, P., Yong, J., Glisovic, T., Wan, L. and Dreyfuss, G. (2011). Structure of a key intermediate of the SMN complex reveals Gemin2's crucial function in snRNP assembly. *Cell* **146**, 384-395.

Zhu, J., Mayeda, A. and Krainer, A. R. (2001). Exon identity established through differential antagonism between exonic splicing silencer-bound hnRNP A1 and enhancer-bound SR proteins. *Molecular cell* **8**, 1351-1361.